การลดลงของระดับเมทิลเลชั่นบนดีเอ็นเอที่ถูกกระตุ้นด้วยอนุพันธ์ออกซิเจนที่ว่องไวในมะเร็งกระเพาะ
ปัสสาวะ ผ่านการเพิ่มขึ้นของ 8-ไฮดรอกซี-2'-ดีออกซีกัวโนซีน

นางสาวพัชราวลัย วงศ์ศิริ

วิทยานิพนธ์นี้เป็นส่วนหนึ่งของการศึกษาตามหลักสูตรปริญญาวิทยาศาสตรดุษฎีบัณฑิต
สาขาวิชาชีวเคมีทางการแพทย์ ภาควิชาชีวเคมี
คณะแพทยศาสตร์ จุฬาลงกรณ์มหาวิทยาลัย
ปีการศึกษา 2560

Reactive Oxygen Species-induced Global DNA hypomethylation in Bladder Cancer is Mediated via Increased Formation of 8-Hydroxy-2'-Deoxyguanosine

Miss Patcharawalai Whongsiri

A Dissertation Submitted in Partial Fulfillment of the Requirements

for the Degree of Doctor of Philosophy Program in Medical Biochemistry

Department of Biochemistry

Faculty of Medicine

Chulalongkorn University

Academic Year 2017

| | |
|---|---|
| Thesis Title | Reactive Oxygen Species-induced Global DNA hypomethylation in Bladder Cancer is Mediated via Increased Formation of 8-Hydroxy-2'-Deoxyguanosine |
| By | Miss Patcharawalai Whongsiri |
| Field of Study | Medical Biochemistry |
| Thesis Advisor | Assistant ProfessorChanchai Boonla, Ph.D. |
| Thesis Co-Advisor | Assistant ProfessorSiriporn Chuchawankul, Ph.D. |
| | Depicha Jindatip, Ph.D. |

Accepted by the Faculty of Medicine, Chulalongkorn University in Partial Fulfillment of the Requirements for the Doctoral Degree

⋯⋯⋯⋯⋯⋯⋯⋯⋯⋯⋯⋯⋯Dean of the Faculty of Medicine

(ProfessorSuttipong Wacharasindhu, M.D.)

THESIS COMMITTEE

⋯⋯⋯⋯⋯⋯⋯⋯⋯⋯⋯⋯⋯Chairman

(ProfessorSittisak Honsawek, M.D., Ph.D.)

⋯⋯⋯⋯⋯⋯⋯⋯⋯⋯⋯⋯⋯Thesis Advisor

(Assistant ProfessorChanchai Boonla, Ph.D.)

⋯⋯⋯⋯⋯⋯⋯⋯⋯⋯⋯⋯⋯Thesis Co-Advisor

(Assistant ProfessorSiriporn Chuchawankul, Ph.D.)

⋯⋯⋯⋯⋯⋯⋯⋯⋯⋯⋯⋯⋯Thesis Co-Advisor

(Depicha Jindatip, Ph.D.)

⋯⋯⋯⋯⋯⋯⋯⋯⋯⋯⋯⋯⋯Examiner

(Roongruedee Chaiteerakij, M.D., Ph.D.)

⋯⋯⋯⋯⋯⋯⋯⋯⋯⋯⋯⋯⋯External Examiner

(Assistant ProfessorPeti Thuwajit, M.D., Ph.D.)

พัชราวลัย วงศ์ศิริ : การลดลงของระดับเมทิลเลชั่นบนดีเอ็นเอที่ถูกกระตุ้นด้วยอนุพันธ์ออกซิเจนที่ว่องไวใน มะเร็งกระเพาะปัสสาวะ ผ่านการเพิ่มขึ้นของ 8-ไฮดรอกซี-2'-ดีออกซีกัวโนซีน (Reactive Oxygen Species-induced Global DNA hypomethylation in Bladder Cancer is Mediated via Increased Formation of 8-Hydroxy-2'-Deoxyguanosine) อ.ที่ปรึกษาวิทยานิพนธ์หลัก: ผศ. ดร.ชาญชัย บุญหล้า, อ.ที่ปรึกษา วิทยานิพนธ์ร่วม: ผศ. ดร.ศิริพร ชื้อชวาลกุล, อ. ดร.เดภิชา จินดาทิพย์, หน้า.

ภาวะเครียดจากออกซิเดชั่นซึ่งเกิดจากการเพิ่มขึ้นของอนุพันธ์ของออกซิเจนที่ว่องไวมีความเกี่ยวข้องกับการเกิด โรคเรื้อรังหลายชนิด รวมทั้งโรคมะเร็ง โดยมีความเกี่ยวข้องผ่านการทำให้เกิดความเสียหายต่อดีเอ็นเอ หรือส่งผลให้การ ควบคุมการแสดงออกของยีนในระดับเหนือพันธุกรรมผิดปกติไป Long interspersed element-1 หรือ LINE-1 เป็น retrotransposible elements ที่ยังคงทำงาน และพบมากถึง 17% ในพันธุกรรมของมนุษย์ การศึกษาก่อนหน้าพบรายงาน การลดลงของระดับเมทิลเลชั่นบนดีเอ็นเอบริเวณ LINE-1 ในมะเร็งกระเพาะปัสสาวะ และจากหลักฐานพบว่าการลดลงของ ระดับเมทิลเลชั่นบนดีเอ็นเอบริเวณ LINE-1 นี้เป็นผลมาจากภาวะเครียดจากออกซิเดชั่น ในการศึกษานี้ ผู้วิจัยได้ศึกษาระดับ การแสดงออกของ 5-methylcytosine (5-mC), 8-hydroxyguanosine (8-OHdG), โปรตีนที่ถูกสร้างจาก LINE-1 (ORF1p), histone H3K9me3 และ HP1 alpha ในเนื้อเยื่อมะเร็งกระเพาะปัสสาวะ นอกจากนี้ ยังทำการศึกษาถึงกลไกของ ภาวะเครียดจากออกซิเดชั่นที่ส่งผลต่อระดับเมทิลเลชั่นบนดีเอ็นเอและการเปลี่ยนแปลงหมู่โปรตีนฮิสโตน ซึ่งนำไปสู่การ แสดงออกที่ผิดปกติของ LINE-1 ในเซลล์มะเร็งกระเพาะปัสสาวะ ผลการศึกษาพบระดับการแสดงออกที่เพิ่มขึ้นของ 8-OHdG, การลดลงของ 5-mC, การเพิ่มขึ้นของโปรตีน ORF1p และการเพิ่มขึ้นของฮิสโตน H3K9me3 ในเนื้อเยื่อมะเร็ง กระเพาะปัสสาวะ ซึ่งเป็นการบ่งบอกถึงการเพิ่มขึ้นของภาวะเครียดจากออกซิเดชั่นและความผิดปกติของการควบคุมการ แสดงออกของยีนในระดับเหนือพันธุกรรม การศึกษาในเซลล์มะเร็งกระเพาะปัสสาวะพบว่า การลดลงของระดับเมทิลเลชั่น บนดีเอ็นเอบริเวณ LINE-1 เกิดผ่านการเพิ่มขึ้นของดีเอ็นเอที่เสียหายบริเวณ LINE-1 promoter จากการทดลองด้วยเทคนิค ChIP พบว่าภาวะเครียดจากออกซิเดชั่นส่งผลทำให้รูปแบบการเปลี่ยนแปลงหมู่โปรตีนฮิสโตนเปลี่ยนแปลงไป โดยเฉพาะ บริเวณ LINE-1 promoter โดยพบว่าระดับของฮิสโตน H3K4me3 และ H3K18Ac บริเวณ LINE-1 promoter เพิ่มขึ้นใน เซลล์ที่กระตุ้นด้วย ROS เมื่อเปรียบเทียบกับกลุ่มควบคุม นอกจากนี้ เซลล์ที่ถูกกระตุ้นด้วย ROS ยังมีระดับ cell migration และ cell invasion ที่สูงขึ้นเมื่อเทียบกับกลุ่มควบคุมด้วย จากการศึกษาสรุปได้ว่า ในเนื้อเยื่อมะเร็งกระเพาะปัสสาวะพบการ เพิ่มขึ้นของความเสียหายของดีเอ็นเอ การเพิ่มขึ้นของโปรตีน ORF1p และความผิดปกติของการเปลี่ยนแปลงหมู่โปรตีนฮิส โตน การทดลองในเซลล์มะเร็งกระเพาะปัสสาวะพบว่า ภาวะเครียดจากออกซิเดชั่นที่ถูกกระตุ้นอนุพันธ์ออกซิเจนที่ว่องไว ส่งผลให้เกิดการลดลงของระดับเมทิลเลชั่นบนดีเอ็นเอบริเวณ LINE-1 และส่งผลให้เกิดการเพิ่มขึ้นของ active chromatin marks บริเวณ LINE-1 promoter ส่งผลให้เกิดการแสดงออกที่เพิ่มขึ้นของโปรตีน ORF1p การศึกษาในครั้งนี้แสดงให้เห็นว่า การเกิด LINE-1 reactivation ที่ถูกกระตุ้นจากภาวะเครียดจากออกซิเดชั่นส่งผลให้เกิดการลุกลามของมะเร็งกระเพาะ ปัสสาวะ ดังนั้น การยับยั้งการแสดงออกของโปรตีน ORF1p และการยับยั้งการเกิดภาวะเครียดจากออกซิเดชั่นน่าจะสามารถ นำมาใช้เป็นเป้าหมายในการรักษามะเร็งกระเพาะปัสสาวะได้ในอนาคต

| ภาควิชา | ชีวเคมี | ลายมือชื่อนิสิต | ......................................... |
|---|---|---|---|
| สาขาวิชา | ชีวเคมีทางการแพทย์ | ลายมือชื่อ อ.ที่ปรึกษาหลัก | ......................................... |
| ปีการศึกษา | 2560 | ลายมือชื่อ อ.ที่ปรึกษาร่วม | ......................................... |
| | | ลายมือชื่อ อ.ที่ปรึกษาร่วม | ......................................... |

# # 5674763330 : MAJOR MEDICAL BIOCHEMISTRY

KEYWORDS: BLADDER CANCER, EPIGENETICS, GLOBAL DNA HYPOMETHYLATION, HISTONE MODIFICATIONS, OXIDATIVE STRESS, ROS, 8-OHDG, LINE-1, CANCER PROGRESSION

PATCHARAWALAI WHONGSIRI: Reactive Oxygen Species-induced Global DNA hypomethylation in Bladder Cancer is Mediated via Increased Formation of 8-Hydroxy-2'-Deoxyguanosine. ADVISOR: ASST. PROF.CHANCHAI BOONLA, Ph.D., CO-ADVISOR: ASST. PROF.SIRIPORN CHUCHAWANKUL, Ph.D., DEPICHA JINDATIP, Ph.D., pp.

Oxidative stress, as a consequence of the elevated reactive oxygen species (ROS), has been implicated in various chronic diseases including cancers by, for examples, causing oxidative DNA damage and altering epigenetic regulation. Long interspersed element-1 (LINE-1) is an only active retrotransposable elements in human DNA, comprising up to 17% of the whole genome. LINE-1 hypomethylation is reported in bladder cancer and evidently it is a consequence of oxidative stress. In this study, we investigated the expression of 5-methylcytosine (5-mC), 8-hydroxydeoxyguanosine (8-OHdG), LINE-1-endoced protein (ORF1p), histone H3K9me3 and HP1 alpha in bladder cancer tissues. Mechanistic insight into how oxidative stress affected DNA methylation and histone modifications that further caused aberrant expression of LINE-1 elements in bladder cancer cells was also explored. Elevated expression of 8-OHdG, decreased 5-mC expression, upregulation of ORF1p expression, and increase in histone H3K9me3 expression were observed in bladder cancer tissues, indicating increases in oxidative stress and epigenetic alterations. The *in vitro* study in bladder cancer cell lines revealed that LINE-1 hypomethylation was occurred through the oxidative DNA damage on LINE-1 promoter. Based on ChIP experiments, oxidative stress disturbed histone modification patterns, especially on LINE-1 promoter. Enrichments of histone H3K4me3 and H3K18Ac at LINE-1 promoter were increased in ROS-treated cells compared to the untreated control. In addition, ROS-treated bladder cancer cells had migration and invasion capability greater than the untreated control cells. In conclusion, elevated formation of oxidative DNA lesions, overexpression of ORF1p, and alteration of chromatin modification were shown in human bladder cancer tissues. Experimentally, oxidative stress induced by ROS caused hypomethylation of LINE-1 and enrichment of active chromatin marks at LINE-1 promoter. These, at least in part, led to increased expression of LINE-1 ORF1p protein. The current findings suggest that LINE-1 reactivation by oxidative stress promotes bladder cancer progression. Therefore, downregulation of LINE-1 expression and attenuation of oxidative stress could be potential targets for bladder cancer therapy in the future.

| | | | |
|---|---|---|---|
| Department: | Biochemistry | Student's Signature | ............................................ |
| Field of Study: | Medical Biochemistry | Advisor's Signature | ............................................ |
| Academic Year: | 2017 | Co-Advisor's Signature | ............................................ |
| | | Co-Advisor's Signature | ............................................ |

# ACKNOWLEDGEMENTS

# CONTENTS

จุฬาลงกรณ์มหาวิทยาลัย

CHULALONGKORN UNIVERSITY

# List of Figures

# List of Tables

จุฬาลงกรณ์มหาวิทยาลัย

CHULALONGKORN UNIVERSITY

## Chapter 1

## Introduction

**Background and rationales**

Oxidative stress is defined as an excessive production of reactive species, mainly reactive oxygen species (ROS), and/or an inadequacy of antioxidants in the cells leading to oxidative damage and cell injury. Increased ROS production leads to oxidative stress and damage that is well recognized to mediate pathogenesis of many chronic diseases including cancers (Betteridge, 2000; Oberley, 2002). Our previous studies demonstrated an increase in oxidative stress in patients with urinary bladder cancer (Patchsung et al., 2012) and hepatocellular carcinoma (Poungpairoj et al., 2015) compared with healthy controls. ROS is produced endogenously as a byproduct of cellular aerobic metabolism and inflammatory reaction, and it is also generated by exogenous source such as UV radiation and ionization. ROS is highly reactive to oxidize biomolecules (lipids, proteins and nucleic acids) within the cells resulting in formation of oxidatively modified damage products. Accumulation of oxidatively modified damage products, especially DNA damage, together with dysfunction of DNA repairing process have been implicated in the carcinogenesis (Betteridge, 2000; Oberley, 2002) and progression of several cancers, for examples, breast cancer (Sova et al., 2010), gastric carcinoma (Borrego et al., 2013) and ovarian carcinoma (Xu et al., 2013). The explanation is that oxidative DNA lesions potentiate both genetic mutations and epigenetic alterations, which are hallmarks of molecular changes in cancers (Klaunig et al., 2010).

Epigenetics, which refers to the chemical modifications above nucleotide sequences, is involved in transcriptional regulation through various mechanisms, for instances, DNA methylation and histone modification (Toraño et al., 2012). Change in DNA methylation pattern is well documented in cancers, and it has a strong association with cancer development (Kitkumthorn & Mutirangura, 2011). Two types of DNA methylation changes that are frequently found in cancers are global

hypomethylation (genome-wide hypomethylation) and promoter hypermethylation (especially in tumor suppressor genes). Loss of global methylation level or global DNA hypomethylation is the first established epigenetic alteration that is verified in various cancers, such as colon cancer (Hernandez-Blazquez et al., 2000), breast cancer (Hon et al., 2012) and prostate cancer (Yang et al., 2013). Moreover, histone modification is evidently involved in carcinogenesis. The modification of histone tails, such as methylation, acetylation and phosphorylation, affects the chromatin structure which is implicated in regulation of gene expression during development and tumorigenesis (Kondo, 2009).

As mentioned above, oxidative stress is increased in cancer conditions, and it is always coincided with DNA methylation alteration, suggesting that a cause-and-effect relationship may exist between these two phenomena. Our previous data clearly showed that ROS was a cause of global DNA hypomethylation (Wongpaiboonwattana et al., 2013). However, the mechanism of how ROS or oxidative stress modifies methylation reaction in DNA is not fully understood. Several mechanisms that drive global DNA hypomethylation under oxidative stress condition have been proposed, and the alteration of DNA methylation via the formation of oxidative DNA damage lesions at the DNA methylation sites (CpG dinucleotides) has been hypothesized (Q. Wu & Ni, 2015). Not only ROS-induced DNA methylation changes, oxidative stress is able to alter histone modification in cancer. It has been reported that histone methylation can be changed in response to oxidative DNA damage. Additionally, the histone modifying enzymes can be oxidized by ROS leading to changes of histone modification patterns resulting in the alteration of gene expression (Kreuz & Fischle, 2016).

Urothelial cancer or urinary bladder cancer is a tumor arising from transitional epithelial cells (also called transitional cell carcinoma) lined at the inner surface of urinary bladder. The well-known risk factors of urothelial cancer are smoking and

occupational exposure to carcinogens, for examples, industrial chemicals, arsenic and alkylating agents (Al Hussain & Akhtar, 2013). There are two main types of bladder cancer classified according to invasiveness of the tumor, superficial and muscle-invasive types. Majority of the cases (approximately 90%) are superficial bladder cancer, which is frequently recurred. The gold standard treatment for bladder cancer consists of transurethral resection of the bladder tumor (TUR-BT for superficial type) and radical cystectomy (for invasive tumor), followed by chemotherapy. The problem is that the rate of recurrence in patients after surgery is relatively high, especially in the patients with superficial type. Seventy percent of superficial cases display one or more recurrences within 5 years. Thus, the molecular mechanistic insight into urothelial carcinogenesis as well as its recurrence and progression needs to be explored to be clinically utilized in diagnosis, prognosis and therapy in the future (Al Hussain & Akhtar, 2013; Besaratinia et al., 2013).

The epigenetic alteration is well recognized in bladder cancer, especially global hypomethylation of DNA. Schulz and colleague firstly demonstrated in 1996 a state of hypomethylation of retrotransposon long interspersed nuclear element 1 (LINE-1 or L1) in bladder cancer (Jürgens et al., 1996). LINE-1 contributes to 17% of the human genome, therefore, it is widely used as a surrogate marker of global hypomethylation (Patchsung et al., 2012; Rodic & Burns, 2013). We previously showed that patients with bladder cancer had LINE-1 hypomethylation, and this LINE-1 hypomethylation was correlated with increased oxidative stress both in bladder cancer patients and normal subjects, suggesting a cause-and-effect relationship between oxidative stress and LINE-1 hypomethylation (Patchsung et al., 2012). In cell culture model, we previously demonstrated that LINE-1 hypomehtylation was induced by ROS (Wongpaiboonwattana et al., 2013). Recently, we further provided the mechanistic evidence that ROS-induced LINE-1 hypomethylation is mediated, at least in part, via depletion of methyl donor S-adenosylmethionine (SAM) (Kloypan et al., 2015). Likewise, histone modification changes have been found in bladder cancer patients. Studies in bladder cancer

tissue microarray revealed that global methylation and global acetylation of histone H3 were altered in bladder cancer tissues comparing to normal tissues (Ellinger et al., 2014; Ellinger et al., 2016; Schneider et al., 2011). This clearly indicated the alteration of histone modification in bladder cancer, but the mechanistic factor that interferes histone changes in bladder cancer has not been explored yet. Therefore, apart from the depletion of SAM, we hypothesized that ROS induced oxidative DNA lesion formation, particularly 8-hydroxydeoxyguanosine (8-OHdG) at CpG dinucleotides, to further interfere DNA methylation and histone modification, and consequently causes LINE-1 hypomethylation and aberrant expression of LINE-1 elements. We also think that the epigenetic changes following oxidative stress would contribute to the progression of bladder cancer.

In this study, we aimed to histologically investigate expression of 5-methylated cytosine (5mC), 8-OHdG, LINE-1-endoced protein (ORF1p), H3K9me3 and HP1$\alpha$ bladder cancer tissues. Also, we explored the epigenetic changes in terms of DNA methylation and histone modification in LINE-1 elements in bladder cancer cells under oxidative stress condition. Whether the formation of oxidative DNA damage (8-OHdG) was associated with global DNA hypomethylation and histone modification changes in bladder cancer were evaluated in both human tissues and cell culture model. Additionally, we asked if ROS-induced LINE-1 expression promoted the progression of bladder cancer.

**Keywords**

Bladder cancer, Epigenetics, Global DNA hypomethylation, Histone modifications, Oxidative stress, ROS, 8-OHdG, LINE-1, Cancer progression

**Research questions**

1. Do global DNA hypomethylation, increased oxidative DNA damage and altered histone modification occur in human bladder cancer tissues?

2. Does the ROS-induced 8-OHdG formation inhibit DNA methylation on LINE-1 promoter in bladder cancer cell lines?

3. Does ROS alter histone modification patterns on LINE-1 element in bladder cancer cell lines?

4. Does ROS-induced epigenetic alteration cause the increased expression of LINE-1 protein?

5. Whether ROS was capable of increasing tumor aggressiveness in bladder cancer cells?

## Objectives

1. To investigate the expression of 5-mC(DNA methylation indicator), 8-OHdG (oxidative DNA lesion), ORF1p, histone H3K9me3 (inactive chromatin or heterochromatin mark), and HP1$\alpha$ in bladder cancer tissues compared to the nearby non-cancerous bladder tissues

2. To evaluate the correlation among expressions of 5-mC, 8-OHdG, ORF1p, H3K9me3 and HP1$\alpha$ in bladder cancer tissues

3. To investigate the effect of ROS on global DNA hypomethylation, 8-OHdG formation in bladder cancer cell lines

4. To investigate the effect of ROS on histone modification changes on LINE-1 element in bladder cancer cell lines

5. To investigate the role of ROS-induced epigenetic alteration on LINE-1 protein (ORF1p) expression

6. To investigate the role of ROS on migration and invasion capability in bladder cancer cells

## Hypothesis

8-OHdG that was excessively produced in bladder cancer cells under oxidative stress condition inhibited DNA methylation at CpG sites in 5'-UTR promoter of LINE-1 elements leading to LINE-1 hypomethylation and increased LINE-1 expression. In addition, ROS altered cellular histone modification patterns, and

favored formation of active chromatin on LINE-1 elements allowing derepression of LINE-1 proteins. Taken together, we think that the ROS-induced epigenetic changes could enhance expression of LINE-1 elements and aggressive capability of the bladder cancer cells.

**Ethical consideration**

A part of this research was conducted in human bladder cancer tissues. However, the research protocol was reviewed and approved by the Institutional Review Board, Faculty of Medicine, Chulalongkorn University and the Institutional Ethics Committees, Buriram Hospital.

**Benefits and applications**

1. The expression levels of 5-mC, 8-OHdG, ORF1p, H3K9me3 and HP1$\alpha$ compared between bladder tumor tissues and adjacent non-cancerous tissues obtained from Thai bladder cancer patient.

2. The mechanistic insight into how ROS and oxidative DNA damage formation contribute to LINE-1 hypomethylation and altered histone modification in order to promote progressive activity of bladder cancer cells was obtained.

3. Reduction of LINE-1 expression through epigenetic regulators and attenuation of oxidative stress by natural antioxidants could be promising therapeutic means for bladder cancer in the future.

# Chapter 2

# Literature review

**Oxidative stress: ROS generation, antioxidant systems and oxidative damage**

Oxidative stress is defined as an imbalance between the generation of oxidants and the elimination systems by antioxidants leading to cellular injury as a result of the attack of reactive species to cellular biomolecules. Reactive species that contain unpaired electrons are known as free radicals which are highly active molecules. Reactive oxygen species (ROS) is the most abundant reactive species in the cells, and it is an unavoidable by-product of biochemical processes, for example aerobic metabolism, inflammation, UV radiation, which continuously generated from oxygen molecules used in the reaction (Betteridge, 2000; Franco et al., 2008).

Major ROS includes superoxide anion ($O_2^{\cdot-}$), hydrogen peroxide ($H_2O_2$) and hydroxyl radicals ($HO^{\cdot}$) (Reuter et al., 2010). In cells, superoxide anion ($O_2^{\cdot-}$) is produced mainly in mitochondria (in electron transport chain) or by NADPH oxidases enzymes (NOXs) (Figure 1). Superoxide anion is further converted to hydrogen peroxide ($H_2O_2$) by superoxide dismutase enzymes (SODs). $H_2O_2$ can be detoxified to $H_2O$ by catalase or glutathione (GSH). In contrast, $H_2O_2$ can be converted to hydroxyl radical ($HO^{\cdot}$) which is the most potent oxidant and capable of attacking cellular macromolecules to cause oxidative damage, consequently resulting in cellular injury and eventually cell death (Schieber & Chandel, 2014). Chemical reactions of cellular ROS generation and generation of hydroxyl radical by Fenton reaction is shown in Figure 2.
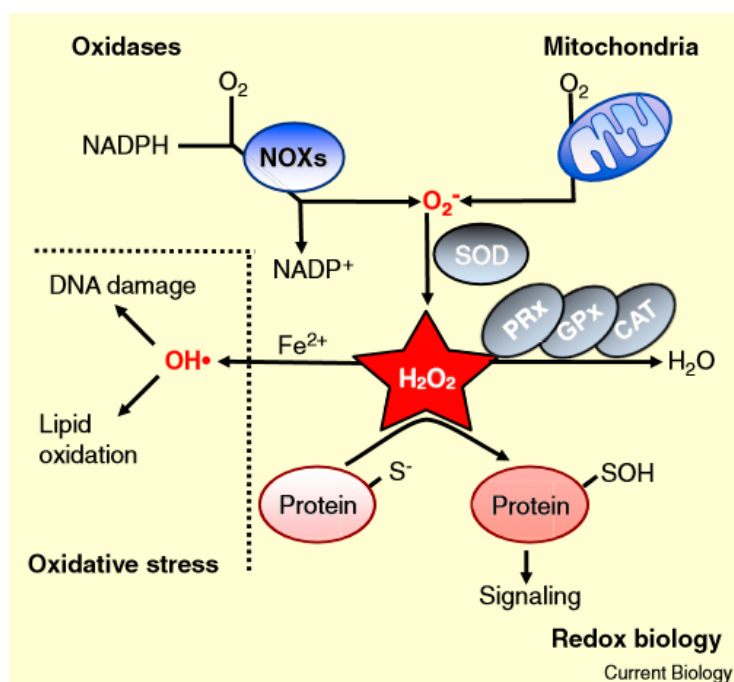
**Figure 1** Basics of Reactive oxygen species including superoxide anion ($O_2^{\cdot-}$), hydrogen peroxide ($H_2O_2$) and hydroxyl radicals ($HO^{\cdot}$) (Schieber & Chandel, 2014)

(For education only)

**Generation of ROS via reduction of molecular oxygen**

$O_2 + e^- \rightarrow O_2^{\cdot-}$ (superoxide anion)

$O_2^{\cdot-} + H_2O \rightarrow HO_2^{\cdot}$ (hydroperoxyl radical)

$HO_2^{\cdot} + e^- + H \rightarrow H_2O_2$ (hydrogen peroxide)

$H_2O_2 + e^- \rightarrow OH^- + OH^{\cdot}$ (hydroxyl radical)

**Fenton reaction**

$$H_2O_2 + Fe^{2+} \rightarrow OH^- + OH^{\cdot} + Fe^{3+}$$
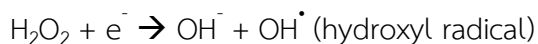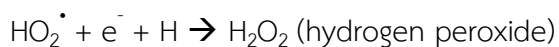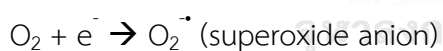
**Figure 2** Intercellular oxidant (ROS) generation (Klaunig et al., 2010)

(For education only)

To moderate the harmful effect of ROS, the antioxidant defense mechanisms have been evolved to protect the organism from ROS attack by scavenging or inhibiting the oxidation of free radicals. The antioxidant systems have been divided

into enzymatic antioxidants, for example SOD, glutathione peroxidase (GPx), glutathione reductase and catalase, and non-enzymatic antioxidants, such as glutathione, thioredoxin, vitamin C and vitamin E (Oberley, 2002; Reuter et al., 2010).
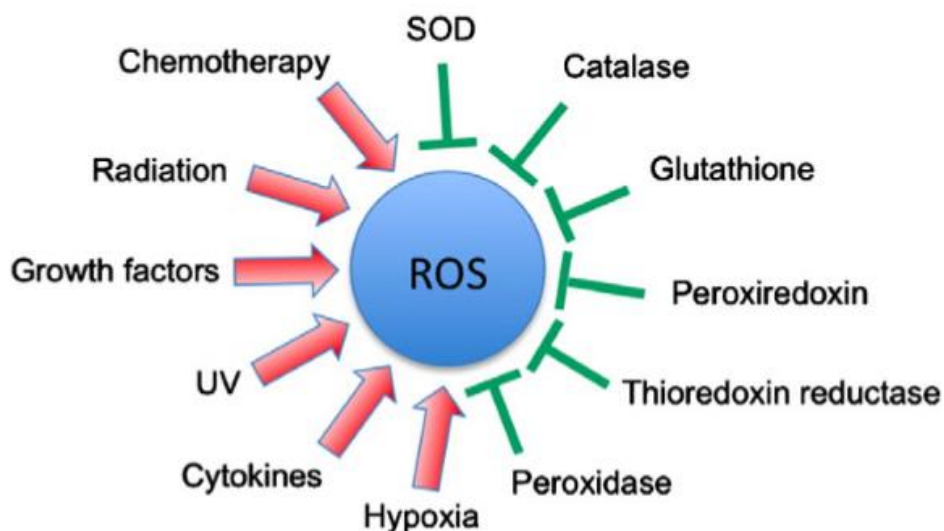


**Figure 3** Activators (arrows) and inhibitors of reactive oxygen species (ROS) production (Reuter et al., 2010) (For education only)

However, under long-term defect of antioxidant systems, oxidative stress is occurred leading to cell injury. Since ROS are highly reactive and unstable, they can react with other macromolecules to be more stable by which lipids, proteins and DNA are the most possible oxidative targets. ROS is able to oxidize lipid on cell membrane provoking lipid peroxidation and also oxidize amino acid residues and nucleic acid causing protein and DNA damage, respectively. Therefore, oxidative damage, consisting of lipid peroxidation, protein oxidation and DNA oxidation, together with the depletion of antioxidants can be measured by biochemical assays for the assessment of oxidative stress (Betteridge, 2000; Oberley, 2002). The oxidatively modified products of lipids, proteins and DNA that are widely used as oxidative damage markers include malondialdehyde (MDA), 4-hydroxynonenal (4-HNE), protein carbonyl and 8-OHdG.

**The implication of ROS in carcinogenesis via oxidative DNA damage**

Due to an oxidative stress condition under chronic inflammation, ROS are chronically and persistently produced and ultimately damage cell structure and function. ROS have been involved in pathogenesis of various diseases, for examples, Alzheimer, cardiovascular disease, diabetes and, especially, cancers (Reuter et al., 2010). Since oxidative DNA damage is critically linked to DNA mutation, ROS have been implicated in multistep carcinogenesis including initiation in which the accumulation of DNA mutation takes place, promotion and progression by which the initiated mutated cells are highly proliferated or resistant to apoptosis (Figure 4) (Klaunig et al., 2010).
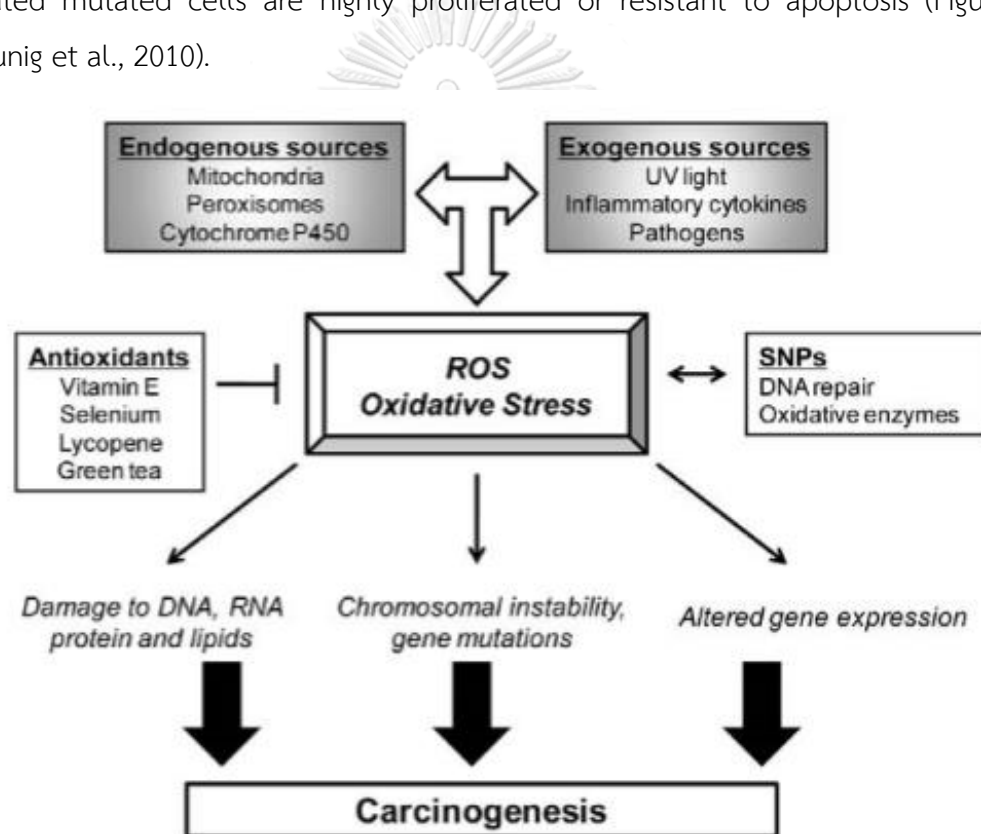
**Figure 4** Roles of ROS in the development of human cancers (Klaunig et al., 2010) (For education only)

Oxidative DNA damage is produced from the interaction between hydroxyl radicals (OH$^{\bullet}$) and nucleotide bases on DNA strands, especially guanine, leading to the formation of 8-hydroxy-2'-deoxyguanosine (8-OHdG) or its keto-enol tautomerism form, 8-oxo-7,8-dihydro-2'-deoxyguanosine (8-oxo-dG) (Figure 5). The 8-OHdG and 8-

oxo-dG are defined as the same compound in the scientific literature (Valavanidis et al., 2009; L. L. Wu et al., 2004).
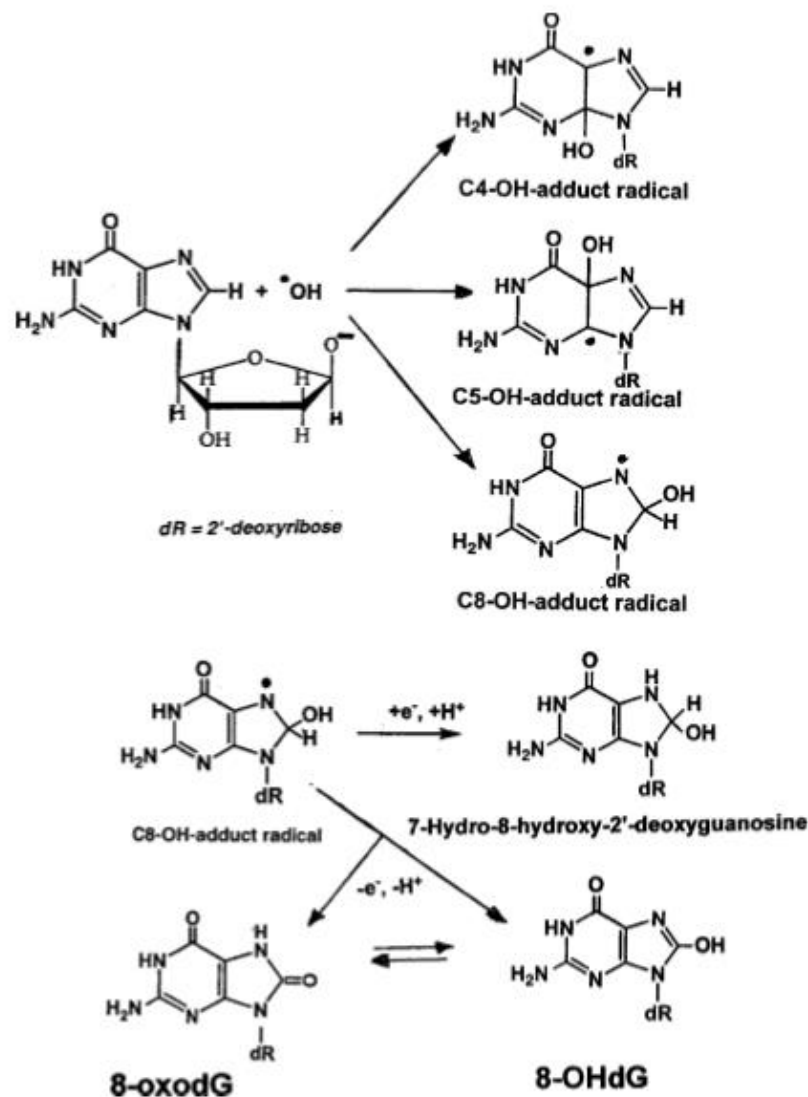


**Figure 5** The formation of 8-OHdG and its tautomerism 8-oxodG by ROS
(Valavanidis et al., 2009) (For education only)

8-OHdG, the most abundant oxidative DNA lesion throughout the genome, is easily formed and potentiates mutagenesis (Valavanidis et al., 2009). To maintain the integrity of DNA, base excision repair (BER) is used to remove and to fix the oxidative base lesion (Figure 6). The 8-oxoguanine DNA glycosylase or OGG1 is a key enzyme in base excision repair that recognizes 8-OHdG lesions and removes these abnormal guanine bases followed by the incorporation of DNA polymerase to eventually

restore the normal G•C base pair. Contrarily, the failure of 8-OHdG repair before replication results in DNA mispairing by which adenine base (A) will be added by DNA polymerase instead of cytosine (C) and causes GC→TA transversion mutation (David et al., 2007). In mouse model, the genomic DNA extracted from repair protein-deficient mice showed high rate of GC→TA transversion mutation (David et al., 2007). Moreover, cells with defect of base excision repairing process by OGG1 predispose to DNA single-strand break leading to increase in genomic instability (Campalans et al., 2015).
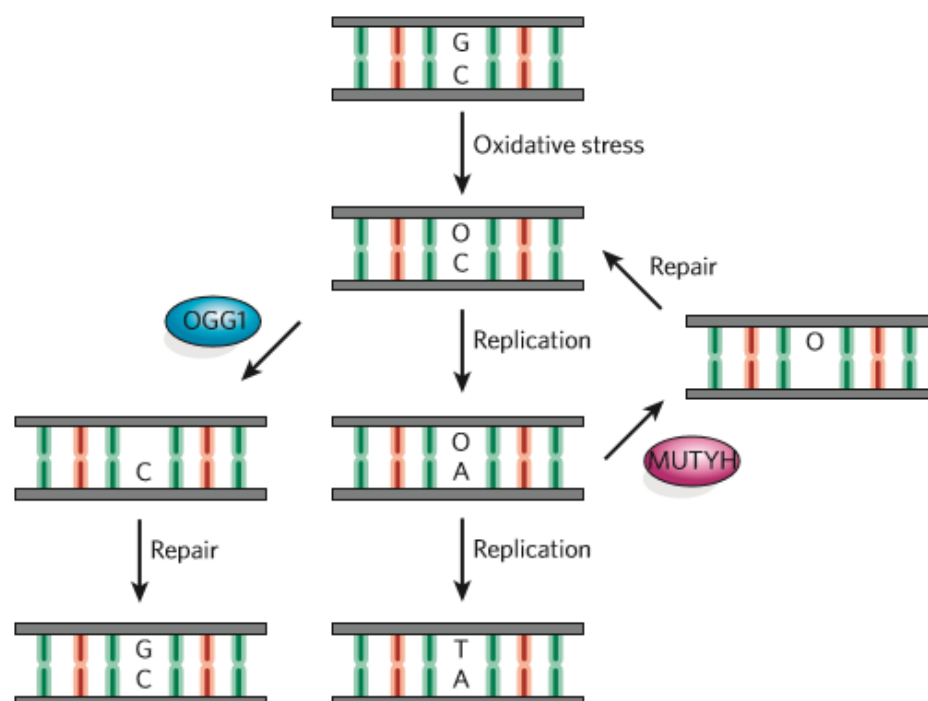


**Figure 6** Base excision repair (BER) of oxidative DNA damage by OGG1

(David et al., 2007) (For education only)

The formation of 8-OHdG is extensively used as an oxidative stress marker in cancers (L. L. Wu et al., 2004). Comparing to normal tissues, the expression of 8-OHdG is increased in cancerous tissues and its level of expression is associated with the progression of many cancers, such as breast cancer (Sova et al., 2010), gastric carcinoma (Borrego et al., 2013) and ovarian carcinoma (Xu et al., 2013). There have been several studies reported that loss of OGG1 activity leads to accumulation of 8-OHdG (Borrego et al., 2013; Habib et al., 2010; Xu et al., 2013). Moreover, OGG1

polymorphism is found to be associated with increased risk of cancer (Ali et al., 2015; Q. Li et al., 2013). These indicated that OGG1, a key enzyme in base excision repair, plays a role as defender to protect cells from oxidative damage and prevent the genomic instability (Campalans et al., 2015; Ruchko et al., 2011).

**Epigenetics and its alteration in cancer**

The term of epigenetics is initially established by Conrad Waddington in 1942 to define the study of heritable and reversible changes in gene expression without changes in primary DNA sequence to control gene expression that occurs during cell cycle, differentiation, development and either in response to environmental stimuli (Toraño et al., 2012). The mechanism of epigenetics is arisen through the incorporation of chemical modifications comprising of DNA methylation, histone modification, and microRNAs regulation. The alteration of epigenetics resulting in the aberrant gene expression and cellular signalling pathway is considered as one of the hallmarks of cancers, and it is evidently experimentally proved to play a vital role in the carcinogenesis (Sharma et al., 2010).

DNA methylation is the most widely studied epigenetic mechanism in cancers, and it is well known that change in DNA methylation plays an important role in the regulation of gene expression and chromatin architecture in cancers (Sharma et al., 2010). In the DNA methylation reaction, a methyl group ($CH_3$) from S-adenosylmethionine (SAM), a methyl donor, will be added to the 5'-carbon atom of cytosine base to form 5-mC and this consequently leads to gene silencing. The specific site for DNA methylation is CpG dinucleotides, which is commonly found in the gene promoters, so called CpG islands. DNA methylation is carried out by DNA methyltransferases (DNMTs), a methyltransferase family consisting of DNMT1, DNMT3A and DNMT3B. The main function of DNMT1 is to maintain the methylation pattern during DNA replication, whereas DNMT3A and DNMT3B play a role in *de novo* methylation mechanism (Toraño et al., 2012).

Changes in DNA methylation are documented in cancers, and at least 2 types of the alterations are classified, including CpG island promoter hypermethylation and global hypomethylation (Toraño et al., 2012). In cancers, CpG islands in promoter

regions of genes, particularly tumor suppressor genes and DNA repair gene, are found to be hypermethylated leading to gene inactivation. Remarkably, the overall level of DNA methylation in tumors is decreased compared with the adjacent-normal tissues, so called global DNA hypomethylation or genome-wide DNA hypomethylation (Esteller, 2008). It has been demonstrated in several cancers, for examples, breast cancer (Hon et al., 2012), colon cancer (Hernandez-Blazquez et al., 2000) and prostate cancer (Yang et al., 2013).

Global DNA hypomethylation has been implicated in the carcinogenic process because it can cause reactivation of transposable elements, potentially, leading to chromosomal instability and mutagenesis (Esteller, 2008). It has been suggested that global DNA hypomethylation may be caused by various putative etliological factors such as altered chromatin structure and changes in DNA methyltransferase activity (Figure 7), and the hypomethylated regions are usually occurred in the transposable elements, for instance, long interspersed nuclear element 1 (LINE-1) (Wilson et al., 2007).
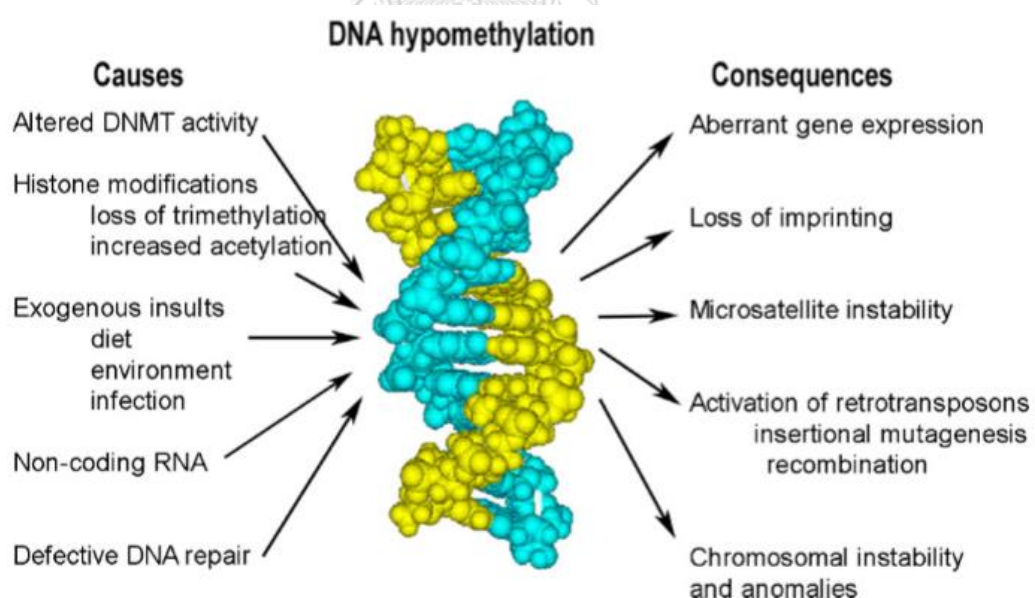


**Figure 7** Potential causes and consequences of global DNA hypomethylation
(Wilson et al., 2007) (For education only)

Apart from DNA methylation, gene expression can be regulated through histone modifications as well. Basically, genomic DNA is packed into condensed structure called chromatin by which 147 bp DNA is wrapping around histone protein complex including histone H2A, H2B, H3 and H4. Histone modifications are post-translational modifications to either N-terminus or C-terminus of histone tails. The chemical modifications, such as methylation, acetylation, phosphorylation and ubiquitylation, are processed on certain amino acid residues on histone tails (as shown in figure 8) affecting the chromatin structures which divided into heterochromatin, a condensed and transcriptionally repressive form, and euchromatin, a relaxed and transcriptionally active form (Kondo, 2009; Sawan & Herceg, 2010).
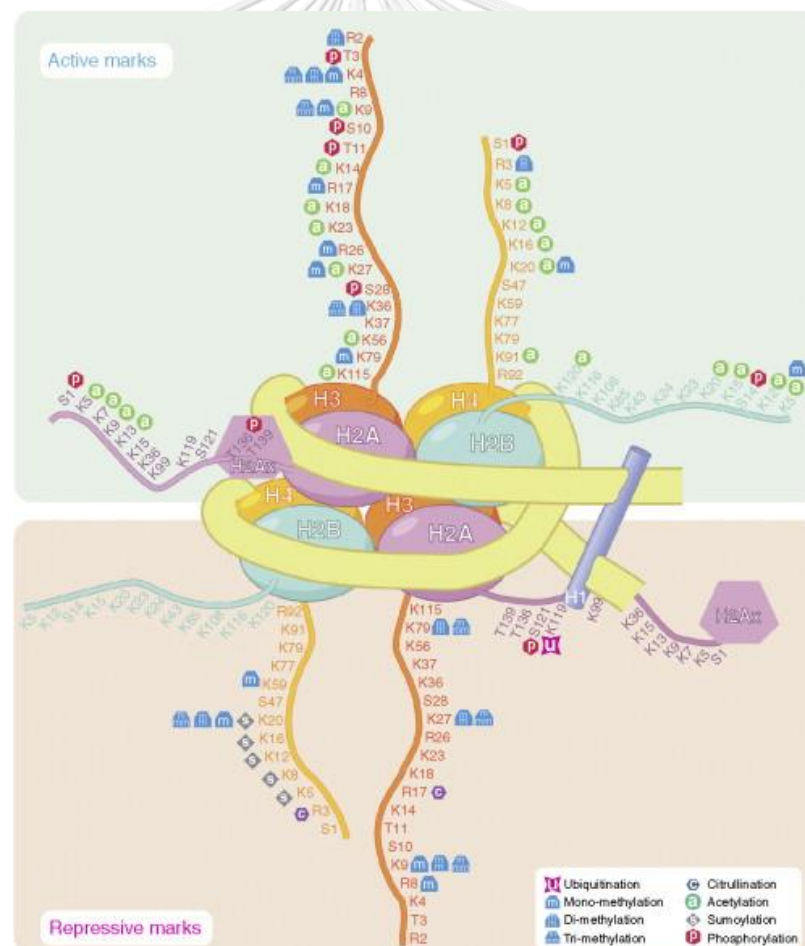
**Figure 8** Histone modifications on histone octamers. The chemical modifications are processed on histone tails leading to gene activation and gene repression (Sawan & Herceg, 2010) (For education only)

The histone modifications are mediated by histone modifying enzymes functioning as writer or eraser, for instance histone methyltransferases (HMTs) and histone acetylases (HACs) as writers, whereas histone demethylases (HDMs) and histone deacetylases (HDACs) as erasers. Some amino acid residues, such as lysine, arginine, are subject for these chemical modifications resulting in chromatin organization. Lysine, as an example in figure 9, can be tri-methylated by SUV39H1 (HMT) at lysine 9 on histone H3 (H3K9me3) or by EZH2 (HMT) at lysine 27 on histone H3 (H3K27me3) leading to heterochromatin formation and transcriptional repression. In contrast, histone H3 can be tri-methylated by MLL (HMT) at lysine 4 (H3K4me3) or acetylated by p300 (HAC) at lysine 18 (H3K18Ac) resulting in euchromatin formation and transcriptional activation. However, the dynamic chromatin structure through histone modification is advantage for gene function in many cellular processes such as development, transcription, DNA replication and DNA repair (Bannister & Kouzarides, 2011; Sawan & Herceg, 2010).
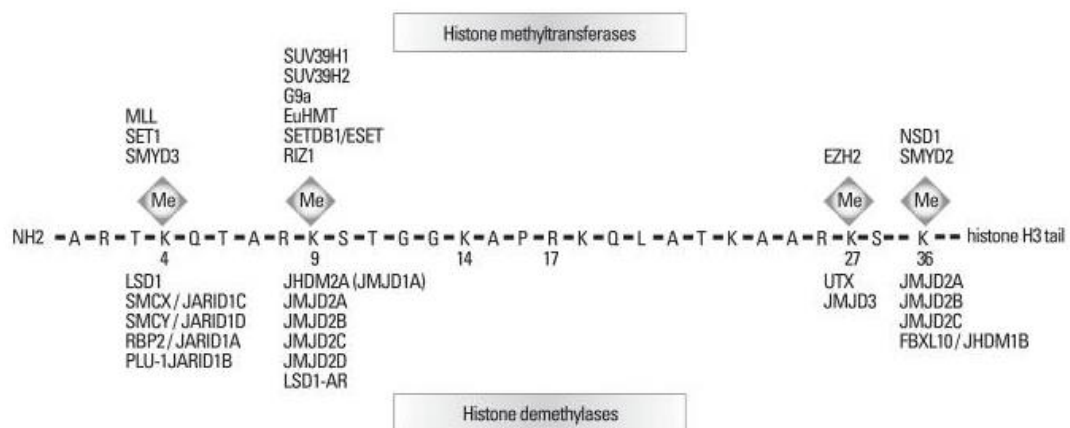


**Figure 9** Histone methylation by histone modifying enzymes.

Histone H3 can be methylated or demethylated at some amino acid residues by HMTs or HDMs enzymes (Kondo, 2009) (For education only).

Similar to DNA methylation, the deregulation of histone modifications, either by the aberrant histone modification patterns or the dysregulated activity of histone modifying enzymes, leading to the alteration of cellular processes is associated with carcinogenesis (Bannister & Kouzarides, 2011; Sawan & Herceg, 2010). There have been many studies reported about the aberrant pattern of histone modifications.

EZH2 has been found elevated in cancer, for example in breast cancer (Holm et al., 2012) and global level of histone H3K27me3 was altered and associated with cancer progression in breast and prostate cancer (Holm et al., 2012; Ngollo et al., 2017). The increased level of histone H3K9me3 was associated with colon cancer progression. Moreover, *in vitro* study revealed that SUV39H1 overexpression increased tumour formation in colon cancer cell line and H3K9me3 was associated with increased cell migration in breast cancer cell line (Yokoyama et al., 2013). Regarding histone acetylation, the increased H3K12Ac and elevated HDAC2 expression were correlated with the progression of colon cancer (Ashktorab, 2009). HDAC expression was found highly expressed in renal cell carcinoma (Fritzsche et al., 2008) and, moreover, histone H4Ac, H3Ac and H3K18Ac were notably high in renal cell carcinoma (Mosashvilli et al., 2010). These strongly indicated the aberrant histone modification in various cancers. However, since DNA methylation and histone modifications are chemically reversible, epigenetics could be a potential targets for cancer therapy (Ahuja et al., 2016; Mair et al., 2014).

**Long interspersed nuclear element 1 (LINE-1)**

Transposable elements are repetitive DNA sequences that are able to integrate themselves into the genome at different region and are classified into DNA transposons and retrotransposons. DNA transposons integrate into genome at the other site by cut and paste mechanism, whereas the insertion process of retrotransposons is mediated through copy and paste mechanism (Han & Boeke, 2005; Wilson et al., 2007).

Long interspersed nuclear elements or LINEs are subfamily of retrotransposons which are divided into LINE-1 (or L1) and LINE-2 (or L2). LINE-1, the major retrotransposon, contains approximately 17% distribution entire the human genome (Figure 10) (Rodic & Burns, 2013). LINE-1 contains two open reading frames: ORF1 and ORF2 (Figure 11) (Han & Boeke, 2005). The copy and paste mechanism of LINE-1 is initiated from transcription of genomic LINE-1 by RNA polymerase II. LINE-1 RNA is translated into two encoded proteins: ORF1p which is an RNA-binding protein, and ORF2p which functions as a reverse transcriptase and endonuclease.

Subsequently, these proteins and LINE-1 RNA are formed as ribonucleoprotein (RNP) complex and transferred into nucleus. Finally at target-primed reverse transcription (TPRT) step, endonuclease activity of ORF2p cleaves the target region and inserts newly synthesized strand from reverse transcription reaction resulting in the integration of LINE-1 into the new site of genomic DNA (Figure 12) (Han & Boeke, 2005; Rodic & Burns, 2013).
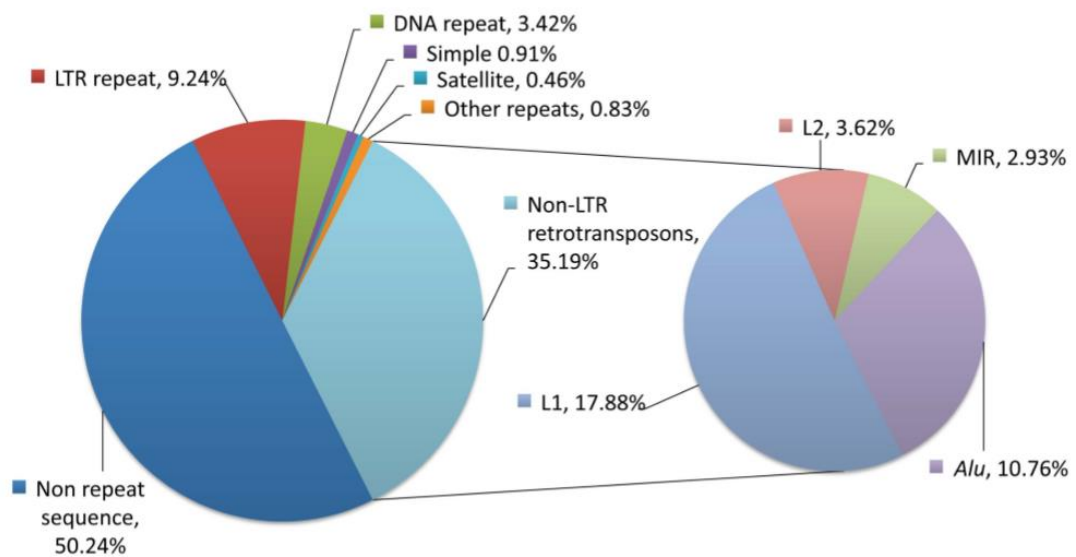


**Figure 10** Repetitive sequences in human genome (Rodic & Burns, 2013)

(For education only)



**Figure 11** Structure of LINE-1 containing two ORFs (Han & Boeke, 2005)

(For education only)
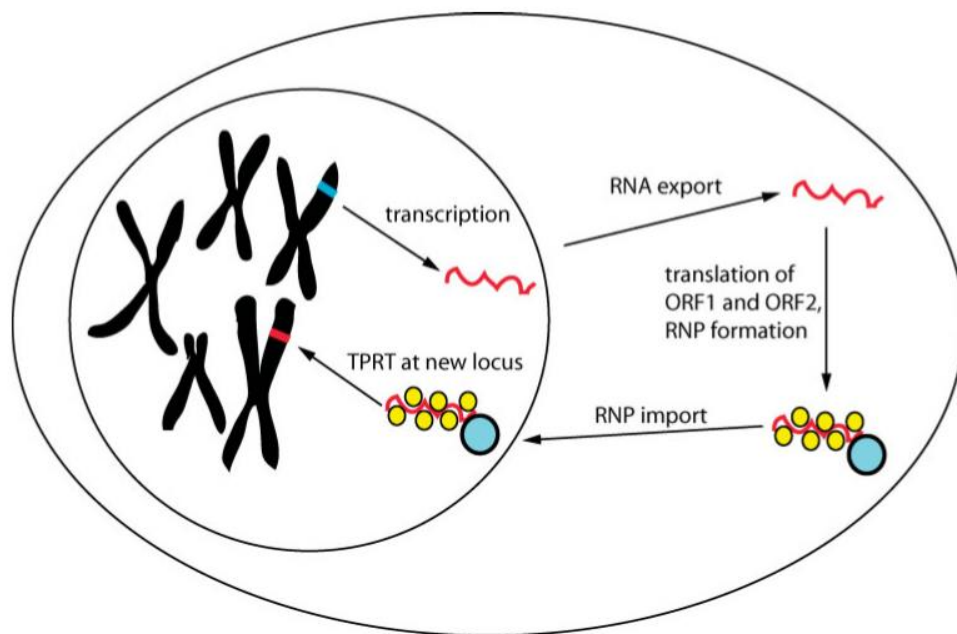
**Figure 12** LINE-1 machinery containing transcription, translation and TPRT steps
(Han & Boeke, 2005) (For education only)

Since insertion of LINE-1 may cause genomic instability, the expression of LINE-1 is repressed in normal germline and somatic cells by DNA methylation at LINE-1 promoter as a host defense mechanism (Figure 13) (Rodic & Burns, 2013). On the other hand, many studies report that methylation level at LINE-1 promoter in cancer is decreased compared with the normal counterpart (Chalitchagorn et al., 2004; Hernandez-Blazquez et al., 2000; Kitkumthorn & Mutirangura, 2011). This indicates that LINE-1 hypomethylation is obviously involved in the carcinogenesis, possibly due to the consequence of LINE-1 reactivation that causes disturbed gene expression and genomic instability (Rodic & Burns, 2013; Yang et al., 2013).
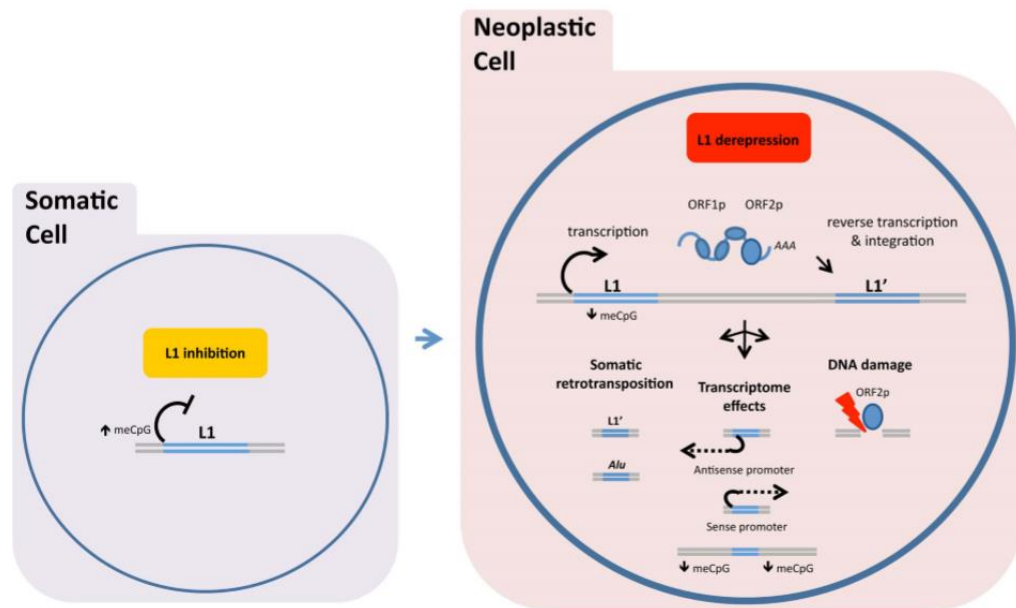
**Figure 13** Inhibition of LINE-1 by DNA methylation in somatic cell and reactivation of LINE-1 transposition by DNA hypomethylation in neoplastic cell (Rodic & Burns, 2013) (For education only)

Moreover, the moderation of LINE-1 expression via histone modifications has been investigated *in vitro*. In embryonic carcinoma cell, histone deacetylase enzyme was required for LINE-1 silencing at the integration site (Garcia-Perez et al., 2010). In addition to DNA methylation, histone demethylase G9a coupled with histone H3K9me2 were essential for the repression of LINE-1 elements in germ line (Giacomo et al., 2014). Furthermore, LINE-1 silencing pathway in embryonic stem cells was controlled by histone H3K9me3 and H3K27me3 at the promoter region. Contrarily, regarding the high expression of LINE-1, the 5'UTR was found enriched in histone H3K4me3 (Walter et al., 2016). Therefore, these indicated that LINE-1 expression is obviously regulated by histone methylation and histone acetylation as well.

**The involvement of oxidative stress in epigenetic alterations: global DNA hypomethylation and changes in histone modification**

Oxidative stress can conduce to carcinogenesis not only by mutagenesis and disturbance in signalling pathway, but also through epigenetic alteration (Franco et al., 2008). Oxidative stress can affect the DNA methylation pattern through the formation of DNA damage. Oxidative DNA damage lesion or 8-OHdG, that is formed especially adjacent to cytosine at CpG dinucleotides, can inhibit activity of DNMTs resulting in global hypomethylation (Weitzman et al., 1994). Moreover, from the base excision repair, 8-OHdG formations on DNA strand are removed by OGG1 followed by APEX1 enzyme which possibly removes the adjacent 5-mC base. Therefore, 8-OHdG formation in accompany with base excision repair may cause global hypomethylation. In addition, 5mC base can be transformed to 5-hydroxymethyl C (5-hmC) which takes part in demethylation processes leading to global hypomethylation. (Figure 14) (Q. Wu & Ni, 2015).
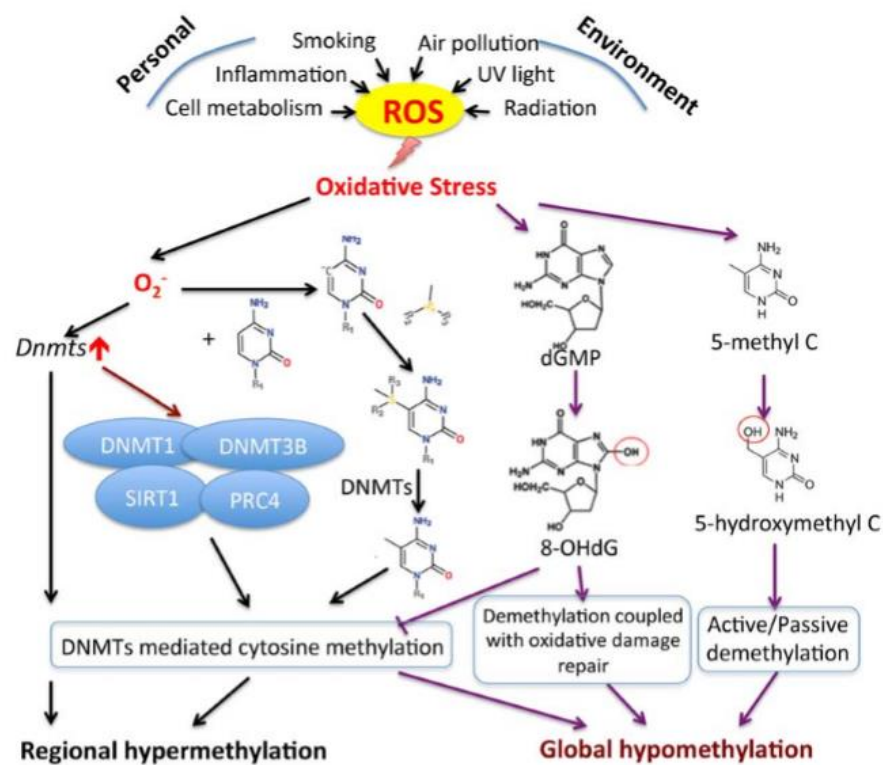


**Figure 14** The aberrant of DNA methylation pattern in consequence of oxidative stress (Q. Wu & Ni, 2015) (For education only)

Moreover, oxidative stress can influence chromatin remodeling through many aspects, by directly altering the chromatin structure or affecting the activity of histone modifying enzymes (Kreuz & Fischle, 2016). Long-term $H_2O_2$ exposure in human kidney cells (HK-2) led to significant increases of HDAC1 and HMT1 expressions but significantly decreased HAT1 expression. The aberrant expression of these histone modifying enzymes was associated with increased level of histone acetylation (H3K14Ac and H3K9Ac) and increased level of histone methylation (H3K27me3 and H3K4me3) (Mahalingaiah et al., 2017). Study demonstrated in human bronchial epithelial cells (BEAS-2B) showed that JmjC-domain-containing histone demethylase activity was inhibited by oxidative stress leading to increased histone methylation level (H3K4me3, H3K9me3 and H3K27me3) (Niu et al., 2015). $H_2O_2$ and cigarette smoke condensate (CSC) exposure on alveolar epithelial cells (A549) increased histone acetylation on histone H4 by triggering HAT activity and interfering HDAC activity (Moodie et al., 2004). In hepatocellular carcinomas, the accumulation of oxidative DNA damage, 8-OHdG, was associated with increased level of histone H3K27me3 and decreased level of histone H3K4me3 and H3K16Ac leading to inactivation of tumor suppressor genes (Nishida et al., 2013). Evidently, oxidative stress is implicated in global DNA hypomethylation and histone modification changes in cancers.

**Oxidative stress and global DNA hypomethylation in urothelial carcinoma**

Urothelial carcinoma or urinary bladder cancer is the fifth common cancer worldwide, usually found in patients aged between 50 and 70 years old. The global age standardized incident rate (ASR) is 10.1 and 2.5 cases per 100,000 in males and females respectively, whereas ASR of Thai bladder cancer patients is 4.6 cases in males and 1.0 case in females per 100,000 (Jantip et al., 2013; Kandimalla et al., 2013). Because urinary bladder cancer is arisen from transitional epithelium, 90% of bladder cancer cases are transitional carcinoma (TCC) or non-muscle invasive tumors (including non-invasive carcinoma (Tis) or flat carcinoma in situ (CIS), non-invasive papillary carcinoma (Ta) and T1 stages), of which approximately 70% of TCC patients

have one or more recurrence within 5 years after transurethral resection. Moreover, more than 15% of the patients will progress into invasive tumors (including T2, T3 and T4 stages) and metastasis and ultimately lead to mortality (Figure 15) (Al Hussain & Akhtar, 2013; Besaratinia et al., 2013).
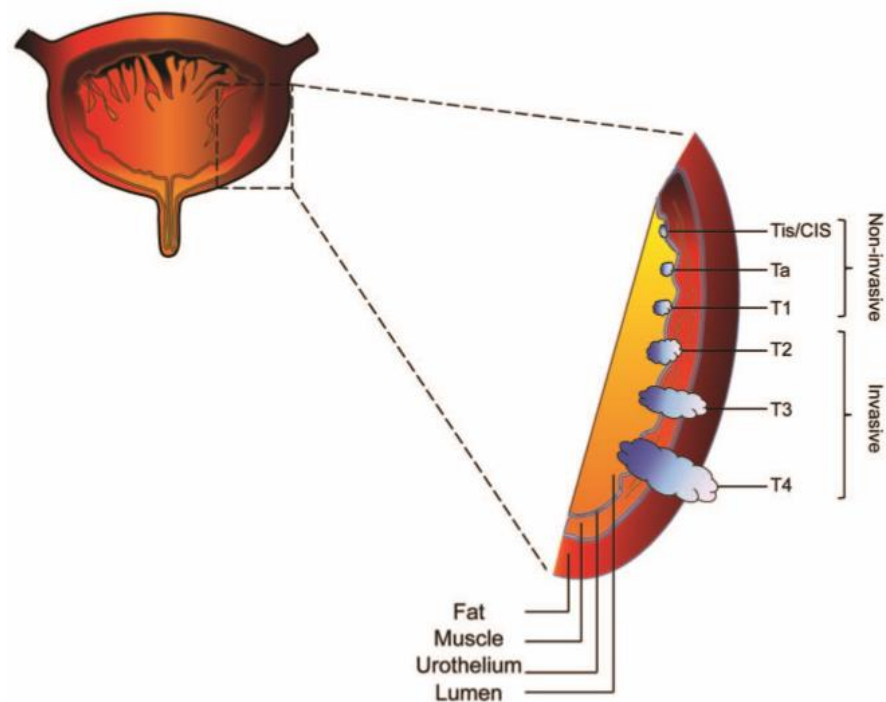


**Figure 15** Stages of transitional cell carcinoma of urinary bladder including non-invasive and invasive types (Besaratinia et al., 2013) (For education only)

The risk factors of bladder cancer have been identified. The most important factor is tobacco which approximately 50% of all cases are smokers. Moreover, the risk is increased in patients who long-term expose to other causative agents for 30-50 years, such as industrial chemicals, arsenic and aromatic amines that are excreted through urine and subsequently induce chronic inflammation on transitional epithelium of bladder. As a consequence of chronic inflammation, reactive oxygen species can be generated by neutrophils, monocytes and macrophages leading to oxidative damage and eventually bladder cancer development (as shown in figure 16) (Al Hussain & Akhtar, 2013; Choudhury et al., 2008; Michaud, 2007).

Model for role of inflammation in bladder carcinogenesis

**Figure 16** The role of chronic inflammation in bladder carcinogenesis (Michaud, 2007)

(For education only)

The oxidative stress, defined as condition with increased ROS production and decreased antioxidants, has been reported in bladder cancer patients compared with the healthy controls (Badjatia et al., 2010; Gecit et al., 2012; Hempel et al., 2009; Opanuraks et al., 2010; Patchsung et al., 2012; Salim et al., 2008). Likewise, DNA damage indicated by comet assay together with 8-OHdG level in the patients is higher than the healthy controls (Akçay et al., 2003; Opanuraks et al., 2010; Romanenko et al., 2002; Salim et al., 2008; Schabath et al., 2003). Moreover, OGG1 exhibits the higher activity after exposure to oxidative milieu (Romanenko et al., 2002) and OGG1 mutation contributes to the increased risk of bladder cancer (X. Wu et al., 2006). These findings indicated that ROS-induced DNA damage and OGG1 function are critically involved in the development of bladder cancer. However, whether how ROS-induced oxidative DNA lesion is mechanistically linked to the

global DNA hypomethylation in order to enhance the bladder cancer genesis and progression is not known.

Apart from genetic mutations consisting of FGFR3 mutation in low-grade tumors and p53 mutation in muscle invasive bladder cancer (Al Hussain & Akhtar, 2013), epigenetic alterations have been explored in bladder cancer as well. It is well recognized that global DNA hypomethylation is strongly associated with bladder cancer development. The measurement of 5-mC level in leukocyte DNA of patients with bladder cancer and controls revealed that blood DNA hypomethylation was associated with increased risk of bladder cancer (Moore et al., 2008). Immunohistochemical staining of 5-mC exhibited that low level of 5-mC was more pronounced in invasive urothelial cancer (Chung et al., 2015).

LINE-1 hypomethylation was firstly demonstrated in bladder cancer by Schulz and colleagues (Jürgens et al., 1996) and it was associated with increased bladder cancer risk. The level of LINE-1 promoter methylation was changed in bladder cancer tissues by which LINE-1 promoter was highly methylated in normal bladder tissues but hypomethylated in tumors. Moreover, the decreased methylation of LINE-1 promoter led to elevated expression of LINE-1 transcripts in bladder cancer (Florl et al., 1999; Kreimer et al., 2013). Therefore, in addition to the expression of 5-mC, LINE-1 methylation level can be utilized as a marker for global DNA hypothylation to the assess risk for bladder cancer onset (Cash et al., 2012; Phokaew et al., 2008; Wilhelm et al., 2010).

The association between LINE-1 hypomethylation and oxidative stress has been explored. The study by Patchsung and colleagues showed that LINE-1 hypomethylation in Thai bladder cancer patients was increased compared with the healthy controls and it was correlated with increased oxidative stress (Patchsung et al., 2012). Furthermore, Wongpaiboonwattana and colleagues experimentally proved that ROS was a cause of LINE-1 hypomethylation bladder cancer cell lines (Wongpaiboonwattana et al., 2013). Mechanistically, Kloypan et al. demonstrated that ROS induced oxidative stress that led to SAM depletion and further caused hypomethylation of LINE-1 (Kloypan et al., 2015). However, we think that ROS-induced LINE-1 hypomethylation in bladder cancer cells may not be solely mediated

via SAM depletion. ROS-induced 8-OHdG formation at LINE-1 CpG dinucleotides may also act in concert to stimulate LINE-1 hypomethylation under oxidative stress condition.

**The alteration of histone modifications in bladder cancer**

Bladder carcinogenesis is strongly associated with the accumulation of genetic mutations. Comparing with other cancers, bladder cancer showed higher frequency of the mutation in histone modifying genes (H.-T. Li et al., 2016; Schulz & Goering, 2016). The comprehensive molecular studies in bladder cancer revealed that 76% of bladder tumors contained at least one mutation of histone modifying gene whereas 41% showed at least two mutations of these regulators. The inactive mutation of histone modifying genes were reported, for example 15% of tumours showed mutation in *EP300* gene (histone acetyltransferase), 27% had mutation of *MLL3* gene (histone methyltransferase) and 24% had mutation of *KDM6A* gene (histone demethylase) (The Cancer Genome Atlas Research, 2014). Comparing between bladder cancer staging, it had been found that *MLL2* mutation was more frequent in muscle invasive bladder cancer but *KDM6A* showed higher rate in non-muscle invasive bladder cancer (Kim et al., 2015). *MLL* mutation were found in 23.5% of recurrent bladder tumours and associated with increased H3K4me3 level. This indicated that *MLL* mutagen was associated with the recurrence of bladder cancer (S. Wu et al., 2016). These evident suggested that histone modification patterns in bladder cancer might be fluctuated as a result of the mutation of histone regulators.

The global level of histone marks was explored in bladder cancer. Immunohistochemistry staining and tissue microarray for histone marks were performed in bladder cancer tissues, both non-muscle invasive and muscle invasive tumors, comparing with normal urothelium. Global histone methylation analyses showed that methylation levels exploring in H3K4, H3K20, H3K9 and H3K27 were decreased from normal urothelium towards muscle invasive tumors (Ellinger et al., 2014; Schneider et al., 2011). Similarly, global histone acetylation on histone H3Ac, H3K18Ac and H4Ac were explored. The result showed that level of histone H3Ac was also decreased from urothelium towards muscle invasive tumors but histone H318Ac

and H4Ac were not different among groups (Ellinger et al., 2016). These studies indicated that histone modification pattern, both histone methylation and histone acetylation, was altered in bladder cancer. However, the molecular mechanisms and factors driving the alteration of histone modifications in bladder cancer have not been explored yet. Thus, in this study, oxidative stress was purposely investigated as a potential factor that alters the pattern of histone marks in bladder cancer.

# Chapter 3

# Materials and Methods

**Sample population for immunohistochemical study**

The subjects in this study were the patients who diagnosed as bladder cancer patients and admitted in Buriram hospital, Buriram province, Thailand. Sample size for this study was calculated using Stata/SE 12.0 software (Figure 17) based on data of 5-mC level in bladder cancer tissues from the study by Chung and colleagues (Chung et al., 2015). They found that the percent of 5-methylcytosine (5-mC) positive in normal urothelium and bladder cancer tissues were of 91% and 57%, respectively. Based on the 'sampsi' command of the Stata software, the result indicated that number of subjects per group to be recruited was 39.



```
Estimated sample size for two-sample comparison of proportions

Test Ho: p1 = p2, where p1 is the proportion in population 1
                  and p2 is the proportion in population 2
Assumptions:

         alpha =   0.0500  (two-sided)
         power =   0.9000
            p1 =   0.9100
            p2 =   0.5700
         n2/n1 =   1.00

Estimated required sample sizes:

            n1 =        39
            n2 =        39
```

**Figure 17** Sample size calculation by Stata/SE 12.0 software

**Subject recruitment**

Patients diagnosed as bladder cancer patients at Buriram hospital were recruited according to the following inclusion and exclusion criteria.

**Inclusion criteria**

1. Age ≥ 18 years old

2. Both males and females

3. Diagnosed as bladder cancer patients with histological proof

**Exclusion criteria**

1. Inflicted with other urogenital disorders and malignancy, e.g. urinary bladder stone and prostate cancer

2. Pregnant women

All subjects were informed about research protocol, background and rationale, objectives, methodology, benefits and risks. They also received the Patient Information Sheets. Decision to participate in the study was entirely based upon the voluntarily of the subjects. The subjects had enough time for consideration whether he or she would or would not participate. Neither force nor pressure was applied to the subject's authority. Any decisions made by the subjects did not affect to the further treatment plan.

**Tissue collection**

Cancerous bladder tissue specimens were collected by Dr. Chaowat Pimratana (the urologist and a co-investigator) during TUR-BT operation at Buriram hospital, Buriram province. In this research, adjacent/nearby non-cancerous bladder tissues (0.5 cm$^3$) were also collected from the same patients in order to use as a control tissue. All tissues were preserved in 10% neutral buffered formalin, and kept at 4$^\circ$C until tissue processing.

**Tissue processing for histological examination**

The tissue specimens preserved in 10% neutral buffered formalin were dehydrated following these steps:

| | | |
|---|---|---|
| 70% Ethanol | 1 | hour |
| 80% Ethanol | 1 | hour |
| 90% Ethanol | 1 | hour |
| 100% Ethanol | 1 | hour |
| Xylene I | 30 | minutes |
| Xylene II | 30 | minutes |

Subsequently, dehydrated tissues were embedded in the paraffin wax. The formalin fixed-paraffin embedded tissues were cut into 3 µm section and placed on slides for further histological examination.

However, paraffin embedded tissues have been kept at the research laboratory, room 806, 8th floor, Pattayapat building under the supervision of Assistant Professor Dr. Chanchai Boonla.

**Hematoxylin and eosin (H&E) staining**

H&E staining was performed to examine the difference of cellular morphology between cancerous and adjacent non-cancerous tissues. The 3 µm sections were deparaffinized and rehydrated according to the following steps:

| | | |
|---|---|---|
| Xylene I | 5 | minutes |
| Xylene II | 5 | minutes |
| Xylene III | 5 | minutes |
| 100% Ethanol I | 2 | minutes |
| 100% Ethanol II | 2 | minutes |
| 90% Ethanol | 2 | minutes |
| 80% Ethanol | 2 | minutes |
| 70% Ethanol | 2 | minutes |
| Distilled water | 2 | minutes |

Later, H&E staining was performed by:

| | | |
|---|---|---|
| Hematoxylin | 3 | minutes |
| Bluing | 30 | seconds |
| Tap water | 5 | minutes |
| 95% Ethanol | 1 | minute |

| Eosin | 40 | seconds |
|-------|-----|---------|

After staining, slides were dehydrated as following:

| 70% Ethanol | 30 | seconds |
|-------------|-----|---------|
| 80% Ethanol | 30 | seconds |
| 90% Ethanol | 30 | seconds |
| 100% Ethanol I | 30 | seconds |
| 100% Ethanol II | 30 | seconds |
| Xylene I | 1 | minute |
| Xylene II | 1 | minute |
| Xylene III | 1 | minute |

Slides were then mounted using mounting medium, and visualized under light microscope. Histological grading of tissues was evaluated and classified as papillary, superficial, muscle invasion, low grade and high grade type by the pathologist at Faculty of Medicine, Chulalongkorn University (Dr. Anapat Sunpawat).

**Immunohistochemistry staining for 5-mC, 8-OHdG, OGG1/2, 4-HNE, ORF1p, H3K9me3 and HP1α in bladder cancer tissues**

Immunohistochemistry staining was performed to detect the expression of antigens of interest within tissues. Initially, the tissue sections were deparaffinized and rehydrated as described in the H&E staining above. Antigen retrieval was performed via heat-induced method. Tissues were immerged in citrate buffer pH 6.0 and boiled in microwave for 10 minutes. In addition for 5-mC staining, tissues were then incubated with proteinase K ready-to-use (Dako) at room temterature for 1 minute. Subsequently, the endogenous peroxidase was blocked by 0.3% $H_2O_2$ in methanol for 30 minutes followed by blocking of non-specific binding in normal blocking serum at room temperature for 20 minutes. Primary antibodies, including **Anti-5-Methylcytosine clone33D3 #ab10805 (abcam) at 1:100 dilution, Anti-8-Hydroxyguanosine [N45.1] #ab48508 (abcam) at 1:2,000 dilution, Anti-OGG1/2 (G-5) #sc-376935 (Santa Cruz Biotechnology) at 1:200 dilution, Anti-4-Hydroxynonel #ab46545 (abcam) at 1:2,000 dilution, Anti-LINE-1 ORF1p clone**

**4H1 #MABC1152 (Millipore) at 1:20,000 dilution, Anti-Histone H3K9me3 #ab8898 (abcam) at 1:500 dilution and anti-HP1α #2616 (Cell Signaling Technology) at 1:200 dilution,** were applied and incubated with tissues at $4^{\circ}$C overnight. After incubation, slides were washed with PBS-T for 5 minutes 3 times. Following the manufacture of Vectastain® Elite ABC-HRP kit #PK-6200 (Vector Laboratories), tissues were then incubated with biotinylated secondary antibody at room temperature for 20 minutes followed by incubating with ABC reagent for another 30 minutes. To detect the HRP-ABC complex, tissues were developed by ImmPACT™ DAB Substrate #SK-4105 (Vector Laboratories) and counterstained with Haematoxylin. Finally, tissues were dehydrated and mounted following the previous steps. The sections were visualized under light microscope to evaluate the expression level of each antigen of interest.

To evaluate the expression level of specific antigens in tissues stained by immunohistochemistry (IHC) method, 16-point scale scoring was created and calculated from the multiplication of grayscale intensity score (0-4) and score of %positive cells (0-4) as shown in table 1. Therefore, the calculated IHC score ranged between 0 and 16. Figure 18 shows representative micrographs of different levels and scores (0-4) of grayscale intensity in IHC stained bladder sections.

**Table 1** 16-point scale scoring criteria used for calculation of the IHC score

| Grayscale intensity | | Positive cells | |
|---|---|---|---|
| Intensity level | Score | %positive cells | Score |
| >170-200 | 0 | 0% | 0 |
| >140-170 | 1 | >0-25% | 1 |
| >110-140 | 2 | >25-50% | 2 |
| >80-110 | 3 | >50-75% | 3 |
| 50-80 | 4 | >75-100% | 4 |
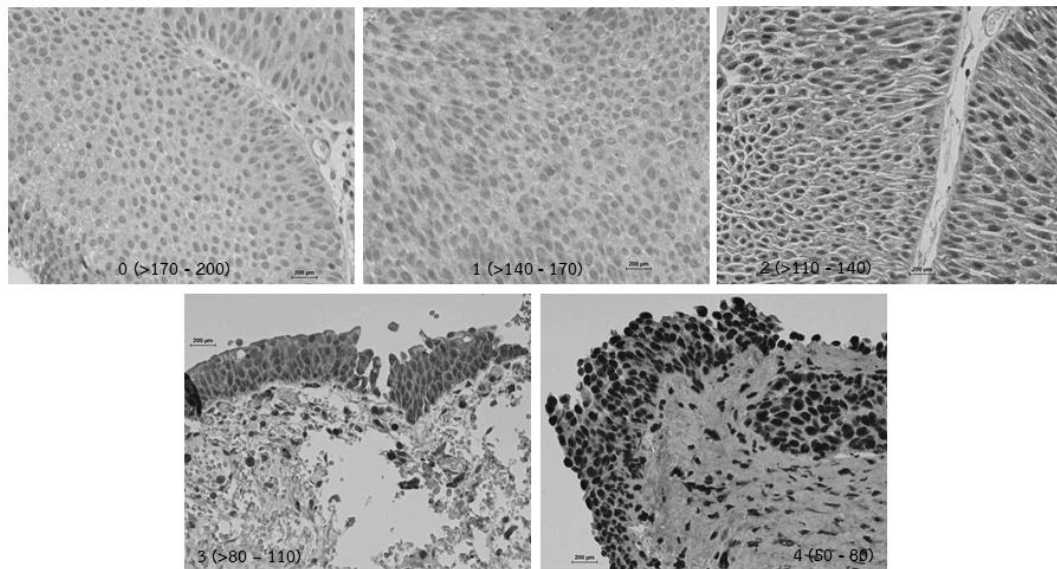
**Figure 18** Representative micrographs showing different levels and scores (0-4) of grayscale intensity in IHC stained bladder tissues detected by HRP-ABC-DAB complex system. Magnification: 400x

## Cell culture for *in vitro* study

Urinary bladder cancer cell lines were employed for the experiments including UMUC-3, RT112, VMCUB1 and BFTC905. The cells were maintained in EMEM with high glucose media, 10% fetal bovine serum and 1% penicillin-streptomycin, at $37^{\circ}C$ and 5% $CO_2$ with saturated humidity.

In the experiments, the cells were treated for 72 hours with different conditions, comprising of 1) control group (serum-free media treatment), 2) $H_2O_2$ treatment at sub-lethal dose, 3) co-treatment between $H_2O_2$ and antioxidants.

## Cell viability assay

To find the optimal concentrations of $H_2O_2$ and antioxidants (Tocopherol acetate and HydroZitLa) against cell lines, 5,000 cells/well were seeded into 96-well plate and cells were treated by various concentrations of $H_2O_2$ (10, 20, 30, 40, 50, 100 and 200 µM), Tocopherol acetate (150, 300, 600, 1200 and 2400 µM) and HydroZitLa (10, 20, 30, 40, 50 and 100%). After 72-hour treatment, cells were

incubated with 0.5 mg/mL MTT at 37$^{\circ}$C for 1 hour. The MTT product, formazan, was dissolved in DMSO and the absorbance was measured at 560 nm using microplate reader Tecan Infinite® 200 Pro. Cell viability was calculated following this equation:

$$\%\text{cell viability} = \left[ \frac{OD_{Treatment}}{OD_{Control}} \right] \times 100$$

## DNA extraction from cell culture

After cell treatments, cells were washed by PBS to remove cell debris and trypsinized by 0.25% trypsin-EDTA for 5 minutes. Medium containing 10% FBS was added to stop the trypsinizing reaction. Cell suspension was centrifuged at 1500 rpm for 5 minutes, supernatant is discarded, and cell pellet was collected. The pellet was resuspended with 200 μL of PBS for DNA extraction.

DNA was extracted by QIAamp DNA Mini Kit (QIAGEN). Following the manufacture, proteinase K and buffer AL were added to cell suspension and incubated at 50$^{\circ}$C overnight. Later, DNA was precipitated by 100% Ethanol and applied to column for purification. DNA was cleaned up in column by buffer AW1 followed by buffer AW2. Finally, DNA was eluted by DNase-free water and stored at -20$^{\circ}$C for downstream experiments. The DNA concentration was measured by Nanodrop 2000 spectrophotometer (Thermo Scientific, USA).

## Protein extraction from cell culture

After 72-hour treatments, cells were washed by cold PBS twice. RIPA buffer containing protease inhibitor cocktail (#5871S, Cell Signaling) was added and incubated on ice for 5 minutes to break the cells. Cells were completely disrupted using cell sculpture and, subsequently, cell lysate was transferred into new micro-centrifuge tube and incubated on ice for another 30 minutes with interval vortex. Later, cell lysate was centrifuged at 12,000g, 4$^{\circ}$C for 5 minutes to remove cell debris. After centrifugation, the supernatant was collected and stored at -80$^{\circ}$C for protein expression study and oxidative stress marker. The concentration of extracted protein was determined by Bradford assay.

**Bradford assay for total protein concentration estimation**

Total protein concentration can be measured by Bradford assay which is based on the reaction between Coomassie Billian Blue G-250 and amino acids. The red form of Coomassie can be converted into blue form when it reacts with amino acid. The absorbance of blue form can be measured at 595 nm and it is proportional to the protein concentration in the solution. To estimate protein concentration, 5 µL of cell lysate extracted from cell culture was mixed with 250 µL of Coomassie reagent from Protein Kit #110306 (Millipore) and incubated for 5 minutes. Bovine serum albumin (BSA) at 0.25, 0.5 and 1 mg/mL were used as standard concentration. The absorbance was measured at 595 nm by microplate reader Tecan Infinite® 200 Pro. The standard curve was created by Microsoft Excel for the calculation of protein concentration.

**Oxidative stress markers**

Protein carbonyl assay

Protein carbonyl assay is one of oxidative stress marker that can detect the carbonyl group in amino acids as protein damage oxidized by ROS. Protein extracted from cell culture (minimally at the concentration of 1 mg/mL) was incubated with 10mM DNPH for 1 hour in the dark at room temperature. The cold 20% trichloroacetic acid (TCA) was added and incubated at $4^\circ$C for 10 minutes. After that, centrifugation at 10,000g, $4^\circ$C for 15 minutes was performed to precipitate the pellet from the reaction. The pellet was washed by Ethanol: Ethyl acetate (1:1 V/V) and centrifuged at 10,000g, $4^\circ$C for 15 minutes. After removing the supernatant, 6M guanidine hydrochloride was added and incubated at $60^\circ$C for 30 minutes to dissolve the pellet. The absorbance at 375 nm was measured to calculate the protein carbonyl level within protein sample following this equation:

$$\text{Protein carbonyl (nmol/mg)} = \frac{\text{A375} \times 45.45 \text{ (nmol/mL)}}{\text{Total protein concentration (mg/mL)}}$$

Dichloro-dihydro-fluorescein diacetate (DCFH-DA) assay

DCFH-DA assay is a tool to detect ROS by fluorometric probe. Theoretically, DCFHA-DA (non-fluorescent) will enter into cells and be converted into DCF (fluorescent) by intracellular ROS. To examine whether $H_2O_2$ could induce intracellular ROS, cells were seeded in 96-well plate for 5,000 cells/well and incubated overnight. After that, cells were incubated with 0.5 mM DCFH-DA in serum-free medium at $37^{\circ}C$ for 30 minutes and quickly washed by PBS for 2 times. $H_2O_2$ and/or antioxidant were added to DCFH-DA-treated cells. Immediately, fluorescent intensity, excitation at 480 nm and emission at 535 nm, was measured at the initial time ($T_0$). Cells were incubated at $37^{\circ}C$ for 1 hour. Finally, fluorescent intensity was measured again ($T_{60}$) to calculate the Arbitrary fluorescent unit (AFU) following this equation:

$$\text{Arbitrary Flourescent Unit (AFU)} = \frac{\text{Fluorescent intensity}_{T60}}{\text{Fluorescent intensity}_{T0}}$$

**DNA bisulfite conversion for DNA methylation study**

Bisulfite conversion reaction is useful for downstream DNA methylation study since unmethylated cytosine will be deaminated and converted to uracil by bisulfite treatment. For this application, EZ DNA methylation-Gold™ Kit (Zymo Reseach) was employed. In detail, 500 ng of genomic DNA was applied and mixed with CT Conversion Reagent in PCR tubes. The PCR tubes were placed in thermal cycler to perform the reactions consisting of denaturation at $94^{\circ}C$ for 10 minutes and bisulfite conversion at $64^{\circ}C$ for 2.5 hours. The mixture was transferred to Zymo-Spin™ IC column and mixed with M-Binding Buffer. The mixture was centrifuged at >10,000g for 30 seconds and then discarded the flow-through. M-Wash Buffer was added to the column to wash DNA and centrifuged to remove wash buffer. At the next step, DNA was incubated with M-Desulphonation Buffer at room temperature for 20 minutes and centrifuged to remove the buffer after incubation. DNA was washed by wash buffer twice. Finally, bisulfite-treated DNA was eluted by M-Elution Buffer and stored at $-20^{\circ}C$ for further experiments.

**Pyrosequecing method for LINE-1 methylation measurement**

The overall methylation level of LINE-1 promoter in UMUC-3 and VMCUB1 cell cultures was examined by Pyrosequencing method. The 10 ng of Bisulfite-treated DNA was applied as a template for PCR. The PCR mixture was prepared with PyroMark® PCR kit (QIAGEN) and LINE-1 primers for pyrosequencing including forward primer and biotinylated reverse primer (as shown in table 1). The PCR reaction was begun with DNA polymerase activation at 95$^\circ$C for 15 minutes followed by 45 cycles of denaturation at 95$^\circ$C for 30 seconds, annealing at 56$^\circ$C for 30 seconds and extension at 72$^\circ$C for 30 seconds and final extension at 72$^\circ$C for 10 minutes. After that, PCR products were immobilized with Streptavidin Sepharose beads for subsequent sequencing. Pyrosequencing was performed by PyroMark® Q24 instrument and the methylation status was analyzed by PyroMark® software.

**Table 2** Primers used for LINE-1 pyrosequencing

| Primers | Sequences | Annealing temperature |
|---|---|---|
| L1_PyRS_F1 | 5'-TTGAGTTAGGTGTGGGATATAGT-3' | 56$^\circ$C |
| L1_PyRS_R1B (Biotinylated) | 5'-AAACCCAAAAAATCAAAAAATTCCCTTTCC-3' | |
| L1_PyRS_S1 (Sequencing) | 5'-GGTGTGGGATATAGTT-3' | 56$^\circ$C |

**Immunofluorescent staining for 8-OHdG in bladder cancer cell lines**

Immunofluorescent staining method was performed to examine the expression 8-OHdG in cell culture model. Initially, UMUC-3 and VMCUB1 at 100,000 cells/well were seeded on sterile glass coverslip in 6-well plate overnight and then treated separately for each experimental condition. After 72-hour treatments, medium were removed and cells were fixed by 4% paraformaldehyde for 10 minutes. After that, cells were pre-treated with 100 µg/mL RNase A at 37$^\circ$C for 30 minutes followed by 2 N HCl for 10 minutes at room temperature and 1 M Tris-HCl

pH 7.5 for another 10 minutes. Cell permeabilization was performed with 0.5% Triton X-100 for 5 minutes and then washed gently by PBS. Cells were then incubated with 2% BSA for 30 minutes for non-specific blocking. Subsequently, cells were incubated with primary antibodies, **Anti-8-Hydroxyguanosine [N45.1] #ab48508 (abcam) at 1:100 dilution in 1% BSA,** at $4^{\circ}$C overnight and next, fluorescence-conjugated secondary antibody was applied. After washing steps, cells on coverslip were counterstained with DAPI and mounted by fluorescent anti-fade mounting medium. The expressions 8-OHdG was visualized and imaged under fluorescent microscope and the fluorescent intensity was measured by ImageJ software.

**Detection of 8-OHdG formation on LINE-1 promoter**

To explore the formation of 8-OHdG on DNA, the DNA immunoprecipitation by 8-OHdG antibody was applied for this study. At the beginning, 1000 ng of genomic DNA extracted from cell culture treatments was prepared in TE buffer pH 8.0 and sheared into 200-800 bp by sonicator following: Time 1:40 min (5 cycles), Pulse 20 sec, Pause 30 sec, Amplitude 20%. The fragment sizes of sheared DNA were checked by 1% agarose electrophoresis. To break double-stranded DNA, DNA fragments were heated at $95^{\circ}$C for 10 minutes and immediately put on ice for 10 minutes to avoid re-annealing. Single-stranded DNA fragments were separated into 2 tubes including 800 ng for immunoprecipitation and 200 ng as input DNA. Subsequently, 800 ng of single-stranded DNA fragments was mix with 1X IP buffer and incubated with 5 µg of **Anti-8-Hydroxyguanosine [N45.1] #ab48508** at $4^{\circ}$C overnight with rotator. After that, DNA-antibody mixture was incubated with SureBeads™ Protein G magnetic beads (Bio-Rad) at $4^{\circ}$C overnight with rotator. DNA-antibody that bound with magnetic beads was isolated by magnetic stand followed by removing the unbound mixture with 1X IP buffer. To elute DNA fragments, magnetic beads was resuspended in digestion buffer with 100 µg of Proteinase K and incubated at $50^{\circ}$C overnight. Finally, DNA was purification by phenol chloroform method.

Firstly, phenol: chloroform (1:1) mixture was added to suspension and vortex gently. Centrifugation was performed at 1300xg at $4^{\circ}$C for 10 minutes and the aqueous upper phase was transferred to a new micro-centrifuge tube. To precipitate

DNA, 3 M sodium acetate (1:10 volume) and 20 µg glycogen were added to aqueous solution. Then 100% Ethanol (2 times volume) was added and incubated at -20$^{\circ}$C for at least 20 minutes. Centrifugation was performed at 1300xg at 4$^{\circ}$C for 20 minutes followed by removing the supernatant. DNA was washed by cold 70% Ethanol and centrifuged again 1300xg at 4$^{\circ}$C for 20 minutes. Supernatant was discarded and DNA was air-dried at room temperature for 10 minutes. Eventually, IP DNA was dissolved in sterilized water and store at -20$^{\circ}$C.

SYBR green based-Quantitative PCR was applied to quantify the amplification of LINE-1 promoter after 8-OHdG antibody isolation. The input DNA from untreated VMCUB1 diluted at 1:10, 1:100 and 1:1000 were applied as standard concentration. IP DNA, input DNA and standard DNA were prepared with SsoAdvanced™ Universal SYBR® Green Supermix (Bio-Rad) and primers following table 2. The qPCR was performed at 95$^{\circ}$C for 2 minutes for enzyme activation and followed by 40 cycles of denaturation at 95$^{\circ}$C, 1 minute, annealing for 1 minute and extension at 72$^{\circ}$C for 1 minute by StepOnePlus™ Real time PCR (Applied Biosystems). The amplification of each sample was calculated by StepOne™ software according to the amplification of standard DNA. Finally the amplification of each gene was calculated as %input following this equation:

$$\%input = \left[ \frac{\text{Amplification of IP DNA}}{\text{Amplification of input DNA}} \right] \times 100$$

Furthermore, the frequency of DNA lesions was calculated as: $\lambda = -\ln (A_D/A_0)$

Which; $\lambda$ = detected lesions/amplicon

$A_D$ = amplification of treatment

$A_0$ = amplification of control

<p align="center">**Table 3** Primers used for qPCR reactions from 8-OHdG immunoprecipitation</p>

| Primers | Sequences | Annealing temperature |
|---------|-----------|----------------------|
| LINE-1-5' | F: 5'-GTACCGGGTTCATCTCACTAGG-3'<br>R: 5'-TGTGGGATATAGTCTCGTGGTG-3' | 55$^{\circ}$C |
| LINE-1-3' | F: 5'-GGGAATTGAACAATGAGATCAC-3'<br>R: 5'-TATACATGTGCCATGCTGGTG-3' | 55$^{\circ}$C |
| GAPDH | F: 5'-TACTAGCGGTTTTACGGGCG-3'<br>R: 5'-TCGAACAGGAGGAGCAGAGAGCGA-3' | 55$^{\circ}$C |

**mRNA extraction and qPCR analysis for mRNA expression**

After 72-hour treatments, cells were washed by PBS and then lysed by Trizol for 10 minutes at room temperature. Lysed cells were transferred to sterilized micro-centrifuge tube. Chloroform was added to Trizol, vortex for 15 seconds and incubated for another 3 minutes at room temperature. After that, the mixture was centrifuged at 12,000g, 4$^{\circ}$C for 15 minutes. The aqueous upper phase was transferred to a new micro-centrifuge tube and 70% Ethanol was added at equal volume followed by vortex for 15 seconds to precipitate RNA. RNA was further purified by RNeasy® mini kit (QIAGEN). According to the manufacture, the lysate was transferred to RNeasy spin column and centrifuged at 8,000g for 15 seconds. Subsequently, RNA was cleaned up in column by buffer RW1 and RPF respectively. Finally, RNA was eluted by RNase-free water and kept at -80$^{\circ}$C for further analyses.

After mRNA extraction, cDNA synthesis was performed by QuantiTect® reverse transcription kit (QIAGEN). Briefly, 1 µg of extracted RNA was initially incubated with gDNA Wipeout buffer at 42$^{\circ}$C for 2 minutes. After that, RNA was mixed with Quantiscript reverse transcriptase, RT buffer and RT primer mix and then incubated at 42$^{\circ}$C for 15 minutes and additionally 95$^{\circ}$C for 3 minutes to inactivate the reaction. The synthesized cDNA was stored at -20$^{\circ}$C for qPCR analysis.

The expression of LINE-1 mRNA was carried out by SYBR green based qPCR. The cDNA from untreated VMCUB1 diluted at 1:10, 1:100 and 1:1000 were applied as

standard expression. The cDNA samples and standard were prepared with QuantiTect SYBR® Green PCR kit (QIAGEN) and primers following table 3. The qPCR was performed at 95$^{\circ}$C for 15 minutes for enzyme activation and followed by 40 cycles of denaturation at 95$^{\circ}$C, 15 seconds, annealing for 30 seconds and extension at 72$^{\circ}$C for 30 seconds by LightCycler® 96 (Roche). The amplification of each sample was calculated according to the amplification of standard cDNA. Eventually, LINE-1 mRNA expression was normalized by α-Tubulin expression.

**Western blot analyses**

Western blot assay was employed to determine the expression of protein of interest including OGG1/2 (base excision repair process) and LINE-1 ORF1p (LINE-1 expression). After protein extraction, 20 μg of total protein of each sample was mixed with loading buffer, which is included 4% SDS and 10% β-mercaptoethanol, and boiled at 95$^{\circ}$C for 5 minutes to denature protein structure. The denatured protein was loaded into the wells of 10% SDS PAGE and firstly run in running buffer at 100 volts for 20 minutes for stacking gel and then continued to 200 volts for about 1 hour in separating gel. After completing electrophoresis, proteins were transferred to PVDF membrane using wet-tank transfer apparatus and run at 180 mA for 1 hour. The membranes were blocked by 5% skimmed milk in TBS-T at room temperature for 1 hour for non-specific blocking and then incubated with primary antibodies **(1:500 Anti-OGG1/2 (G-5) #sc-376935 (Santa Cruz Biotechnology), 1:10,000 Anti-LINE-1 ORF1p clone 4H1 #MABC1152 (Millipore), 1:25,000 Anti-α-Tubulin as an internal control)** at 4$^{\circ}$C overnight with gently shaking. After washing with TBS-T, membranes were incubated with 1:5,000 HRP-conjugated secondary antibody at room temperature for 1 hour followed by washing with TBS-T. Finally, membranes were developed with SuperSignal™ West Femto Maximum Sensitivity Substrate (Thermo Scientific) and signal was detected by LI-COR® C-Digit Blot Scanner. The proteins of interest were observed at 38 kDa for OGG1/2, 40 kDa for LINE-1 ORF1p and 50 kDa for α-Tubulin.

**Chromatin immunoprecipitation assay for histone modification study** *in vitro*

Chromatin immunoprecipitation (ChIP) assay was performed to investigate histone modification patterns. Following the manufacture of ChIP®IT Express Chromatin Immunoprecipitation Kit #53008 (Active Motif), approximately $1.5 \times 10^7$ cells were required for each condition. After 72-hour treatment, cells were fixed with 1% paraformaldehyde for 10 minutes at room temperature. Then, cells were scraped in scraping solution and transferred to 15 mL centrifuge tube. To collect cell pellet, cell suspension was centrifuged at 2,500 rpm, $4^\circ$C for 15 minutes and supernatant was then discarded. Pellet was resuspended in lysis buffer and lysed by homogenizer followed by centrifugation at 5,000 rpm, $4^\circ$C for 10 minutes. The chromatin pellet was collected and resuspended in shearing buffer. Chromatin was then sheared by sonication following: Time 2:20 min (7 cycles), Pulse 20 sec, Pause 30 sec, Amplitude 25%. The expected sized of sheared DNA was around 200 - 1500 bp. The 25 µg of sheared chromatin was incubated with Protein G beads and 3 µg of antibody at $4^0$C overnight with rotator. Antibodies employed in this experiment included **Anti-Histone H3 #39763 (Active Motif), Anti-Histone H3K4me3 #39915 (Active Motif), Anti-Histone H3K9me3 #ab8898 (abcam), Anti-Histone H3K27me3 #39535 (Active Motif) and Anti-Histone H3K18Ac #ab1191 (abcam).** Finally, chromatin was then eluted from magnetic beads and treated with Proteinase K. The IP DNA was stored at -$20^\circ$C for 2-3 weeks for analyses.

The enrichment of LINE-1 element on each modified histone was analyzed by qPCR. Furthermore, the enrichment of GAPDH, CTCFL and GRM6 were also analyzed in order to verify ChIP-qPCR technique. SYBR green based qPCR was carried out following qPCR method for mRNA expression. Primers applied for this experiment were shown in table 3.

**Table 4** Primers used for qPCR reactions from ChIP assay

| Primers | Sequences | Annealing temperature |
|---|---|---|
| LINE-1-5' | F: 5'-GTACCGGGTTCATCTCACTAGG-3'<br>R: 5'-TGTGGGATATAGTCTCGTGGTG-3' | 55°C |
| LINE-1-3' | F: 5'-GGGAATTGAACAATGAGATCAC-3'<br>R: 5'-TATACATGTGCCATGCTGGTG-3' | 55°C |
| GAPDH | F: 5'-TACTAGCGGTTTTACGGGCG-3'<br>R: 5'-TCGAACAGGAGGAGCAGAGAGCGA-3' | 55°C |
| CTCFL | F: 5'-GAACAGCCCATGCTCTTGGAG-3'<br>R: 5'-CAGAGCCCACAAGCCAAAGAC-3' | 60°C |
| GRM6 | F: 5'-GAGAGGGACGCTGGACAC-3'<br>R: 5'-CTCCGTCTCCATCATGGTC-3' | 60°C |

**Wound healing assay for cell migration study**

Wound healing or scratch assay is a basic method to measure the cell migration *in vitro*. It quantifies the migration rate of the cells to fill gap of the scratch or wound made in the cell monolayer. At the beginning, cells were plated in 24-well plate overnight allowing cells to form a monolayer at confluency. Then, p200 pipet tip was used to make a scratch or straight line in the well. Every scratch size in every treatment had to be relatively equal. After scratching, cell debris was removed by gently washing with PBS. The new medium with different treatments was added into each well afterwards. The size of scratch area at starting time was visualized under microscope. After that, cells were incubated at 37°C, 5% $CO_2$ for 6 - 24 hours and the scratch area after incubation was visualized again to analyze the cell migration rate of each treatment condition.

**Boyden chamber assay for cell migration and cell invasion study**

Boyden chamber assay is widely used to study the motility and invasive activity of the testing cells, for example to test metastasis of cancer cells. The test

quantifies number of the cells that migrate or invade through the pore of membrane (covered by extracellular matrix) in transwell compartment. Corning® Transwell insert was applied for cell migration and Corning® Biocoat™ Matrigel transwell insert was applied for cell invasion study. At the beginning, the transwell inserts with 8 μm pore size filter was placed in 24-well plate dividing the well into two parts, upper and lower part. EMEM containing 1% FBS was added to the lower part. Cell suspension in serum-free medium with different treatments (containing 20,000 cells for cell migration in both UMUC-3 and VMCUB1, 30,000 cells for cell invasion in UMUC-3 and 100,000 cells for cell invasion in VMCUB1) was added to the upper part and incubated at $37^{\circ}$C, 5% $CO_2$ for 24 hours to allow the cells migrate and invade through matrix proteins to the other side of filter. After that, cells were fixed by 4% paraformaldehyde for 10 minutes. Cells on the upper side of filter that do not migrate to the lower side were removed by a cotton swap. Cells which were fixed on the lower side were stained by 1% crystal violet in 2% ethanol for 20 minutes and finally destained in 10% acetic acid. The absorbance at 570 nm was measured by microplate reader Tecan Infinite® 200 Pro and the number of migrated or invaded cells was evaluated from standard curve. Cell migration and Cell invasion were calculated as %migration and %invasion respectively by the following equation:

$$\text{\%Migration or \%invasion} = \left[ \frac{\text{Number of migrated or invaded cells}}{\text{Number of initial cells}} \right] \times 100$$

To create a standard curve, cells were seeded at different numbers including 2,500, 5,000, 10,000 and 20,000 cells and incubated at $37^{\circ}$C with 5% $CO_2$ for 24 hours. Then, medium were discarded and cells were stained with 1% crystal violet in 2% ethanol for 20 minutes. Crystal violet was dissolved in 10% acetic acid and the absorbance was measured at 570 nm by microplate reader. Finally, the standard curve was created between number of cells (X-axis) and $OD_{570}$ (Y-axis) by Microsoft Excel for cell number calculation.

**Statistical analysis**

The data was presented as mean ± SEM. Categorical data was presented as frequency and percentage. Student's *t*-test or Mann-Whitney U test was used for comparison of variables between the two independent groups. One-way analysis of variance (ANOVA) or Kruskal-Wallis test followed by multiple comparison tests was used for three or more group comparison. Spearman's rank correlation test was used for assessing correlation of two continuous variables. GraphPad Prism version 5.0 was employed for all graphs and calculations. *P*-value<0.05 was considered as statistically significant.

# Chapter 4

# Results

**The characteristics of studied bladder cancer patients**

This study was ethically approved by The Institutional Review Board (IRB), Faculty of Medicine, Chulalongkorn University and the IRB of Buriram Hospital. A total of 39 bladder cancer patients admitted to Buriram Hospital, Buriram province, Thailand during April 2016 – April 2017 were included in this study. As shown in table 4, these patients had mean age of 70.5 ± 13.7 years old. There were 33 male (84.61%) and 6 female (15.39%). According to the patient history, 50% of these patients were smokers, 82.35% were exposed to pesticides and 17.65% were exposed to other chemicals (for example dye and battery) from their works. Regarding the clinical manifestation, hematuria, a common symptom of bladder cancer, was found at 87.88%. Moreover, 69.23% of cases were new bladder cancer cases whereas 30.77% of the patients had recurrent tumors. All of them have no family history of bladder cancer.

According to the surgical approaches for removing the tumors, 89.47% underwent transurethral resection of bladder tumors (TUR-BT) procedure, while the rest of 10.53% were surgically treated with radial cystectomy. The pathology of tumor was examined by pathologist and revealed that 8.57% were papillary urothelial neoplasm of low malignant potential (PUNLMP), 37.14% were low grade and 51.29% were high grade tumors. According to tumor classification based on muscle invasion, 71.79% were non-muscle invasive tumors (papillary and superficial tumor) and 28.21% were classified as muscle-invasive tumors.

**Table 5** Bladder cancer patient characteristics included in this study

| Characteristic | Frequency (%) |
|---|---|
| Total number of patients | 39 |
| Average age | 70.5 ± 13.7 years old |
| Sex: | |
| Male | 33 (84.61%) |
| Female | 6 (15.39%) |
| Smoking status (n=24): | |
| Yes | 12 (50%) |
| No | 12 (50%) |
| Occupational risks (n=17): | |
| Pesticide exposure | 14 (82.35%) |
| Chemical exposure (Dye/Battery/Coal) | 3 (17.65%) |
| Hematuria (n=33): | |
| Yes | 29 (87.88%) |
| No | 4 (12.12%) |
| Recurrence: | |
| First Diagnosis | 27 (69.23%) |
| Recurrence (>2) | 12 (30.77%) |
| Family history (n=19): | |
| Yes | 0 (0%) |
| No | 19 (100%) |
| Surgical approaches (n=38): | |
| TUR-BT | 34 (89.47%) |
| Radial cystectomy | 4 (10.53%) |
| Histological grading (n=35): | |
| PUNLMP | 3 (8.57%) |
| Low grade | 13 (37.14%) |
| High grade | 19 (54.29%) |
| Type of tumor: | |

| Non-muscle invasive (papillary/superficial) | 28 (71.79%) |
|---|---|
| Muscle invasive | 11 (28.21%) |

## Histological examination of studied tissues and the scoring system of the immunohistochemistry staining

Initially, Haematoxylin and Eosin (H&E) staining was performed in all bladder cancer and their adjacent tissues and the sections were histologically examined by pathologist. According to H&E evaluation, there were 38 cancerous bladder sections and 19 adjacent non-cancerous bladder tissues (used as controls). These sections were used for further immunohistochemical staining (Figure 19).
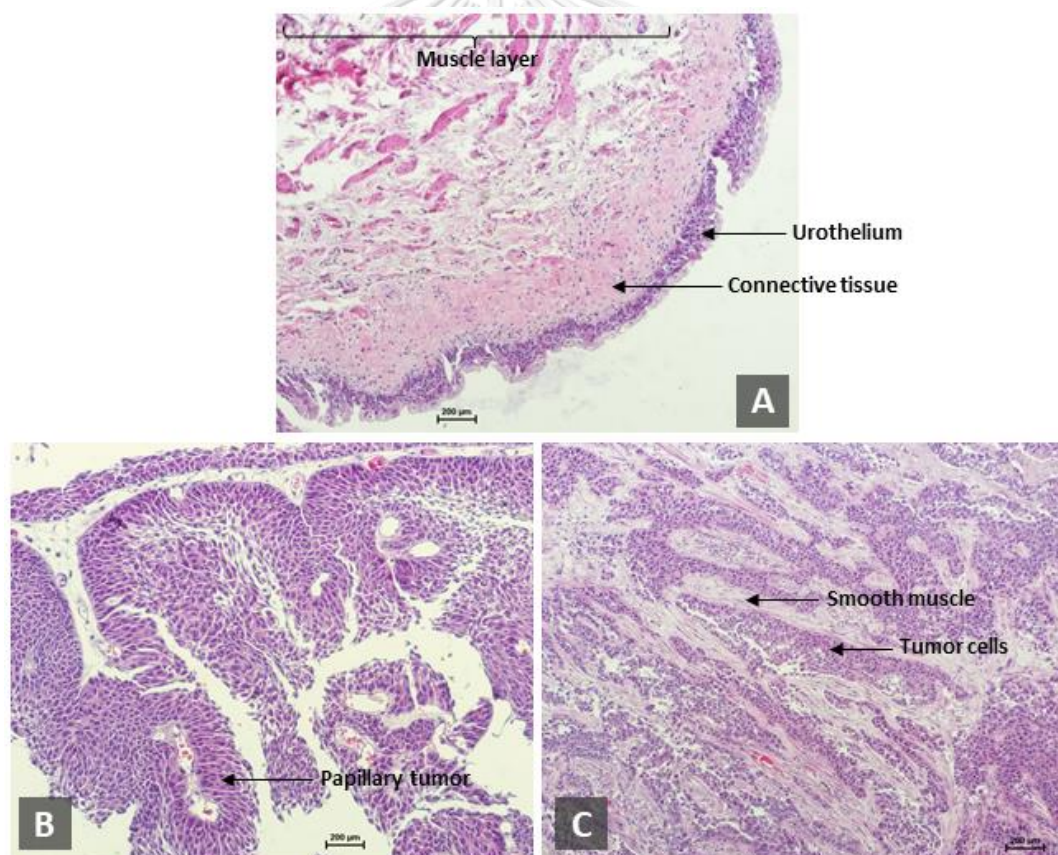


**Figure 19** H&E staining in cancerous and adjacent non-cancerous tissues

A) Adjacent non-cancerous bladder tissue

B) Cancerous bladder tissue (papillary type, low grade),

C) Cancerous bladder tissue (muscle invasive, high grade) Magnification: 100x

**Global DNA hypomethylation in bladder cancer tissues**

   5-mC IHC staining has been used to indicate the level of global DNA methylation in tissues. Seventeen cancerous and 14 adjacent non-cancerous bladder tissues were available for 5-mC staining. The result showed that 5-mC expression level in cancerous tissues was statistically lower than their adjacent tissues (IHC score: 10.97±2.54 vs. 14.35±1.64, *p*=0.0001) (Figure 20, 21). Comparing among different histological grading tumors, 5-mC expression level in high-grade tumors was significantly lower than PUNLMP/low grade (IHC score 9.89±2.26 vs. 11.88±2.83, *p*=0.037) (Figure 22, 23). Evidently, the present data showed that DNA methylation was decreased in cancerous bladder tissues relative to adjacent or non-cancerous bladder tissues. These data indicated global DNA hypomethylation in bladder cancer. Furthermore, global DNA hypomethylation was associated with bladder cancer progression since DNA methylation level was declined in high-grade tumors compared to PUNLMP and low-grade tumors.
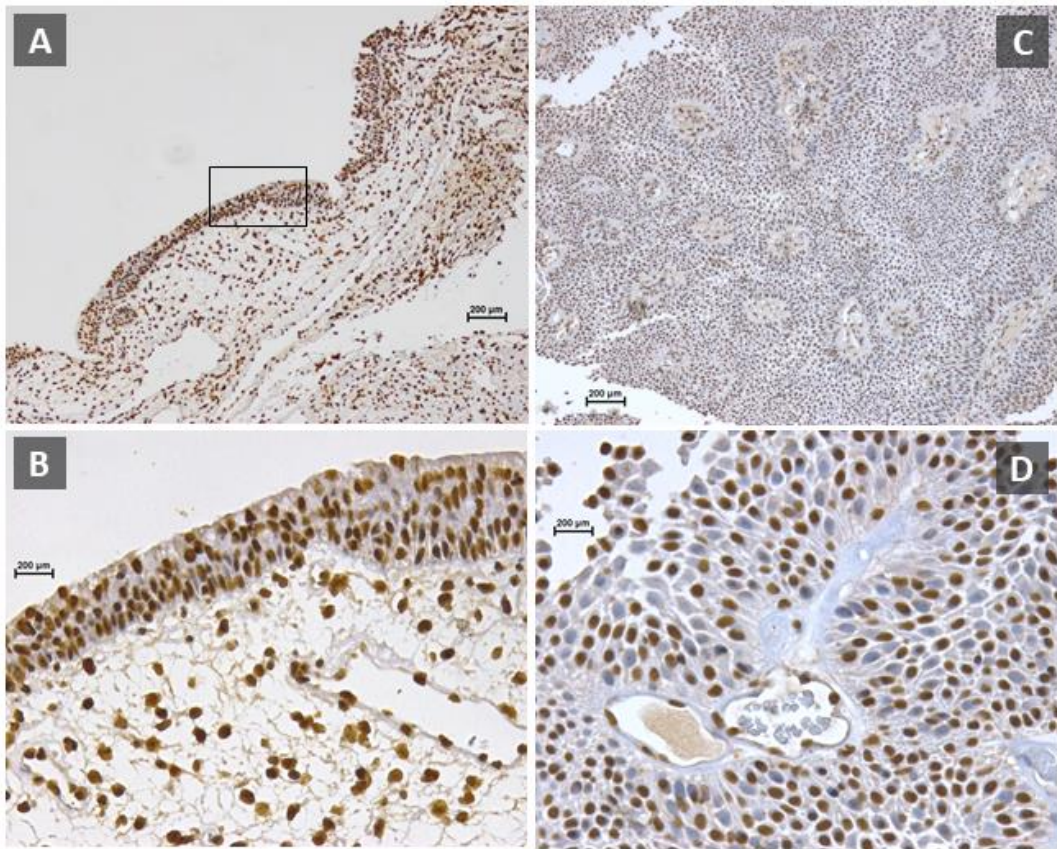
**Figure 20** Global DNA hypomethylation in bladder cancer. 5-mC expression in cancerous tissues (C, D) was lower than non-cancerous tissues (A, B). Magnification: 100x (A, C), 400x (B, D).
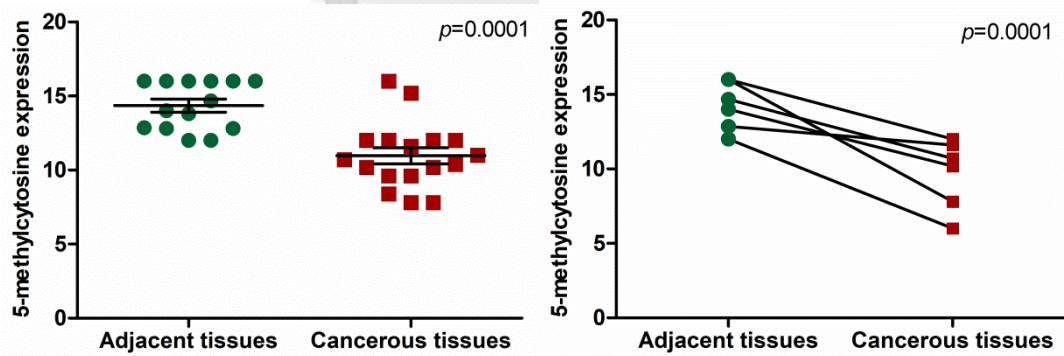


**Figure 21** 5-mc expression level in adjacent non-cancerous (green) and cancerous (red) bladder tissues. Cancerous tissues showed significant lower 5-mC expression than adjacent tissues. Left: Overall comparison (Mann-Whitney U test) Right: Paired comparison (Paired *t*-test)
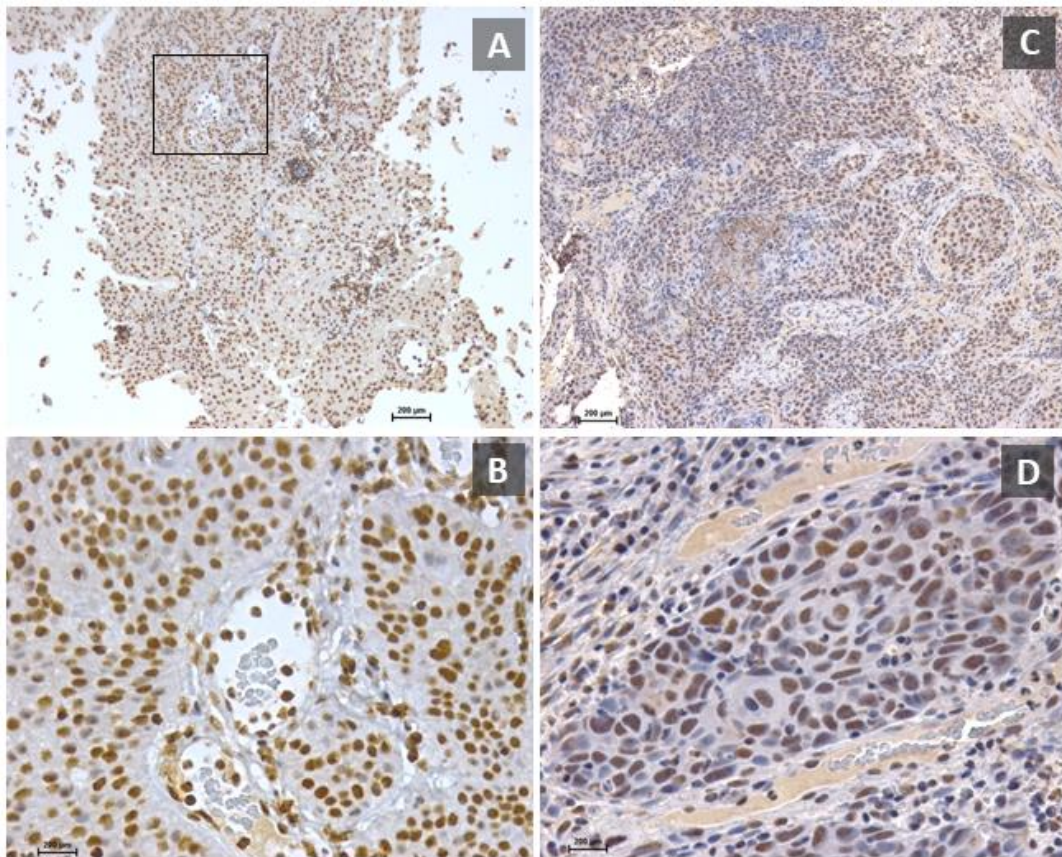
**Figure 22** Association of global DNA hypomethylation with advanced stage of bladder cancer. 5-mC expression in high-grade (C, D) was lower than low-grade tumors (A, B). Magnification: 100x (A, C), 400x (B, D).
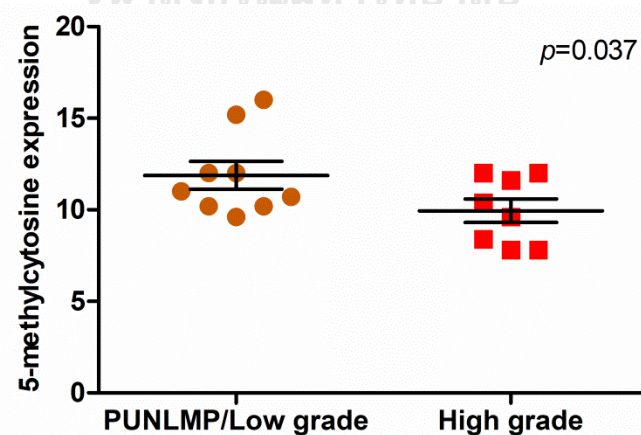


**Figure 23** 5-mC expression in PUNLMP/low-grade tumors (brown) and high-grade tumors (red). Expression of 5-mC was significantly decreased in high-grade tumors compared to low-grade tumors (Mann-Whitney U test).

## Oxidative stress and LINE-1 ORF1p expression in bladder cancer

To examine the oxidative stress status in tissues, 37 cancerous and 11 adjacent non-cancerous tissues were immunohistochemically stained with 4-hydroxynoneol (4-HNE) as an oxidative stress marker (byproduct from lipid peroxidation). It was shown that the expression of 4-HNE in cancerous tissues (IHC score = 7.63±3.17) was significantly higher than adjacent tissues (IHC score = 5.13±2.45) ($p$=0.020) (Figure 24, 25). However, 4-HNE expression was not statistically different between high-grade (IHC score = 8.17±2.86) and low-grade tumors (IHC score = 7.43±3.50) ($p$=0.4219) (Figure 26). Nevertheless, IHC data indicated that oxidative stress was augmented in cancerous bladder tissues.



**Figure 24** Oxidative stress in bladder cancer tissues. 4-HNE expression in cancerous tissues (C, D) was higher than non-cancerous tissues (A, B).

Magnification: 100x (A, C), 400x (B, D).
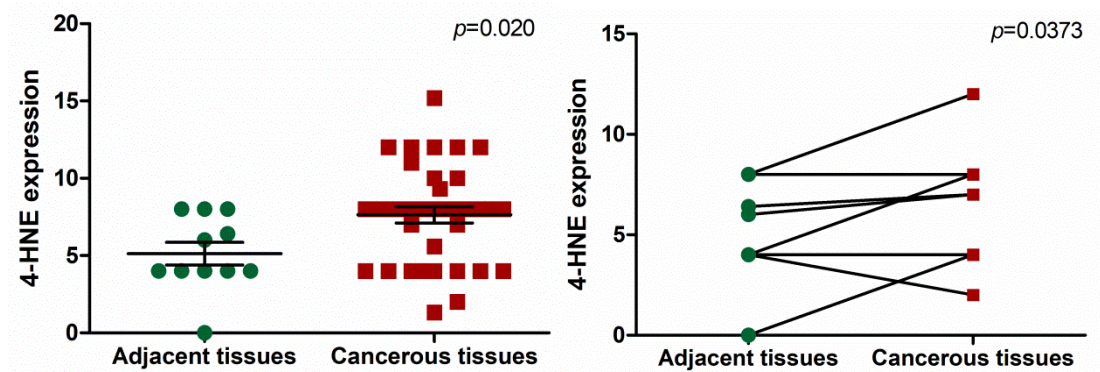
**Figure 25** 4-HNE expression level in adjacent (green) and cancerous (red) bladder
tissues. 4-HNE expression was significantly higher in cancerous than adjacent tissues.

Left: Overall comparison (Mann-Whitney U test)
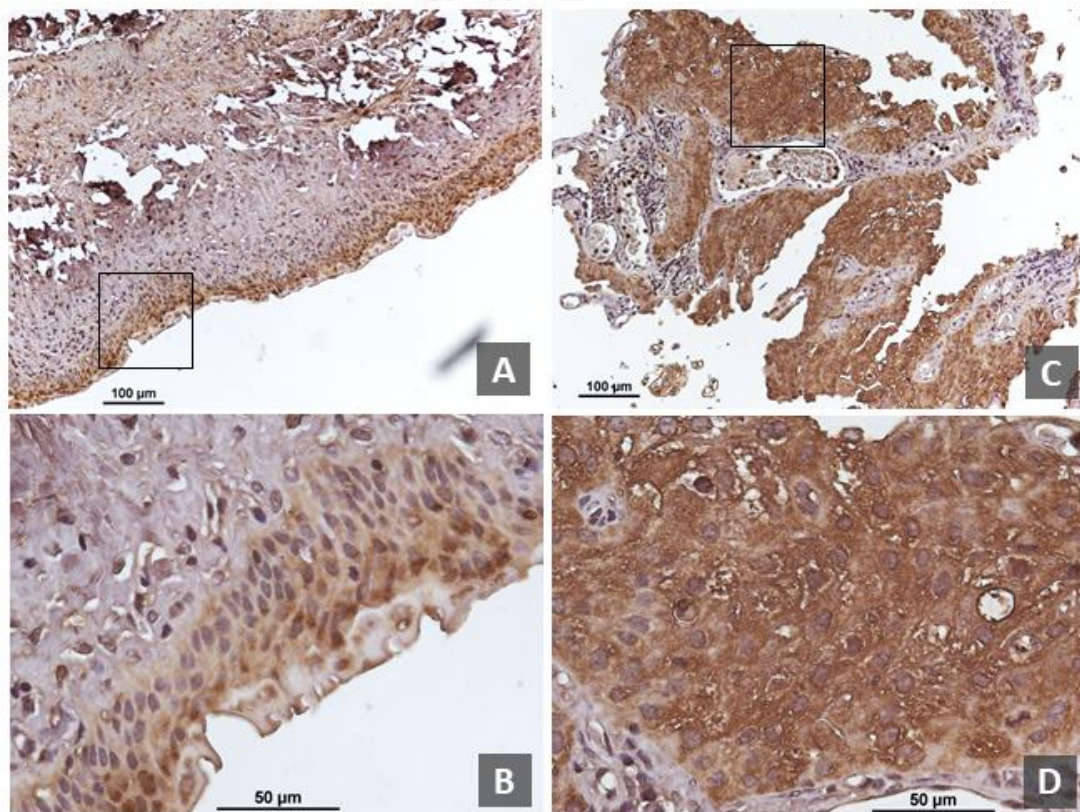
Right: Paired comparison (Paired *t*-test).
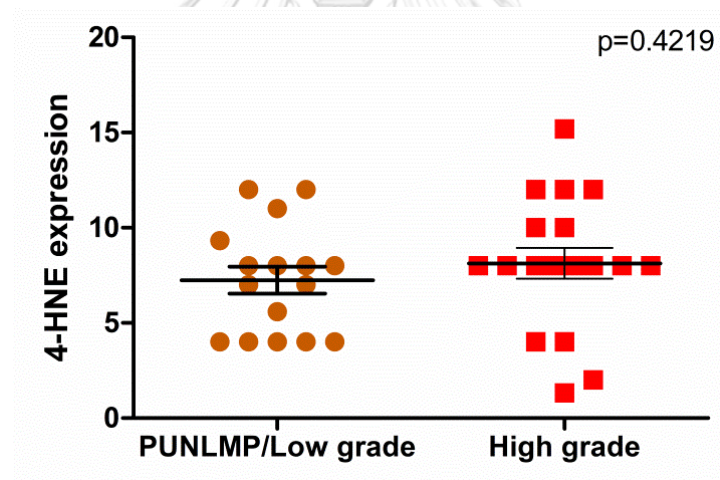


**Figure 26** 4-HNE expression in PUNLMP/low-grade (brown) and high-grade (red)
tumors. Level of 4-HNE expression was not different between PUNLMP/low-grade
and high-grade tumors (Mann-Whitney U test).

Since global DNA hypomethylation was found in bladder cancer, it was
interesting to ask if LINE-1 protein expression was upregulated. In this study, LINE-1
ORF1p expression was investigated in 36 cancerous tissues together with 11 adjacent
tissues as controls. As shown in Figure 27, ORF1p expression was significantly
increased in cancerous tissues (IHC score = 7.71±4.25) compared with adjacent

tissues (IHC score = 5.48±3.48) (*p*=0.0464) (Figure 28). Comparison between PUNLMP/low-grade and high-grade tumors, it showed that ORF1p expression in high-grade tumors (IHC score = 9.45±2.97) was significantly greater than PUNLMP/low-grade tumors (IHC score = 5.63±4.38) (*p*=0.0083) (Figure 29, 30). These findings indicated that ORF1p expression was increased in cancerous bladder tissues and it was associated with bladder cancer progression.

Moreover, we found that the expression of 4-HNE was statistically correlated with ORF1p expression (Spearman rho = 0.5782, p=0.0002) (Figure 31). Therefore, this might implied that the increase in ORF1p expression in bladder cancer tissues was possibly induced by oxidative stress.



**Figure 27** ORF1p expression in bladder cancer tissues. The expression of ORF1p in cancerous (C, D) tissues was higher than non-cancerous tissues (A, B).

Magnification: 100x (A, C), 400x (B, D).
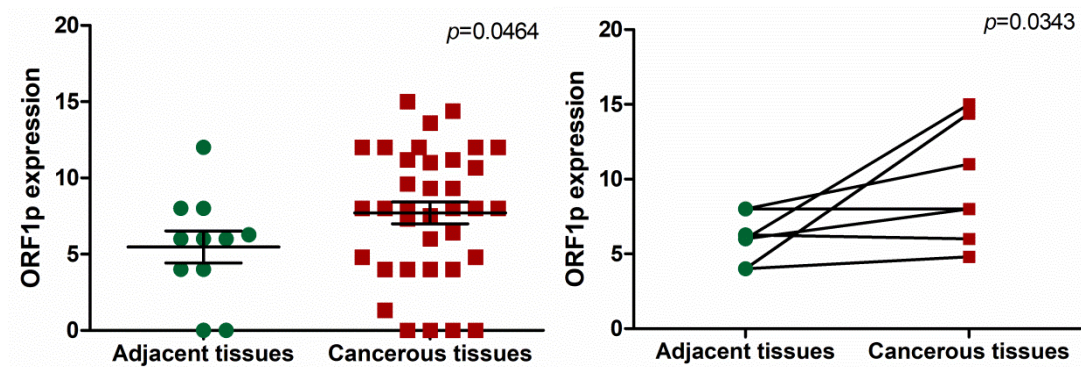
**Figure 28** ORF1p expression level in adjacent (green) and cancerous (red) bladder tissues. ORF1p expression in cancerous was significantly higher than adjacent tissues.

Left: Overall comparison (Mann-Whitney U test)
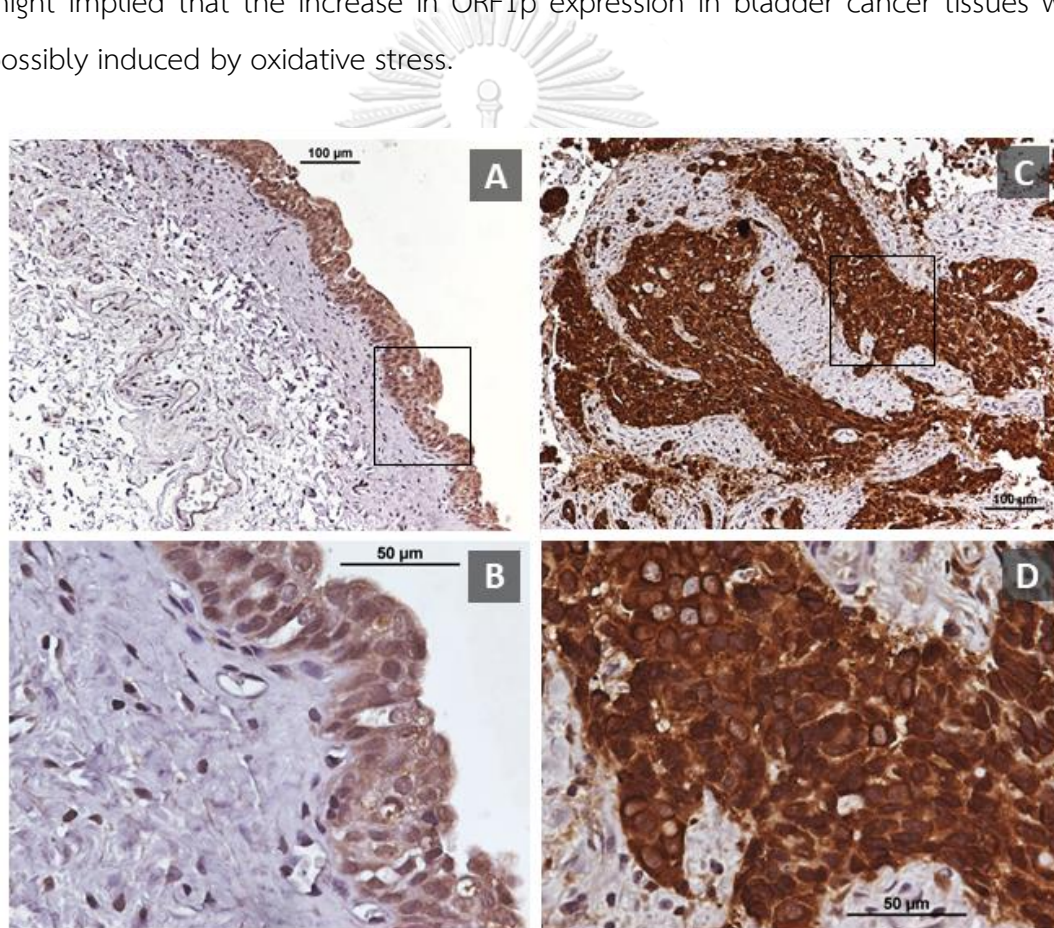
Right: Paired comparison (Paired t-test).



**Figure 29** Association of increased ORF1p expression with bladder cancer progression

ORF1p expression in high-grade (C, D) was higher than low-grade tumors (A, B).

Magnification: 100x (A, C), 400x (B, D).

**Figure 30** ORF1p expression in PUNLMP/low-grade (brown) and high-grade (red) tumors. Level of ORF1p expression in high-grade tumors was significantly higher than PUNLMP/low-grade tumors (Mann-Whitney U test).
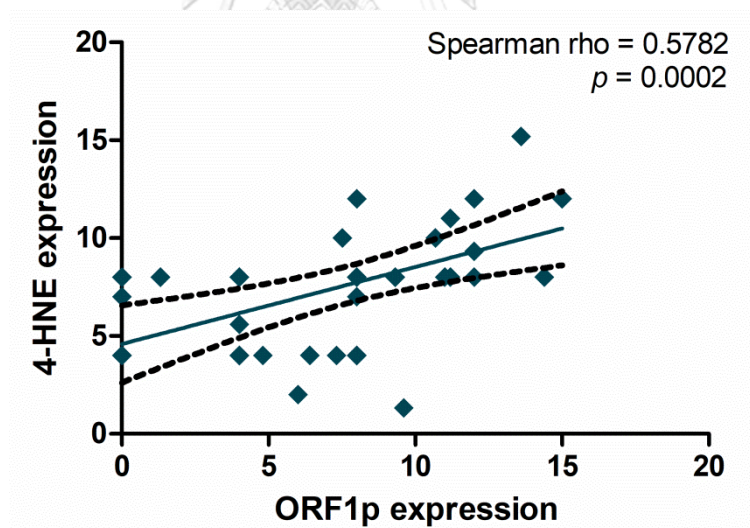


**Figure 31** Positive correlation between ORF1p and 4-HNE expression. Increased ORF1p expression was statistically correlated with increased 4-HNE expression.

**Oxidative DNA damage and base excision repair in bladder cancer**

The previous study demonstrated an increased oxidative stress in bladder cancer tissues. In this study, oxidative DNA lesions 8-OHdG was immunohistochemically investigated in 36 cancerous and 10 adjacent tissues. The data showed that cancerous tissues exhibited significantly higher 8-OHdG expression (IHC score = 9.23±2.42) than adjacent tissues (IHC score = 7.28±3.11) ($p$=0.0206) (Figure 32, 33). Comparing among tumors, it was shown that 8-OHdG expression in high-grade tumors (IHC score = 8.17±2.50) was significantly lower than PUNLMP/low-grade tumors (IHC score = 10.17±1.92) ($p$=0.028) (Figure 34, 35).

OGG1/2, DNA glycosylase enzyme that recognizes 8-OHdG lesions in base excision repair, was also investigated in this study. Nineteen cancerous and 11 adjacent tissue sections were immunohistochemically stained, and the result showed that OGG1/2 expression was significantly increased in cancerous tissues (IHC score = 11.21±3.04) compared to adjacent tissues (IHC score = 9.26±1.94) ($p$=0.0469) (Figure 36, 37). However, the expressions of OGG1/2 in PUNLMP/low-grade (IHC score = 10.16±3.14) and high-grade tumors (IHC score = 12.38±2.37) were not significantly different ($p$=0.0741) (Figure 38). However, the current IHC data revealed that oxidative DNA damage formation was increased, and base excision repair pathway was activated in bladder cancer tissues.

Furthermore, this study found that 8-OHdG expression in cancerous tissues was positively correlated with OGG1/2 expression (Spearman rho = 0.5455, $p$=0.0015) (Figure 39). Therefore, we concluded that oxidative DNA damage was associated with the expression of base excision repair enzyme in bladder cancer tissues.

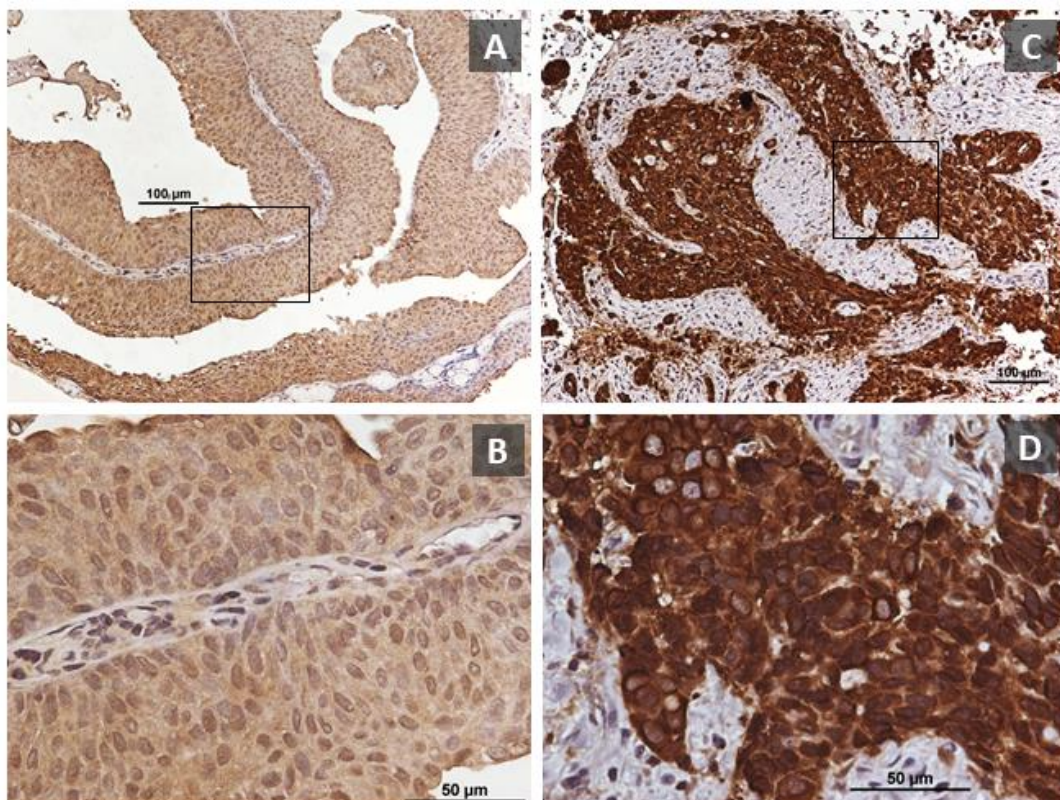**Figure 32** 8-OHdG expression in bladder cancer tissues. 8-OHdG expression in cancerous tissues (C, D) was higher than non-cancerous tissues (A, B). Magnification: 100x (A, C), 400x (B, D).
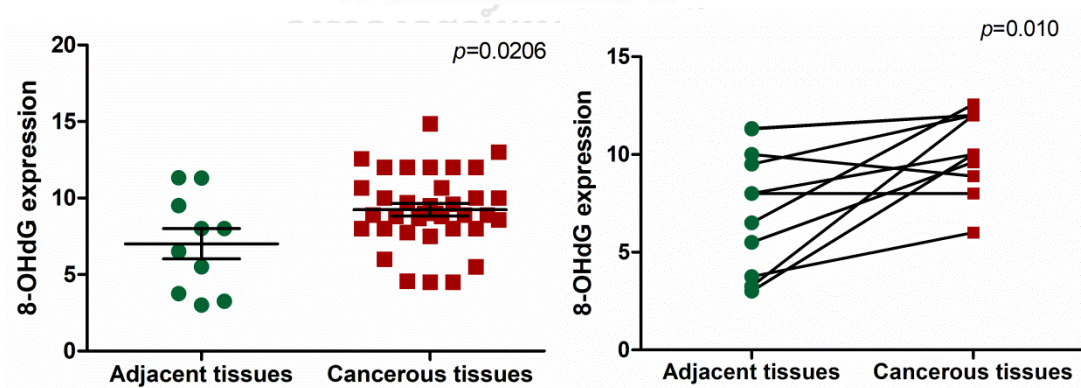


**Figure 33** 8-OHdG expression level in adjacent (green) and cancerous (red) bladder tissues. Level of 8-OHdG expression in cancero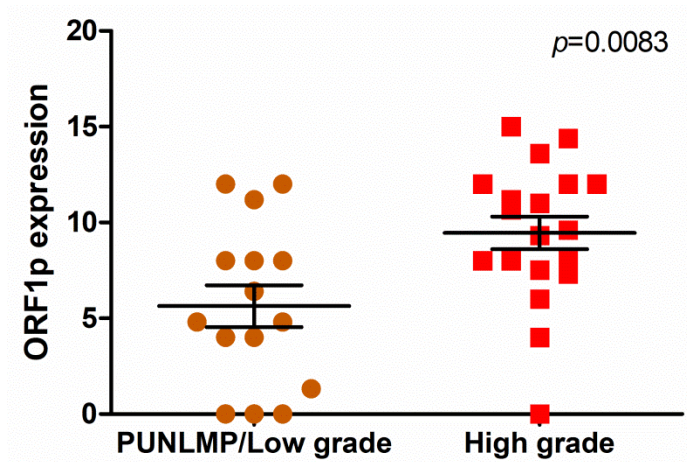us was significantly higher than adjacent tissues. Left: Overall comparison (Mann-Whitney U test) Right: Paired comparison (Paired *t*-test)

**Figure 34** Association of 8-OHdG expression and bladder cancer progression
8-OHdG expression in low-grade (A, B) was higher than high-grade tumors (C, D).
Magnification: 100x (A, C), 400x (B, D).



**Figure 35** 8-OHdG expression in PUNLMP/low-grade (brown) and high-grade (red)
tumors. 8-OHdG expression in high-grade tumors was significantly lower than
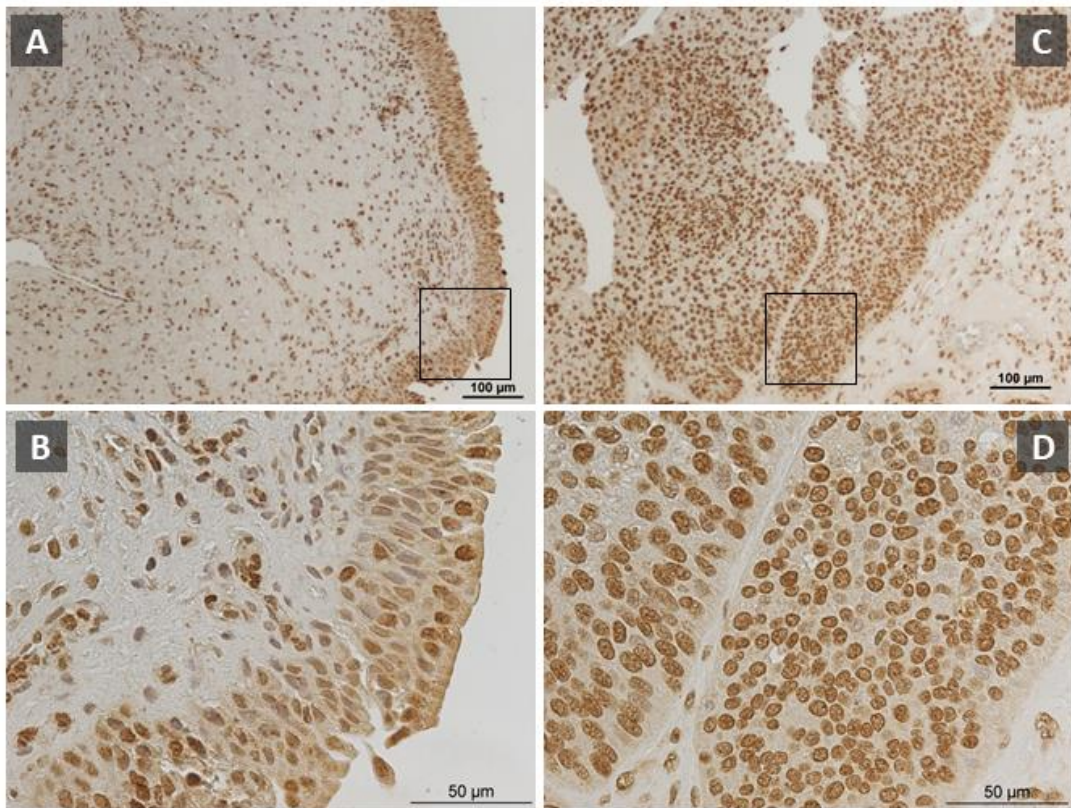PUNLMP/low-grade tumors (Mann-Whitney U test).
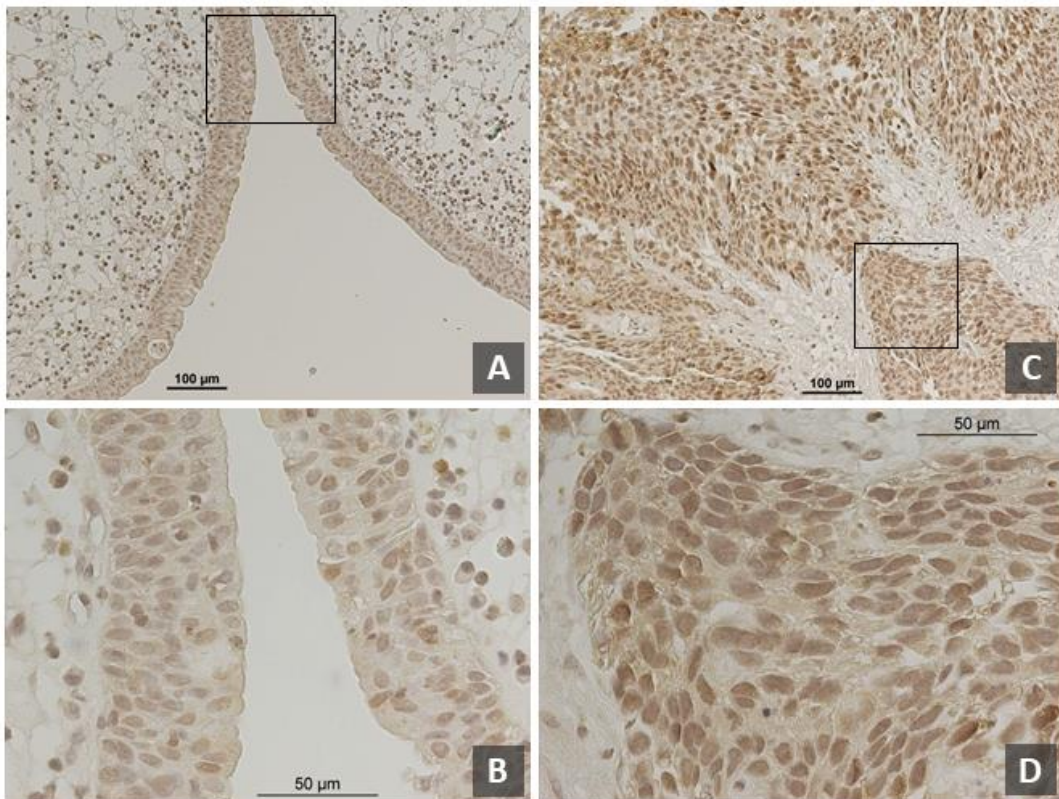
**Figure 36** OGG1/2 expression in bladder cancer tissues. OGG1/2 expression in cancerous tissues (C, D) was higher than non-cancerous tissues (A, B).

Magnification: 100x (A, C), 400x (B, D).
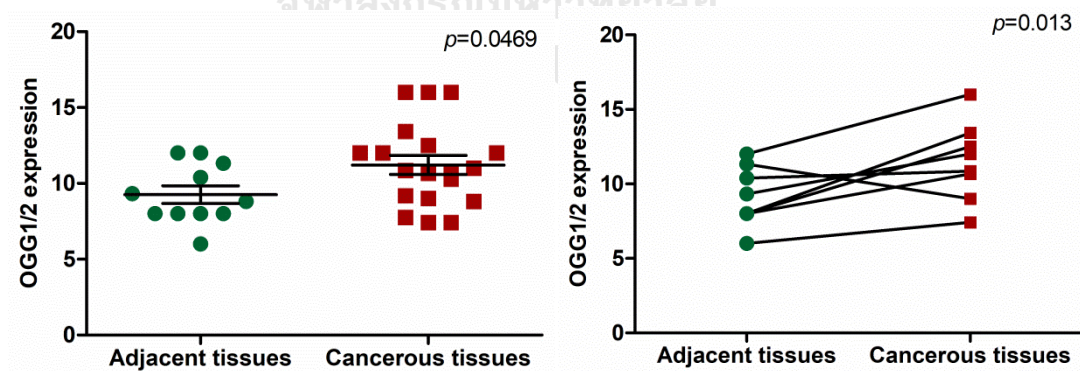


**Figure 37** OGG1/2 expression level in adjacent (green) and cancerous (red) tissues

Level of OGG1/2 expression in cancerous was significantly higher than adjacent

tissues. Left: Overall comparison (Mann-Whitney U test)

Right: Paired comparison (Paired *t*-test)
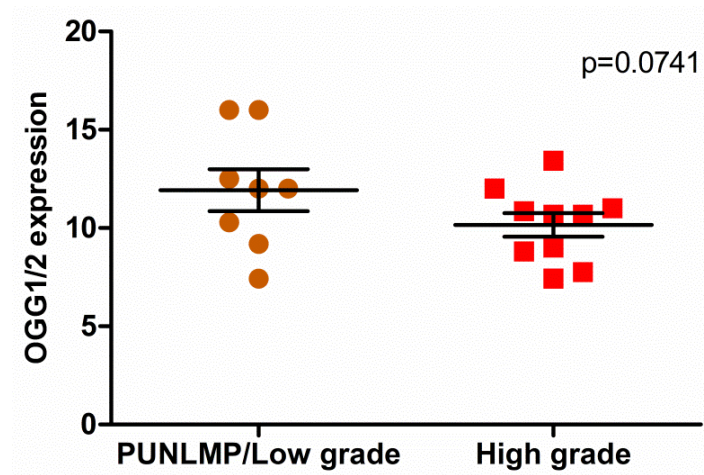
**Figure 38** OGG1/2 expression in PUNLMP/low-grade (brown) and high-grade (red) tumors. OGG1/2 expression was not different between PUNLMP/low-grade and high-grade tumors (Mann-Whitney U test).



**Figure 39** Positive correlation between 8-OHdG and OGG1/2 expression. Increased 8-OHdG expression was significantly associated with increased OGG1/2 expression.

**Histone modification change in bladder cancer tissues**

H3K9me3 is a well-known hallmark of heterochromatin formation, and this chromatin mark is specifically recognized by HP1$\alpha$ proteins. Whether these two heterochromatin hallmarks are changed in bladder cancer tissues was investigated in this study. The level of histone H3K9me3 was investigated in 37 cancerous and 12 adjacent tissues. The IHC results revealed that expression level of histone H3K9me3 was significantly increased in cancerous tissues (IHC score = 8.98±3.48) compared to adjacent tissues (IHC score = 7.03±2.76) (*p*=0.0382) (Figure 40, 41). Additionally, the level of histone H3K9me3 in high-grade tumors was slightly decreased (IHC score = 8.45±2.64), but it was not statistically different from PUNLMP/low grade tumors (IHC score = 9.57±4.14) (p=0.3387) (Figure 42, 43). Nevertheless, these IHC data indicated that histone methylation, particularly H3K9me3 was changed in bladder cancer tissues.

Expression of HP1$\alpha$, a heterochromatin protein that recognizes histone H3K9me3 was corresponded well with histone H3K9me3 expression. HP1$\alpha$ expression level in cancerous tissues (IHC score = 8.21±2.72) was significantly higher than that in adjacent tissues (IHC score = 5.48±2.99) (*p*=0.0433) (Figure 44, 45). HP1$\alpha$ expression tended to decrease in high-grade tumors (IHC score = 6.95±2.55), but it didn't reach the statistical level compared to PUNLMP/low-grade tumors (IHC score = 8.96±2.71) (*p*=0.0508) (Figure 46, 47).
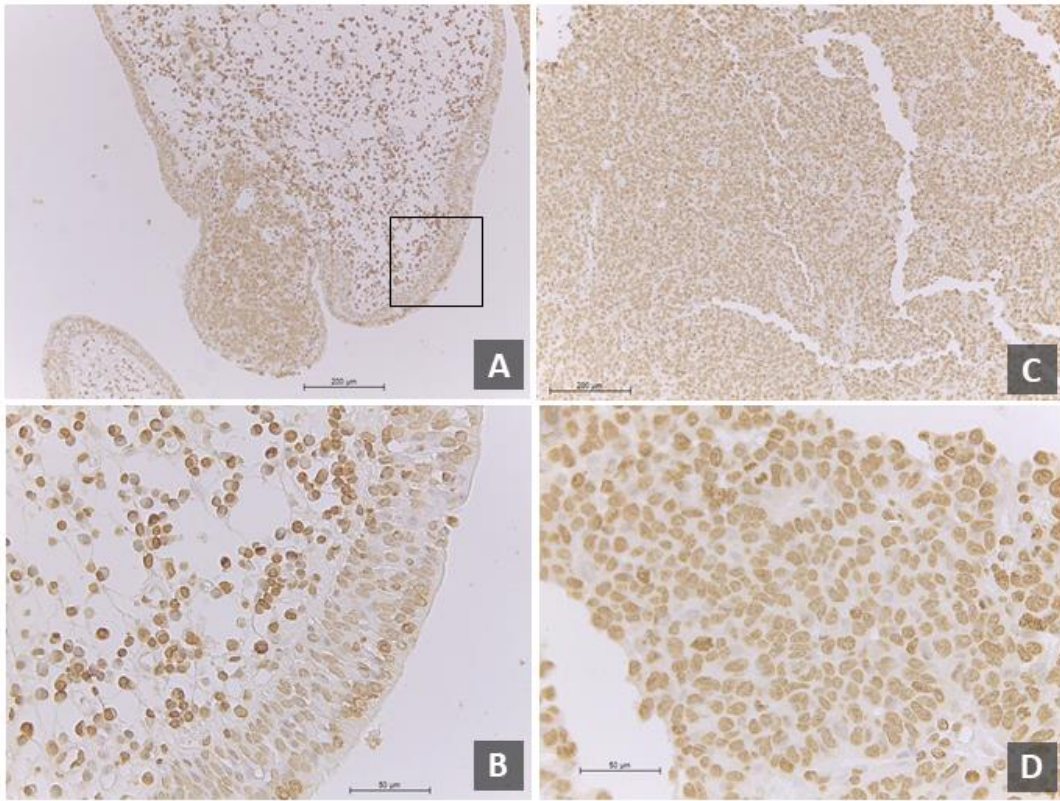
**Figure 40** Histone H3K9me3 expression in bladder cancer tissues. The expression of histone H3K9me3 in cancerous tissues (C, D) was higher than non-cancerous adjacent tissues (A, B). Magnification: 100x (A, C), 400x (B, D).
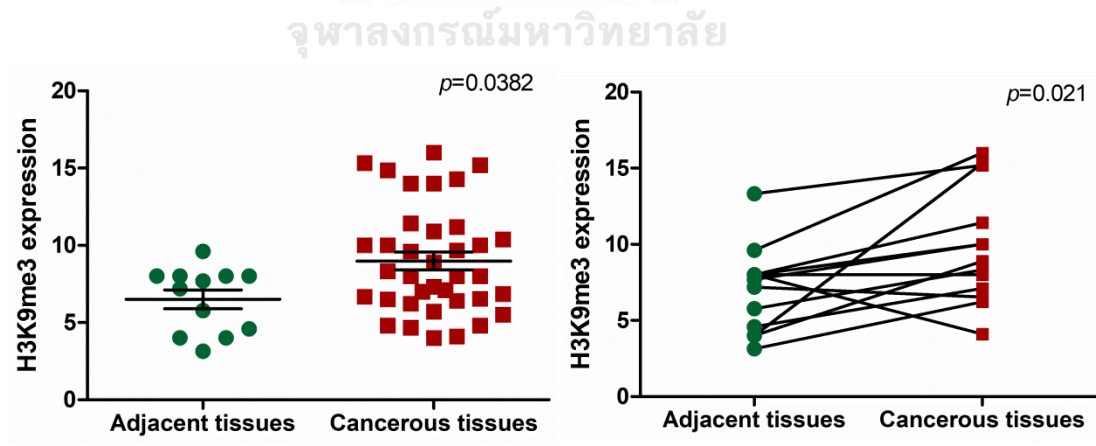


**Figure 41** Histone H3K9me3 expression in adjacent (green) and cancerous (red) tissues. Histone H3K9me3 expression in cancerous was significantly higher than non-cancerous adjacent tissues. Left: Overall comparison (Mann-Whitney U test) Right: Paired comparison (Paired $t$-test)

**Figure 42** Histone H3K9me3 expression in different stage of bladder cancer
Histone H3K9me3 expression was comparable between PUNLMP/low-grade (A, B)
and high-grade tumors (C, D). Magnification: 400x.



**Figure 43** Histone H3K9me3 expression in low grade (brown) and high grade (red)
tumors. Histone H3K9me3 expression was not significantly different between
PUNLMP/low-grade and high-grade tumors (Mann-Whitney U test).
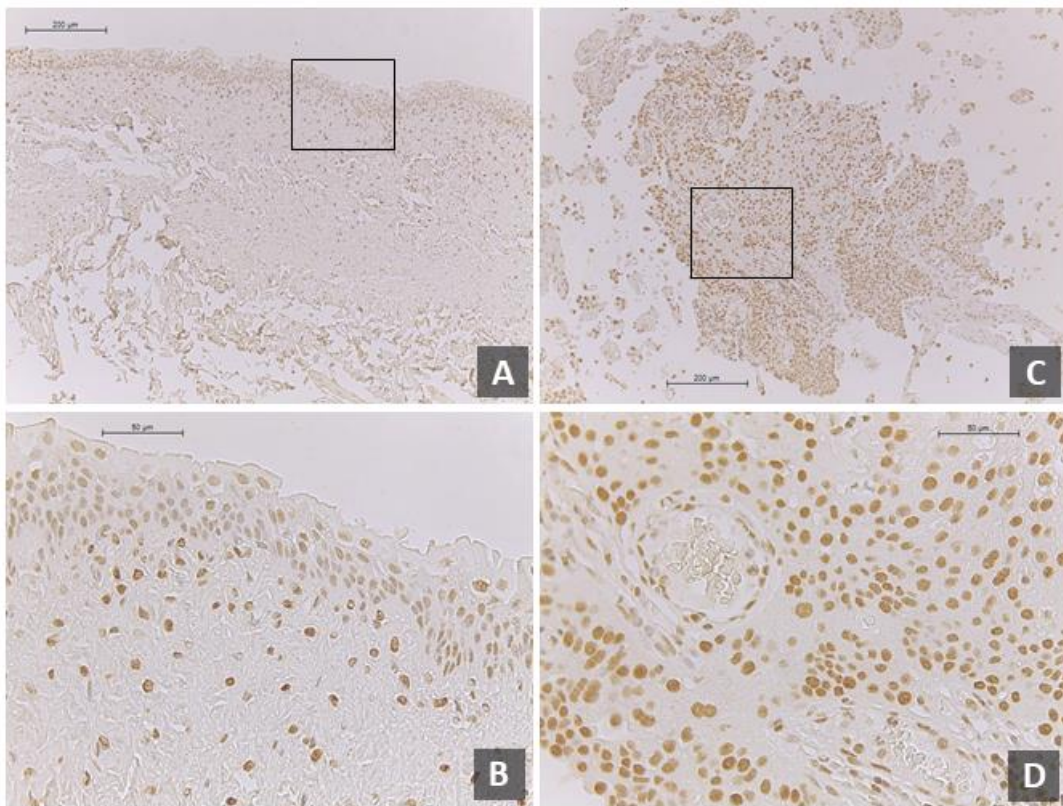
**Figure 44** HP1α expression in bladder cancer tissues.

The expression of HP1α in cancerous tissues (C, D) was higher than adjacent non-cancerous bladder tissues (A, B). Magnification: 100x (A, C), 400x (B, D).
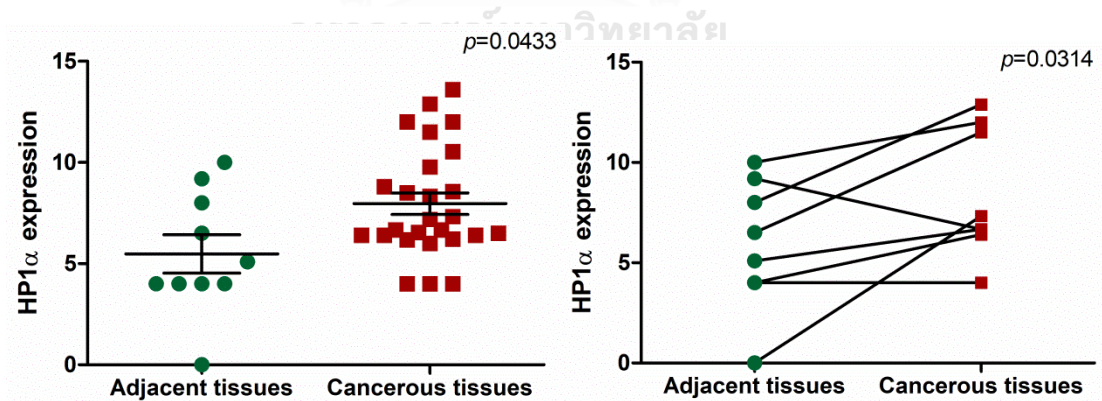


**Figure 45** HP1α expression level in adjacent (green) and cancerous (red) tissues

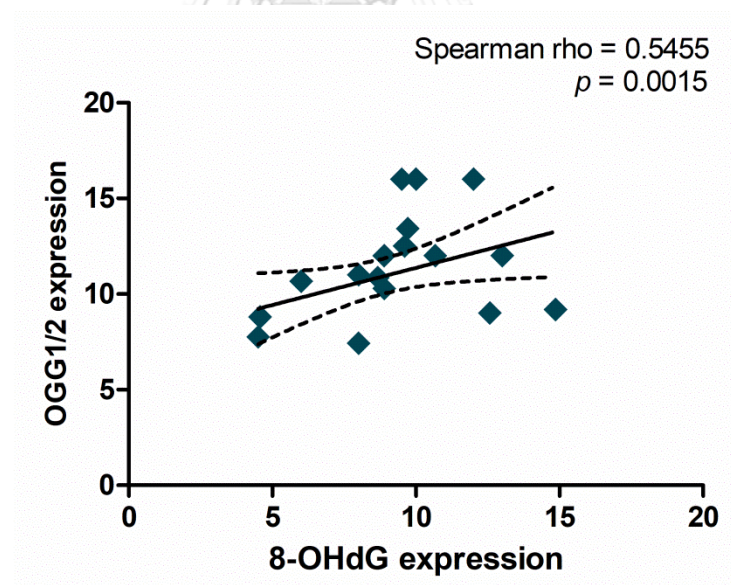HP1α expression in cancerous was significantly higher than non-cancerous adjacent

tissues. Left: Overall comparison (Mann-Whitney U test)

Right: Paired comparison (Paired *t*-test)
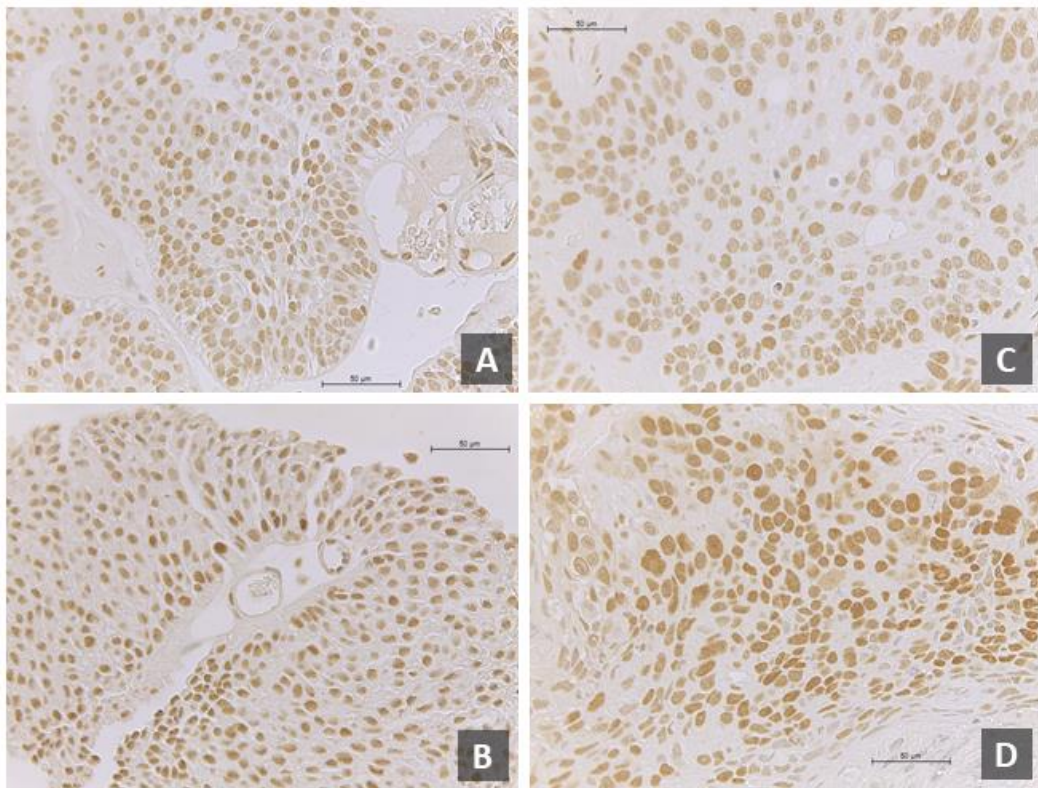
**Figure 46** HP1$\alpha$ expression in different stage of bladder cancer. HP1$\alpha$ expression was relatively similar between PUNLMP/low-grade (A, B) and high-grade tumors (C, D). Magnification: 400x.
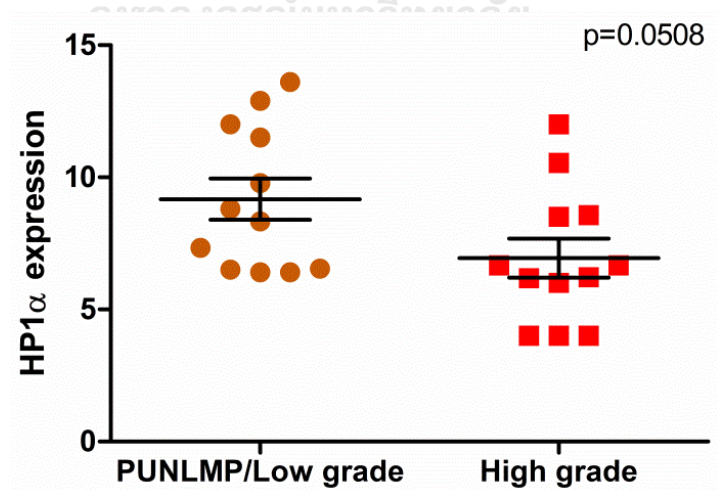


**Figure 47** HP1$\alpha$ expression in PUNLMP/low grade (brown) and high grade (red) tumors. HP1$\alpha$ expression was not significantly different between PUNLMP/low-grade and high-grade tumors (Mann-Whitney U test).

Association of H3K9me3 and HP1α expression with expression of oxidative DNA lesion 8-OHdG were additionally assessed. 8-OHdG expression was positively correlated with both histone H3K9me3 (Spearman rho = 0.4969, *p*=0.0021) and HP1α expression (Spearman rho = 0.4075, *p*=0.0388) (Figure 48). These indicated that change in heterochromatin formation was associated with oxidative stress. Perhaps, increased oxidative stress or DNA damage induces formation of condensed chromatin in bladder cancer tissues (Cann & Dellaire, 2011).

Table 6 summarized changes in IHC expression of each marker in bladder cancer tissues compared to non-cancerous adjacent tissues. The correlation matrix of all IHC staining markers in bladder cancer tissues is shown in Table 7.
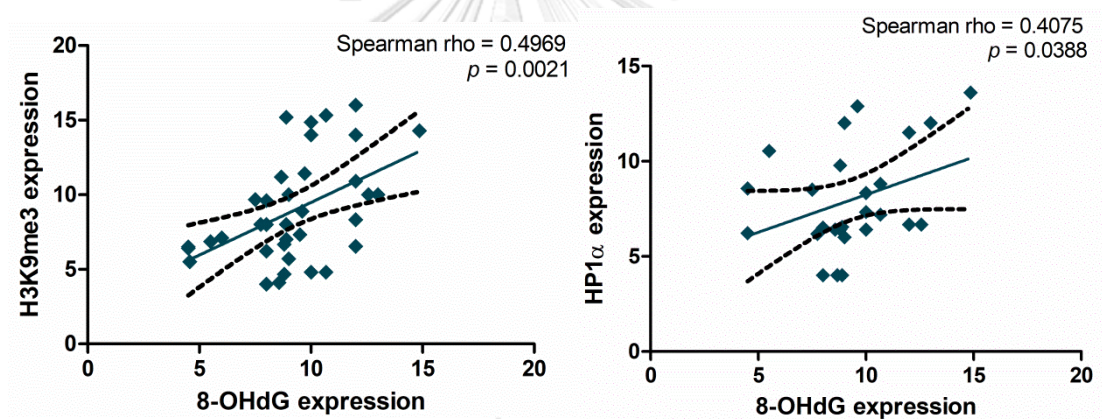


**Figure 48** Positive correlation between 8-OHdG and histone H3K9me3 expression (left) and 8-OHdG and HP1α expression (right). Increased 8-OHdG expression was statistically correlated with increased heterochromatin marks.

**Table 6** Summary result from immunohistochemistry staining in
bladder cancer tissues

| Antibody | Level in cancerous compared to adjacent | Level in high grade compared to low grade |
|---|---|---|
| 5-methylcytosine | Decreased** | Decreased** |
| LINE-1 ORF1p | Increased** | Increased** |
| 8-OHdG | Increased** | Decreased** |
| OGG1/2 | Increased** | Decreased |
| 4-HNE | Increased** | Decreased |
| Histone H3K9me3 | Increased** | Decreased |
| HP1$\alpha$ | Increased** | Decreased |

** = significant difference

**Table 7** Correlation matrix of all IHC staining in bladder cancer tissues

| | ORF1p | 8-OHdG | 4-HNE | OGG1/2 | H3K9me3 | HP1$\alpha$ |
|---|---|---|---|---|---|---|
| ORF1p | | | $r_s$=0.5882 $p$=0.0002 | | | |
| 8-OHdG | | | | $r_s$=0.5455 $p$=0.0015 | $r_s$=0.4969 $p$=0.0021 | $r_s$=0.4075 $p$=0.0388 |
| OGG1/2 | | $r_s$=0.5455 $p$=0.0015 | | | | |
| 4-HNE | $r_s$=0.5882 $p$=0.0002 | | | | | |
| H3K9me3 | | $r_s$=0.4969 $p$=0.0021 | | | | |
| HP1$\alpha$ | | $r_s$=0.4075 $p$=0.0388 | | | | |

$r_s$ = Spearman rho

**Cell viability of bladder cancer cell lines**

To examine the optimal concentrations of hydrogen peroxide ($H_2O_2$), tocopherol acetate (TA) and inhouse natural antioxidant regimen HydroZitLa (HZL) for bladder cancer cell lines, 2 bladder cancer cell lines including UMUC-3 and VMCUB1 were treated with various concentrations of each testing substance. MTT assay was performed after 72 hour treatment and, subsequently, cell viability (% of control) and inhibitory concentration 50% ($IC_{50}$) were analyzed.

Cell viability of UMUC-3 and VMCUB1 against $H_2O_2$ varying from 10 – 200 µM was exhibited in figure 49 showing that cell viability was significantly decreased at 20 µM in UMUC-3 and at 30 µM and higher concentrations in VMCUB1 when compared to untreated control. $IC_{50}$ of $H_2O_2$ was 35.99 µM for UMUC-3, but it was almost double (59.31 µM) for VMCUB1. This obviously indicated that UMUC-3 was more sensitive to $H_2O_2$ than VMCUB1. However, the sub-lethal doses of $H_2O_2$ were used for downstream experiments. Therefore, 20 µM and 30 µM $H_2O_2$ were selected for UMUC-3 and VMCUB1, respectively.
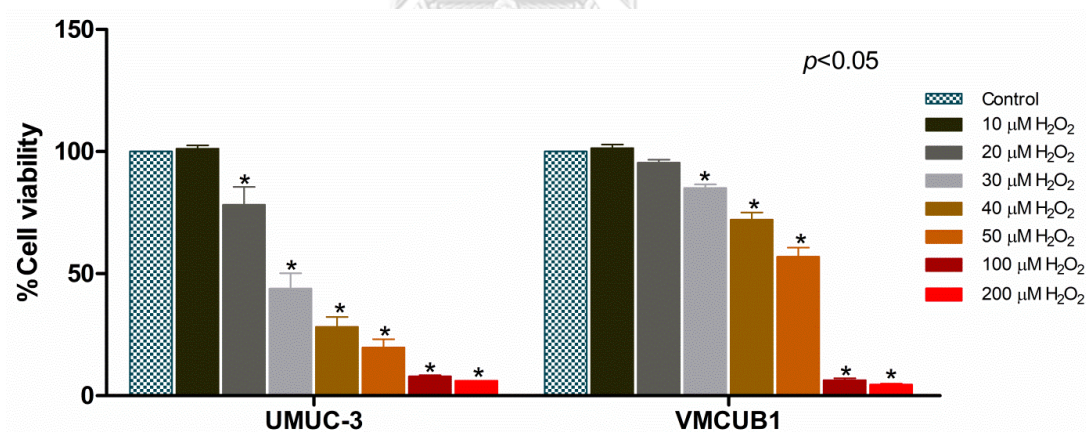


**Figure 49** Cell viability of bladder cancer cell lines against $H_2O_2$

In further experiments, sub-toxic doses of 20 µM and 30 µM $H_2O_2$ were selected for UMUC-3 and VMCUB1, respectively. (* $p<0.05$ vs. control)

The toxicity of antioxidant substances, TA and HZL, was also investigated. TA or vitamin E was applied as a standard antioxidant. HZL is the natural antioxidants-derived regimen developed in our group. One of main ingredient of HZL is alpha-lipoic acid which is a well-known antioxidant involving in inhibitory effect of ROS

production (Hwang et al., 2016). As shown in figure 50, tocopherol acetate, varying from 150 – 2400 µM, showed no toxicity to both UMUC-3 and VMCUB1. However, TA at 600 µM was chosen for further experiment to compete with $H_2O_2$ in co-culture treatment.
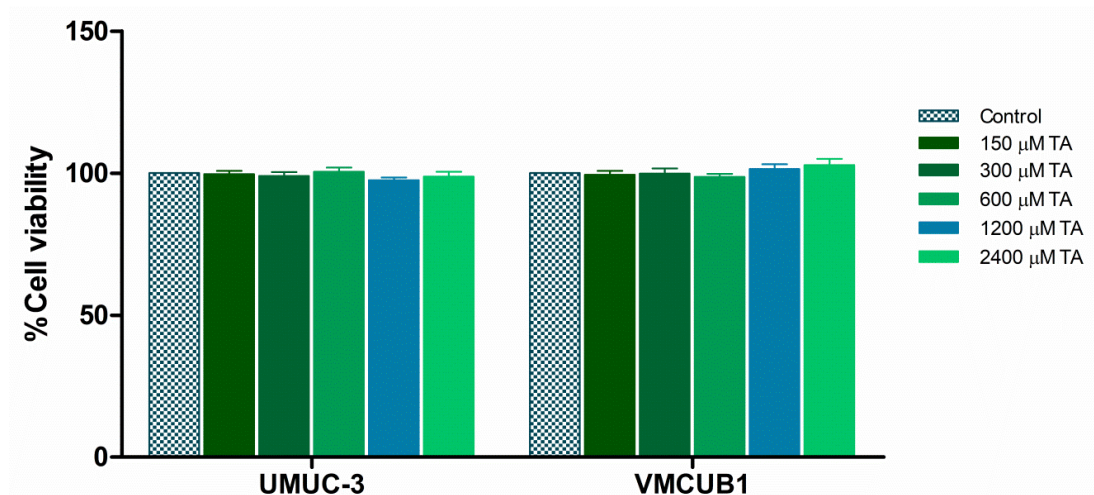


**Figure 50** Cell viability of bladder cancer cell lines against tocopherol acetate (TA). TA at various concentrations from 150-2400 µM, was not significantly toxic to UMUC-3 and VMCUB1.

Cell viability of bladder cancer cell lines against various concentrations of HZL (from 10% - 100% (v/v)) was shown in figure 51. In UMUC-3 comparing to untreated control, cell viability was significantly decreased at 20% HZL. Unlike in VMCUB1, cell viability was significantly decreased at 30% HZL. At low concentrations of HZL (10 - 20%), it significantly induced cell proliferation in VMCUB1, as it showed significantly higher cell viability in the treated cells than the untreated control. $IC_{50}$ values of HZL were 31.32% and 33.99% for UMUC-3 and VMCUB1, respectively. To attenuate oxidative stress induced by $H_2O_2$ in cell culture experiments, 10% HZL was selected to use in both UMUC-3 and VMCUB1.
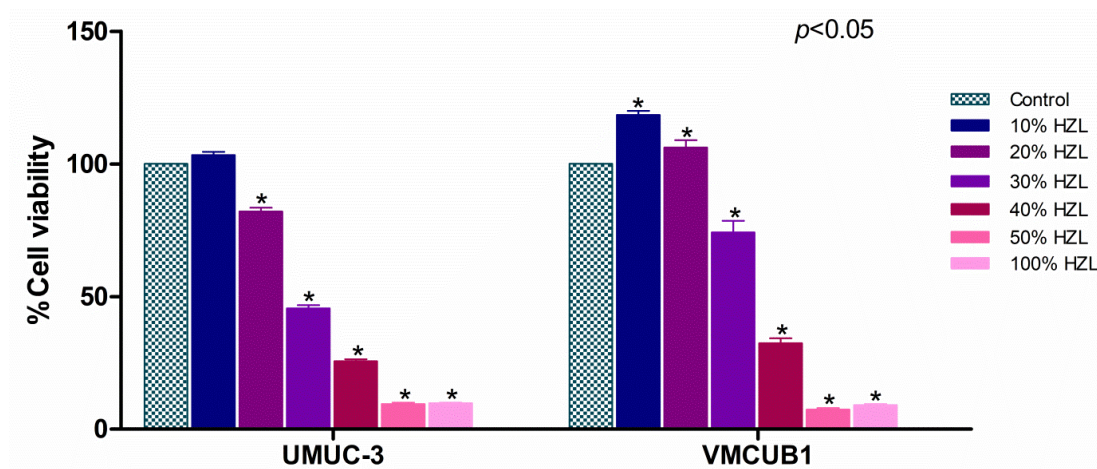
**Figure 51** Cell viability of bladder cancer cell lines against HydroZitLa (HZL)
The 10% HZL was used for both UMUC-3 and VMCUB1 in further experiments.
(* $p<0.05$ vs. control)

## $H_2O_2$ induced oxidative stress in bladder cancer cell lines

To induce the oxidative stress in bladder cancer cell lines, UMUC-3 and VMCUB1 were treated with sub-lethal doses of $H_2O_2$ for 72 hours. Co-treatment with antioxidants (TA and HZL) was used as inhibition model. Two assays were performed afterwards including DCFH-DA and protein carbonyl assay as oxidative stress markers.

The intracellular ROS production was determined by DCFH-DA assay showing that the arbitrary fluorescent unit (AFU that indicates amount of generated ROS) in cells treated with $H_2O_2$ alone, 20 µM in UMUC-3 and 30 µM in VMCUB1, were significantly increased compared to untreated control (Figure 52). Conversely, AFU was decreased in cells co-treated with 600 µM TA and significantly decreased in cells co-treated with 10% HZL compared to cells treated with $H_2O_2$. These results indicated that $H_2O_2$ at sub-lethal concentrations could induce intracellular ROS production in both UMUC-3 and VMCUB1, and the antioxidants, especially HZL could restrain intracellular ROS production induced by $H_2O_2$.
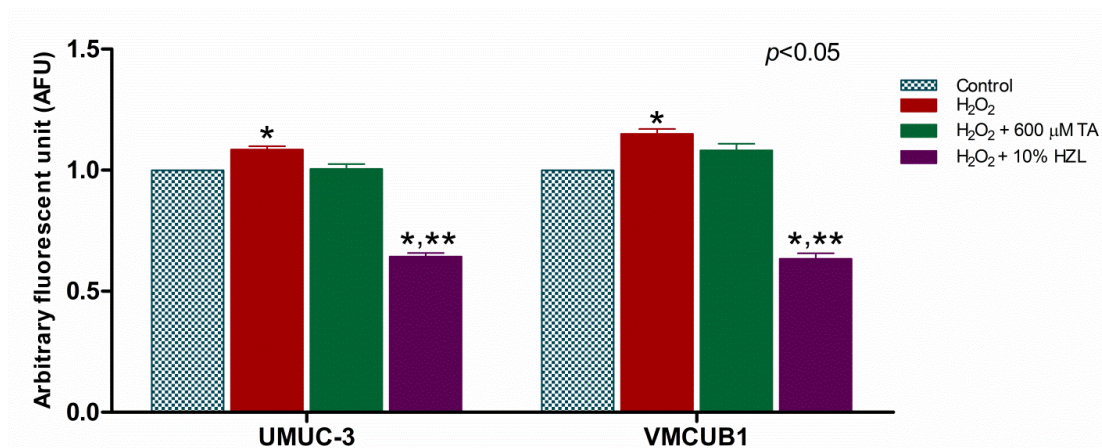
**Figure 52** Intracellular ROS production in bladder cancer cell lines by DCFH-DA assay
The intracellular ROS production was induced by $H_2O_2$, but significantly attenuated
by the antioxidants. (* $p<0.05$ vs. untreated control, ** $p<0.05$ vs. $H_2O_2$-treated cells)

Level of oxidative stress can be monitored by protein carbonyl assay, as
carbonylated proteins are byproducts of protein oxidation. As shown in figure 53, the
level of protein carbonyl content was increased in VMCUB1 treated with 30 μM $H_2O_2$
and significantly increased in UMUC-3 treated with 20 μM $H_2O_2$ compared to the
untreated control. However, the antioxidants, 600 μM TA and 10% HZL, significantly
reduced the protein carbonyl content in both UMUC-3 and VMCUB1 relative to the
$H_2O_2$ treated condition. These results showed that $H_2O_2$ at sub-lethal concentrations
could induce oxidative stress. On the other hand, co-treatment with antioxidants
could reduce the oxidative stress and prevent oxidative damage in bladder cancer
cells.

Together with DCFH-DA assay, it could be concluded that $H_2O_2$ at sub-lethal
doses could induce the oxidative stress by triggering the intracellular ROS production
leading to the oxidative damage in bladder cancer cell lines. Moreover, co-treatment
with the antioxidants was beneficial in preventing the oxidative stress by reducing the
intracellular ROS production that further results in decreased oxidative damage in
cell culture.
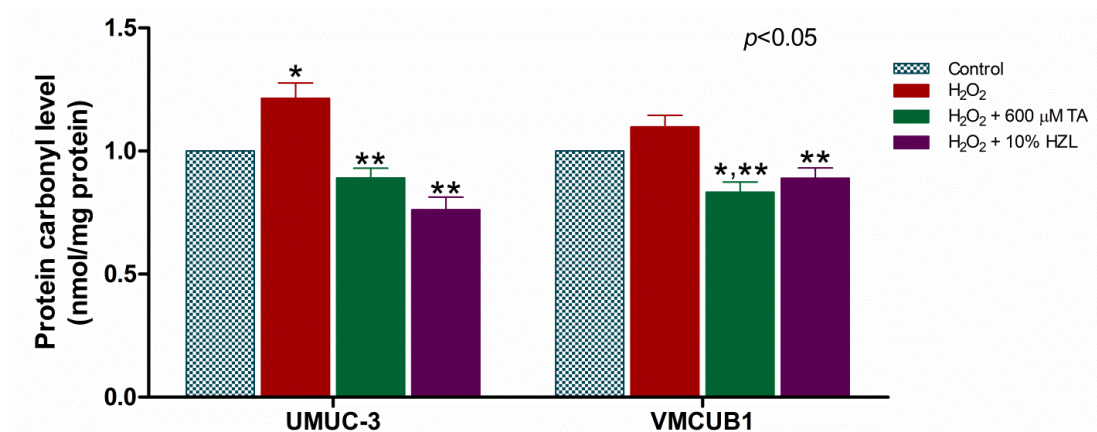
**Figure 53** Protein carbonyl level in bladder cancer cell lines by protein carbonyl assay. The protein carbonyl level was increased in $H_2O_2$-treatment, but significantly decreased in co-treatment with the antioxidants.

(\* $p < 0.05$ vs. untreated control, \*\* $p < 0.05$ vs/ $H_2O_2$-treated condition)

**The formation of 8-OHdG on LINE-1 promoter in bladder cancer cell lines**

DNA can be oxidized by ROS especially at deoxyguanosine (G) base resulting in 8-OHdG formation. In this study, DNA was extracted from UMUC-3 and VMCUB1 after 72-hour treatment followed by 8-OHdG immunoprecipitation (IP) to isolate 8-OHdG-rich DNA. Thereafter, LINE-1 amplification of IP DNA was quantified by qPCR to monitor DNA lesions. Since DNA polymerase activity can be blocked by DNA adducts (Furda et al., 2014), therefore, higher 8-OHdG lesions on DNA templates expectedly leads to a lower qPCR amplification.

First of all, formation of 8-OHdG on genomic DNA of cells treated with $H_2O_2$ was visualized by immunofluorescent staining. Comparing to untreated cells, 8-OHdG expression was slightly increased in bladder cancer cells treated with $H_2O_2$ (Figure 54, 55) indicating that $H_2O_2$ at sub-lethal dose could trigger oxidative DNA damage formation at some extent on genomic DNA. Formation of 8-OHdG in $H_2O_2$-treated cells was not markedly increased. It is possible that base excision repair (BER) is activated in cells exposed to non-toxic dose of $H_2O_2$ in order to fix the oxidized lesions. This might be the reason why expression of 8-OHdG in bladder cancer cells exposed to the sub-toxic dose of $H_2O_2$ was not drastically increased.
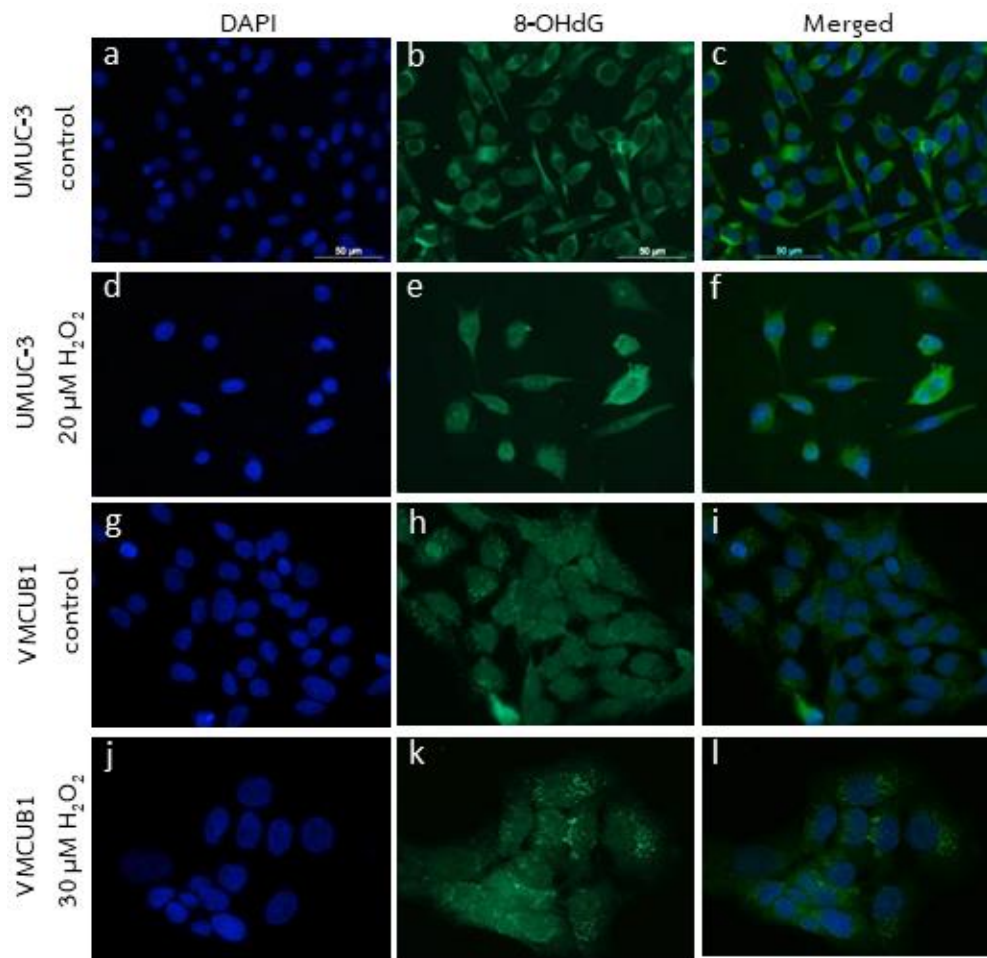
**Figure 54** Oxidative DNA damage in bladder cancer cell lines. 8-OHdG expression was slightly increased in cells treated with sub-lethal dose of $H_2O_2$ (Magnification = 400x). (a-c = UMUC-3 control, d-f = UMUC-3 with $H_2O_2$ treatment, g-l = VMCUB1 control, j-l = VMCUB1 with $H_2O_2$ treatment)
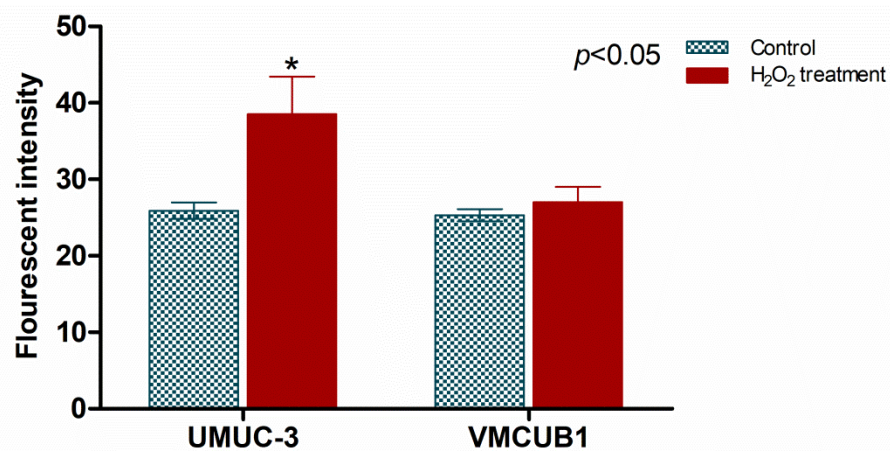


**Figure 55** Fluorescent intensity of 8-OHdG expression in bladder cancer cells. 8-OHdG expression was increased in cells treated with $H_2O_2$.

According to the qPCR result, LINE-1-5' (5'-UTR promoter) amplification was significantly decreased in $H_2O_2$-treated cells compared to the untreated control in both UMUC-3 and VMCUB1. Co-treatment with the antioxidants (TA and HZL) showed a slight increase in LINE-1-5' amplification relative to the $H_2O_2$-treated condition (Figure 56). The detected lesion on LINE-1 promoter was calculated relative to untreated control showing that the lesions on LINE-1-5' in both UMUC-3 and VMCUB1 (1.85 and 1.07 lesions/amplicon, respectively) were significantly increased in $H_2O_2$-treated cells compared to untreated cells (Figure 57). In VMCUB1, the lesions were significantly decreased by HZL co-treatment (0.43 lesions/amplicon) compared to the $H_2O_2$-treated condition (Figure 57). These results suggested that $H_2O_2$ could considerably induce formation of 8-OHdG lesions on LINE-1 promoter.
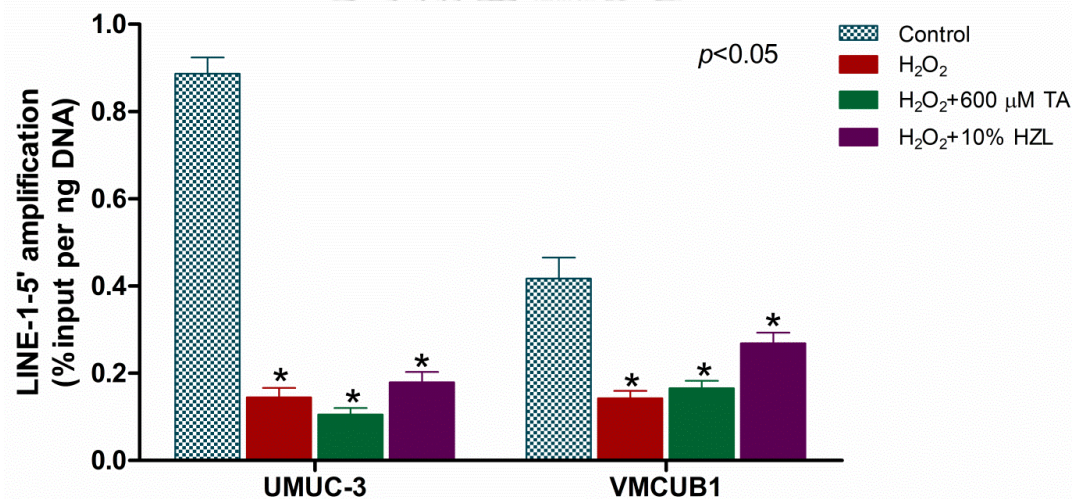


**Figure 56** The amplification of LINE-1 promoter in 8-OHdG IP DNA

LINE-1-5' amplification was significantly reduced in $H_2O_2$ treated cells compared to control. (* $p < 0.05$ vs. control)
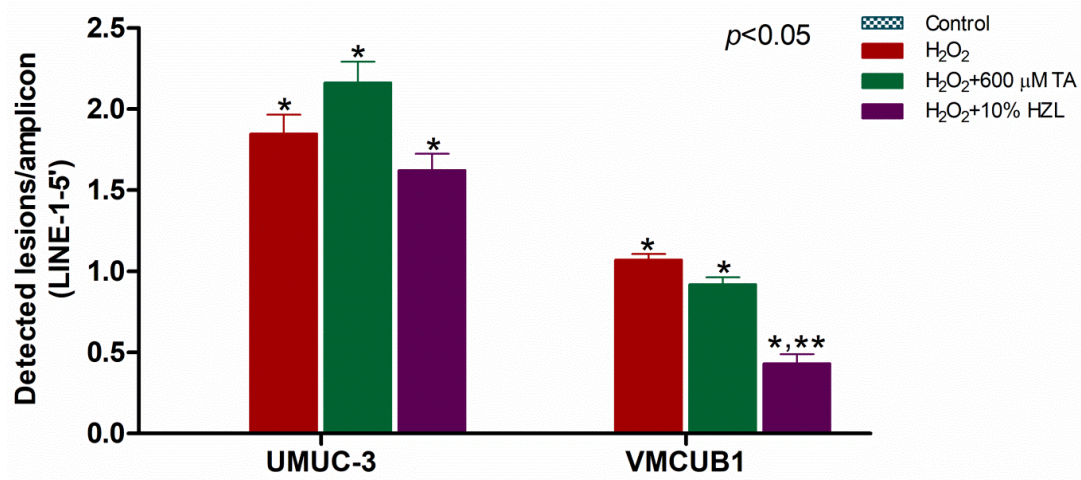
**Figure 57** The detected lesions on LINE-1 promoter in 8-OHdG IP DNA

The relative number of lesions on LINE-1-5' was significantly increased in $H_2O_2$ treated cells compared to the untreated control. HZL efficiently inhibited the lesion formation in VMCUB-1 exposed to $H_2O_2$.

(* $p<0.05$ vs. control, ** $p<0.05$ vs $H_2O_2$ treatment)

In addition to LINE-1-5', qPCR amplifications of LINE-1-3' (3'-UTR of LINE-1) and GAPDH of IP DNA were also investigated. Similar to LINE-1-5', the amplification of LINE-1-3' was significantly reduced in $H_2O_2$-treated cells comparing to untreated control in UMUC-3. In VMCUB1, co-treatment with the antioxidants, especially with 10% HZL, showed the increase in LINE-1-3' amplification compared to $H_2O_2$ treatment (Figure 58). As shown in figure 59, the detected lesions were significantly increased in $H_2O_2$ treated cells (0.65 lesions/amplicon in UMUC-3 and 0.32 lesions/amplicon in VMCUB1), but significantly decreased in VMCUB1 co-treated with antioxidants (0.07 lesions/amplicon in TA treatment and no lesion detected in HZL treatment).

For GAPDH amplification, it was decreased in $H_2O_2$ treatment as well. The lesions detected on $H_2O_2$ treated cells in UMUC-3 and VMCUB1 (0.85 and 0.42 lesions/amplicon, respectively) were shown in figure 60 and 61. Taken together, these results suggested that $H_2O_2$ oxidized the G bases not only on LINE-1 element, but, generally, also on other regions of genomic DNA. However, the antioxidants

showed promising role in preventing oxidative DNA lesion formation on LINE-1 elements and genomic DNA.
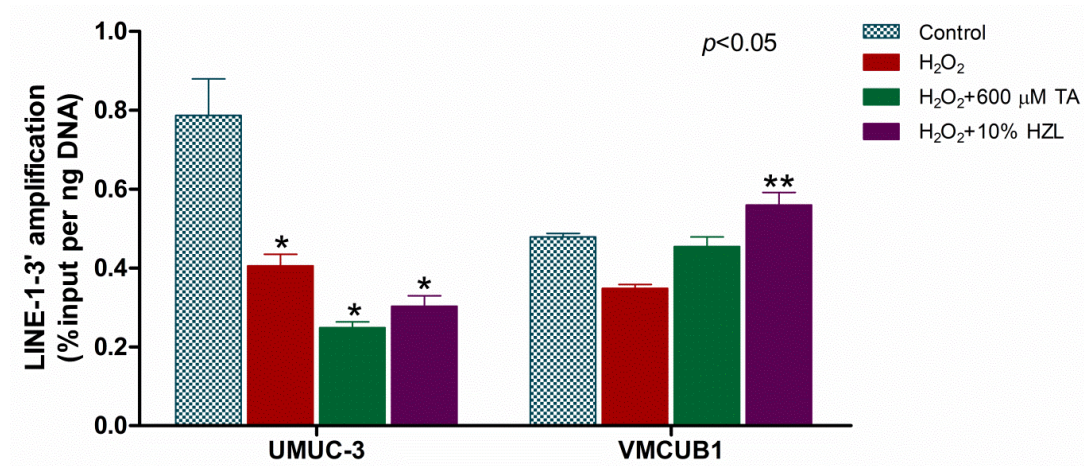


**Figure 58** The amplification of LINE-1 element in 8-OHdG IP DNA

LINE-1-3' amplification was significantly reduced in $H_2O_2$ treated cells.

(* $p<0.05$ vs. control, ** $p<0.05$ vs. $H_2O_2$ treatment)
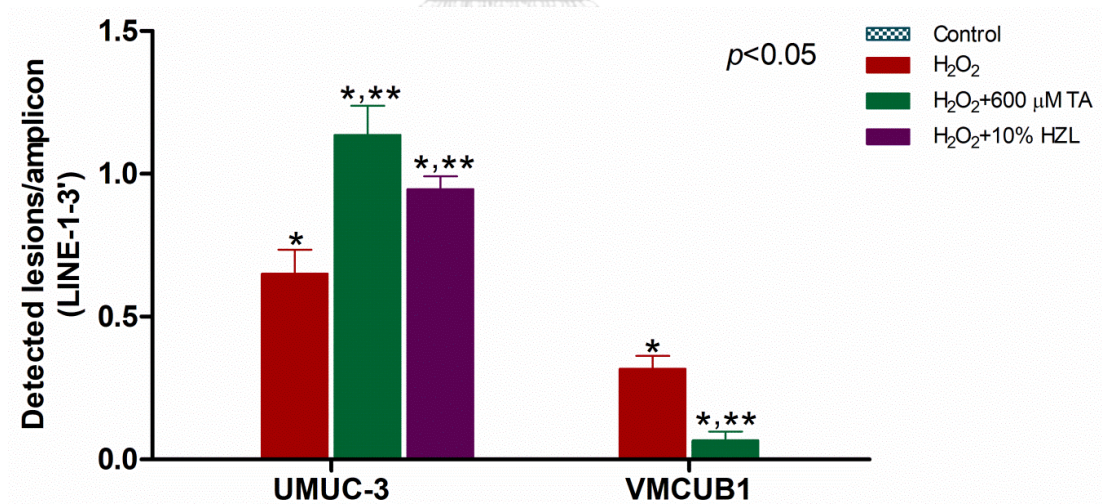


**Figure 59** The detected lesions on LINE-1 elements in 8-OHdG IP DNA

The lesion on LINE-1-3' was significantly increased in $H_2O_2$ treated cells compared to control. (* $p<0.05$ vs. control, ** $p<0.05$ vs $H_2O_2$ treatment)
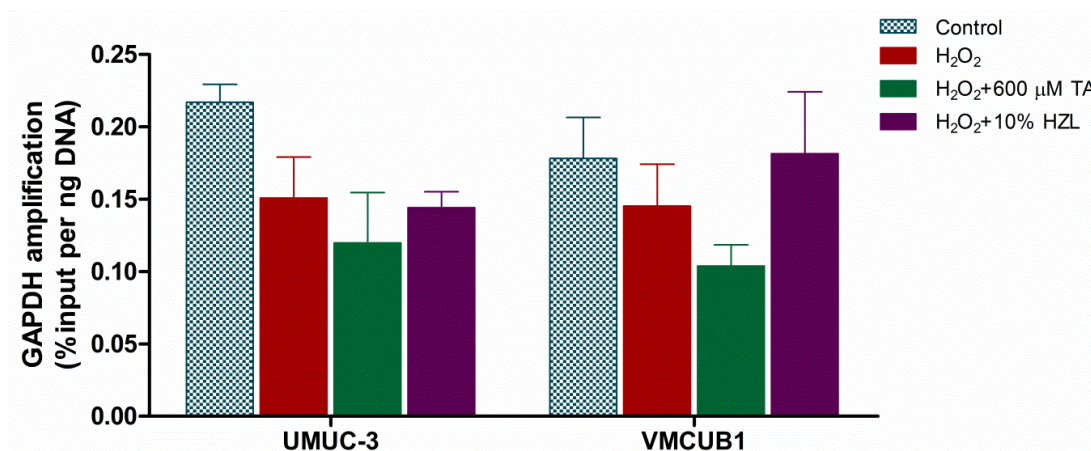
**Figure 60** The amplification of GAPDH in 8-OHdG IP DNA

GAPDH amplification was decreased in $H_2O_2$ treated cells compared to control.
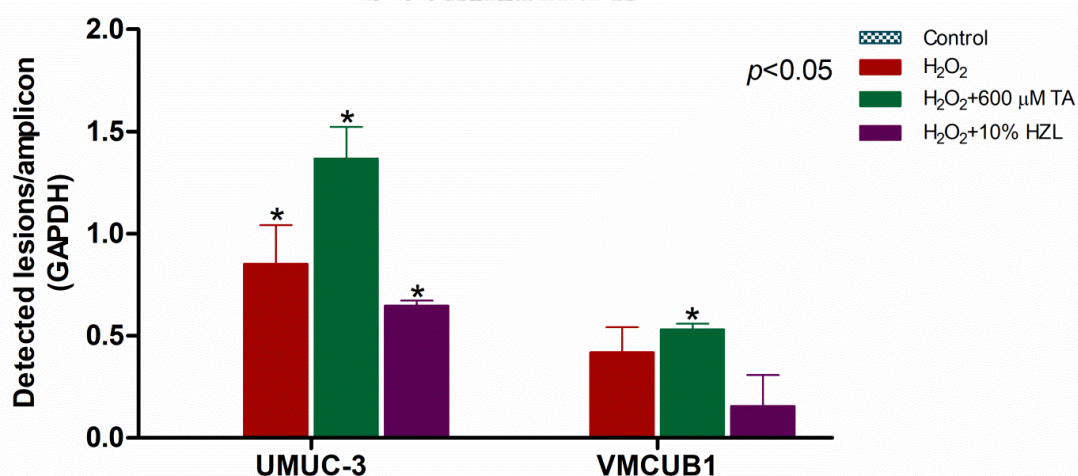


**Figure 61** The lesion on GAPDH was significantly increased creased in $H_2O_2$ treated cells compared to control (* $p<0.05$ vs. control).

As 8-OHdG was increased under oxidative stress condition, expression of OGG1/2 (BER relating enzyme) in $H_2O_2$-treated UMUC-3 and VMCUB1 was further investigated by western blot. It was found that the expression of OGG1/2 was slightly increased in $H_2O_2$ treatment in both UMUC-3 and VMCUB1 and this increment was decreased in VMCUB1 co-treated with TA (Figure 62, 63). However, comparing between these two cell lines, it showed that OGG1/2 expression in UMUC-3 was obviously higher than VMCUB1. This related well to their level of oxidative DNA

lesions that found that the DNA lesions in VMCUB1 were higher than in UMUC-3. Thus, these *in vitro* data suggested that ROS augmented oxidative DNA lesions and activated expression of OGG1/2 in response to DNA damage lesion formation.
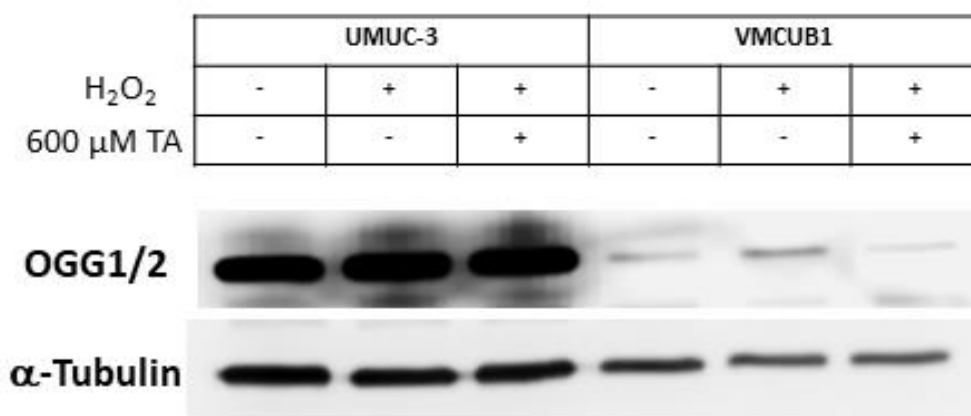


**Figure 62** Western blot analysis of OGG1/2 expression in bladder cancer cell lines OGG1/2 expression was slightly increased in $H_2O_2$ treatment compared to the untreated control.
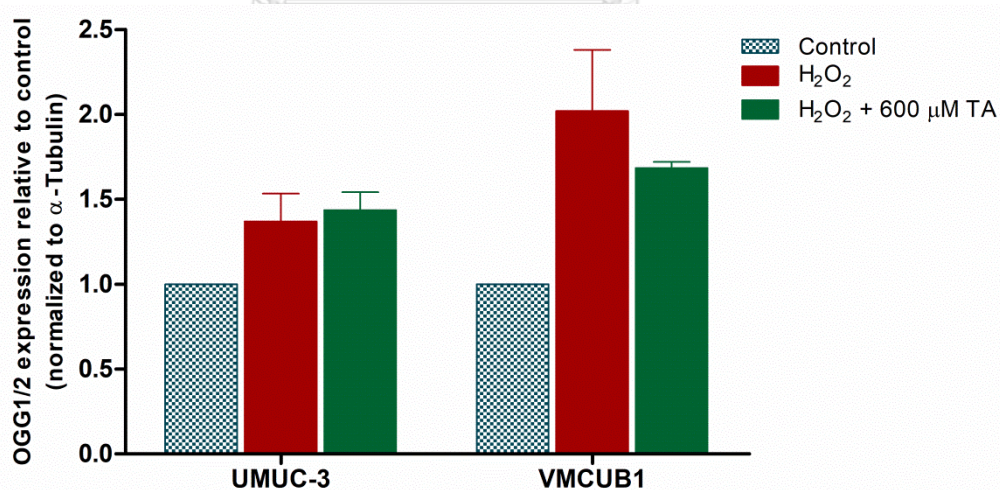


**Figure 63** The expression of OGG1/2 in bladder cancer cell lines relative to control OGG1/2 expression was slightly increased in $H_2O_2$ treatment compared to control.

**Oxidative stress induced LINE-1 hypomethylation in bladder cancer cell lines**

The methylation level of 5'-UTR LINE-1 promoter at 4 CpG sites was analyzed in $H_2O_2$-treated cells (for 72 hours) by Pyrosequencing assay. In UMUC-3, the overall methylation level of LINE-1 promoter was 69.25% in untreated control whereas it was decreased to 64.75% in $H_2O_2$ treatment (Figure 64). The methylation levels were reduced in all four CpG sites. LINE-1 methylation level in UMUC-3 co-treated with TA was restored to 68.25%. Methylations of all 4 CpG sites were increased.

In comparison with UMUC-3, the overall LINE-1 methylation in VMCUB1 was greatly lower (69.25% in UMUC-3 and 40.5% in VMCUB1). The average LINE-1 methylation level in VMCUB1 untreated control was 40.5%. However, the methylation level in $H_2O_2$ treatment was reduced in 3 CpG sites and, in overall, it was slightly decreased to 40%. The methylation of 3 CpG sites were restored in cells co-treated with TA and the overall LINE-1 methylation was increased to 40.5% (Figure 65). Taken together, the findings suggested that $H_2O_2$ could reduce the methylation level of LINE-1 promoter that further led to LINE-1 hypomethylation in bladder cancer cell lines, particularly in UMUC-3. On the other hand, the antioxidant possibly prevented or restored the methylation level of LINE-1 promoter in bladder cancer cells.
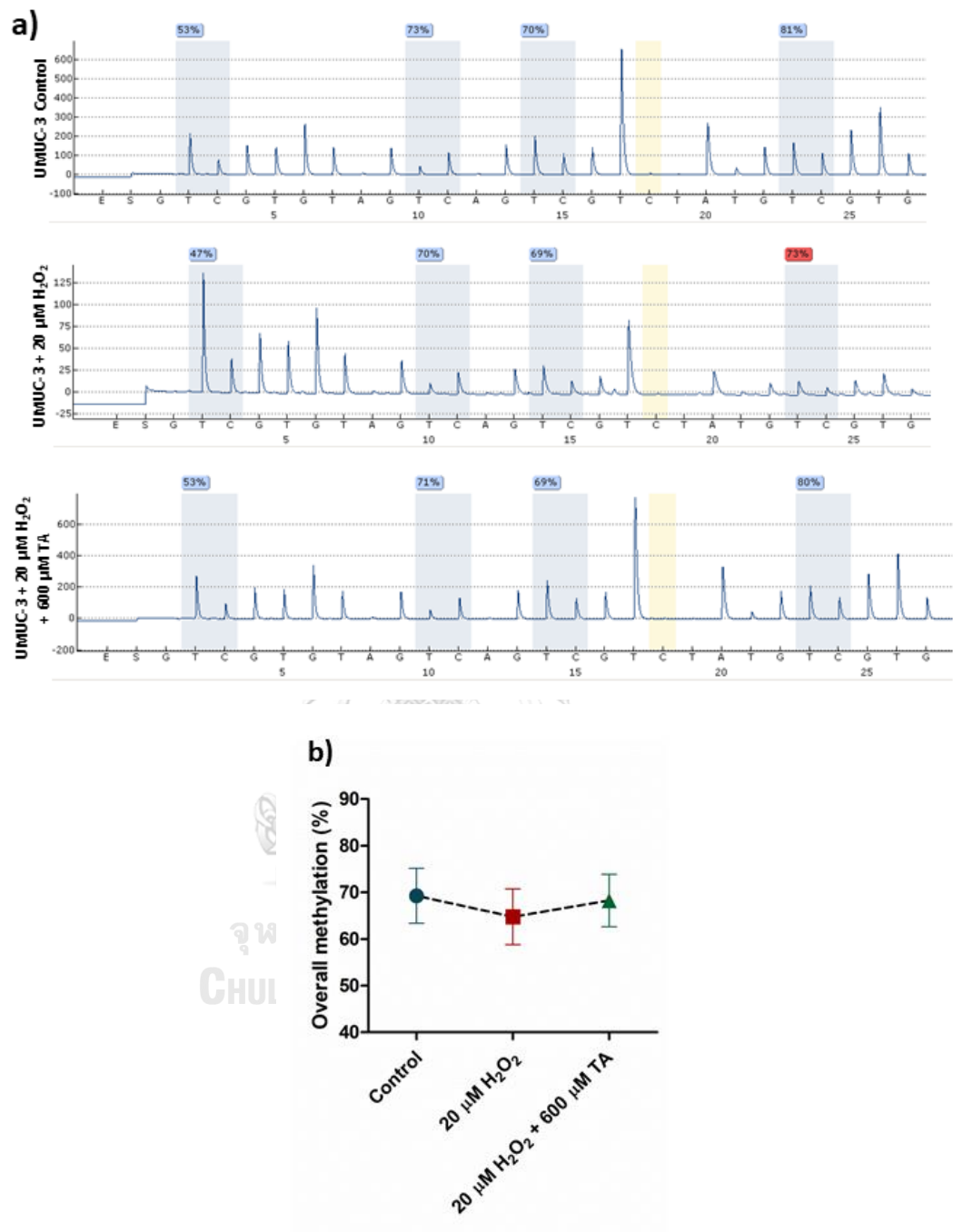
**Figure 64** LINE-1 methylation analysis by Pyrosequencing in UMUC-3

a) Pyrogram showed methylation level (%) in 4 CpG sites of 5'-UTR LINE-1 promoter

b) The overall methylation level (%) averaged from 4 CpG sites showed decreased

LINE-1 methylation level in $H_2O_2$ treatment.
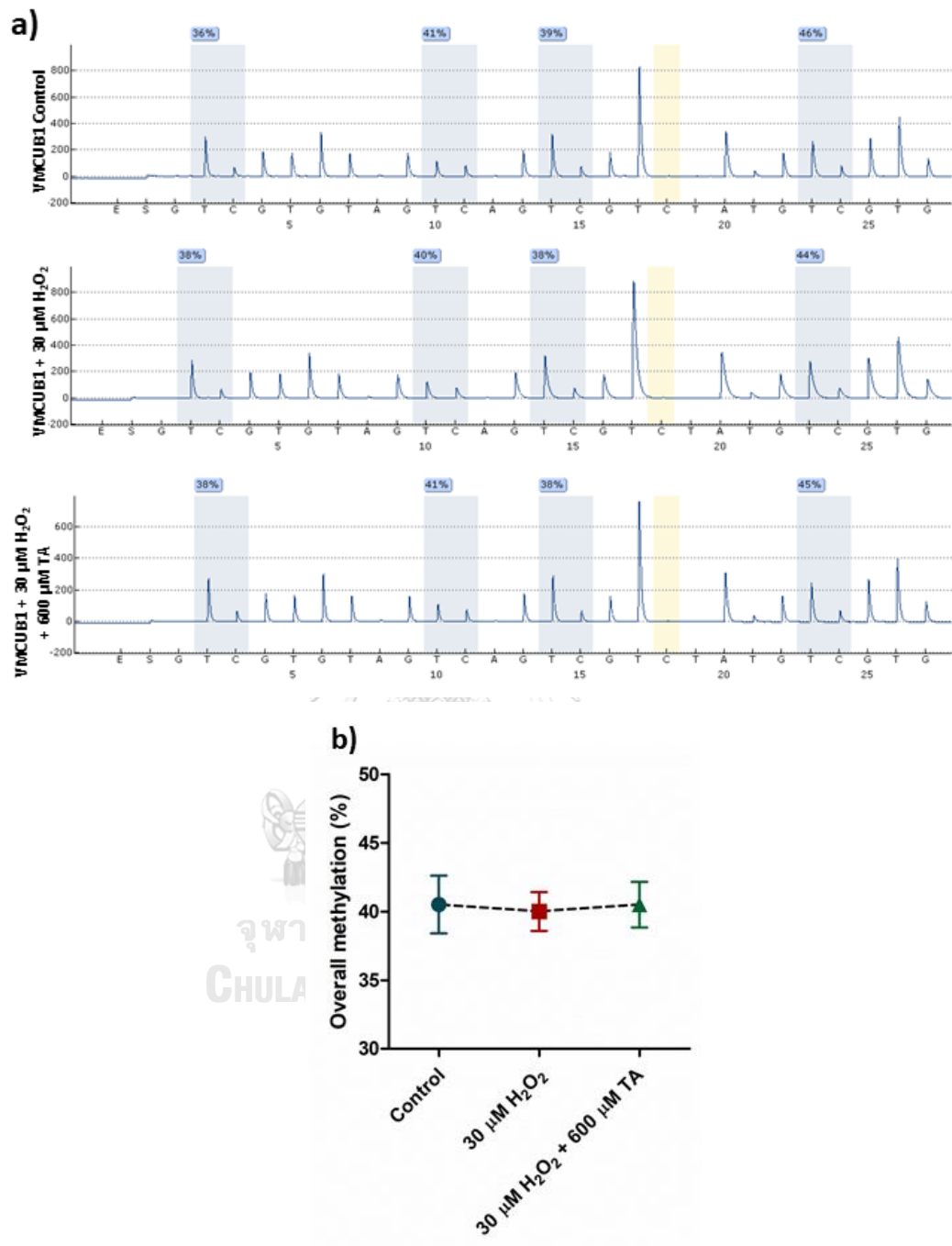
**Figure 65** LINE-1 methylation analysis by Pyrosequencing in VMCUB1

a) Pyrogram showed methylation level (%) in 4 CpG sites of 5'-UTR LINE-1 promoter

b) The overall methylation level (%) averaged from 4 CpG sites showed

slight decreased LINE-1 methylation level in $H_2O_2$ treatment.

The expression of Dnmt1, one of DNA methyltransferase enzymes, was also determined by western blot. Dnmt1 expression was increased in UMUC-3 treated with $H_2O_2$, but it was not significantly changed in VMCUB1 (Figure 66). Therefore, this could be assumed that oxidative stress possibly alter the methylation activity of Dnmt1 resulting in LINE-1 hypomethylation in bladder cancer cell lines.



| | UMUC-3 | | | VMCUB1 | | |
|---|---|---|---|---|---|---|
| $H_2O_2$ | - | + | + | - | + | + |
| 600 µM TA | - | - | + | - | - | + |
| Dnmt1 | | | | | | |
| α-Tubulin | | | | | | |
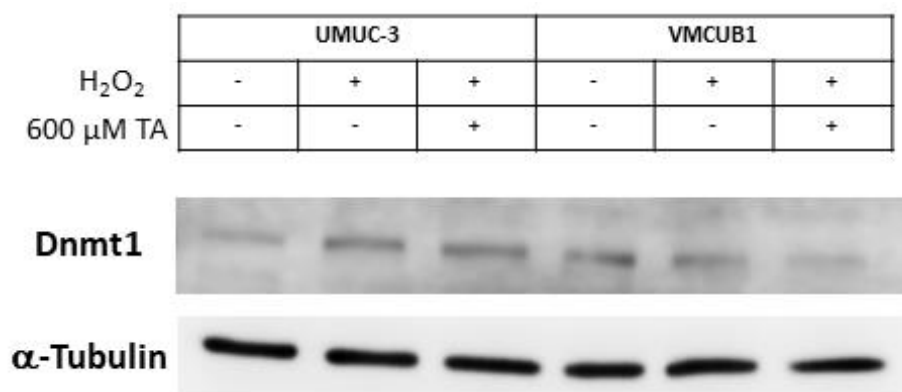
**Figure 66** Western blot analysis of Dnmt1 expression in bladder cancer cell lines Dnmt1 expression was altered in $H_2O_2$-treated UMUC-3 cells, but it did not change in VMCUB1 treated with $H_2O_2$.

LINE-1 ORF1p expression was also explored in $H_2O2$-treated bladder cancer cells. Western blot analysis showed that ORF1p expression was undetectable in UMUC-3 in all treated conditions. In contrast, VMCUB1 showed significantly higher ORF1p expression in $H_2O_2$ treatment compared to the untreated control and co-treatment with TA (Figure 67, 68). This indicated that $H_2O_2$ slightly induced LINE-1 ORF1p expression in VMCUB1. Clearly, $H_2O_2$ was not able to induce de novo expression of ORF1p in UMUC-3 cells. It is interesting to note that the difference in ORF1p expression between UMUC-3 and VMCUB1 might be in regard to the methylation level of LINE-1 promoter since LINE-1 promoter methylation in UMUC-3 (69.25%) was obviously higher than VMCUB1 (40.5%).

| | UMUC-3 | | | VMCUB1 | | |
|---|---|---|---|---|---|---|
| H$_2$O$_2$ | - | + | + | - | + | + |
| 600 µM TA | - | - | + | - | - | + |
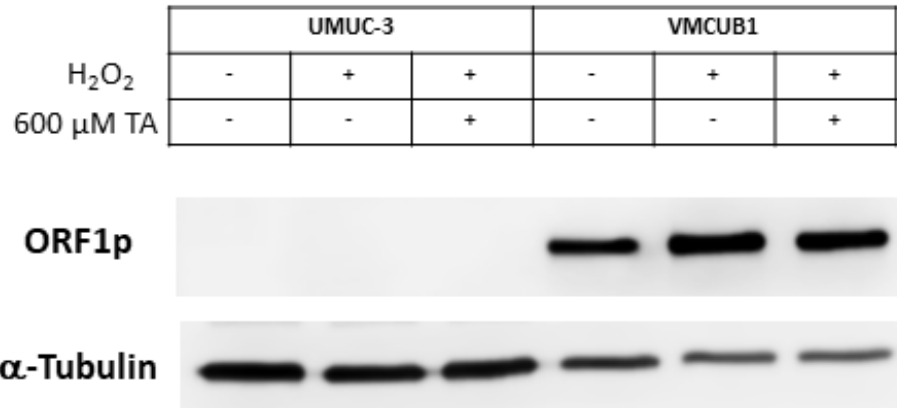
**Figure 67** Western blot analysis of LINE-1 ORF1p expression in bladder cancer cell lines. ORF1p expression was undetectable in UMUC-3. However, H$_2$O$_2$ significantly induced ORF1p expression in VMCUB1.
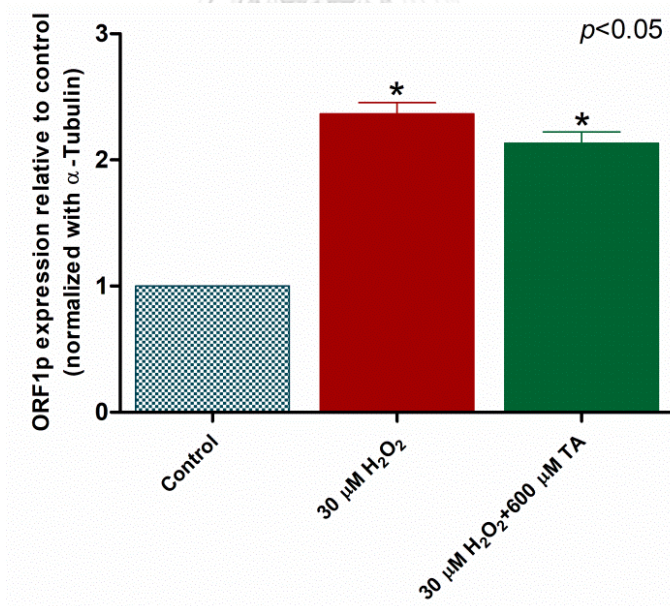


**Figure 68** The expression of LINE-1 ORF1p in VMCUB1 exposed to H$_2$O$_2$ ORF1p expression was significantly increased in H$_2$O$_2$ treatment compared to untreated control.

**LINE-1 ORF1p expression in bladder cancer cell lines through histone modification**

LINE-1 ORF1p expression was explored in various bladder cancer cell lines. It showed that the expression level was varied among cell lines. According to ORF1p expression levels, 4 bladder cancer cell lines were chosen for this study consisting of UMUC-3 as no (undetectable) ORF1p expression, RT112 as low ORF1p expression, VMCUB1 as high ORF1p expression and BFTC905 as very high ORF1p expression.

Cells were treated with $H_2O_2$ at sub-lethal concentrations (20-30 µM) for 72 hours, subsequently LINE-1 mRNA and ORF1p protein expressions were analyzed by qPCR and western blot analyses, respectively. The results showed that LINE-1 transcript expression was different between cell lines. UMUC-3 had the lowest expression followed by RT112 and VMCUB1 and BFTV905. Additionally, $H_2O_2$ slightly induced LINE-1 mRNA expression in UMUC-3, RT112 and VMCUB1 but it was reduced in BFTC905 compared to the untreated control (Figure 69). Western blot analysis showed similar results with mRNA expression (Figure 70). ORF1p expression was undetectable in UMUC-3 and low expressed in RT112. However, it was highly expressed in VMCUB1 and even more in BFTC905. Expression of ORF1p was slightly increased in RT112, VMCUB1 and BFTC905 treated with $H_2O_2$. These findings suggested that LINE-1 ORF1p expression was varied among cell lines, and $H_2O_2$ only enhanced its expression to some extent in bladder cancer cell lines.
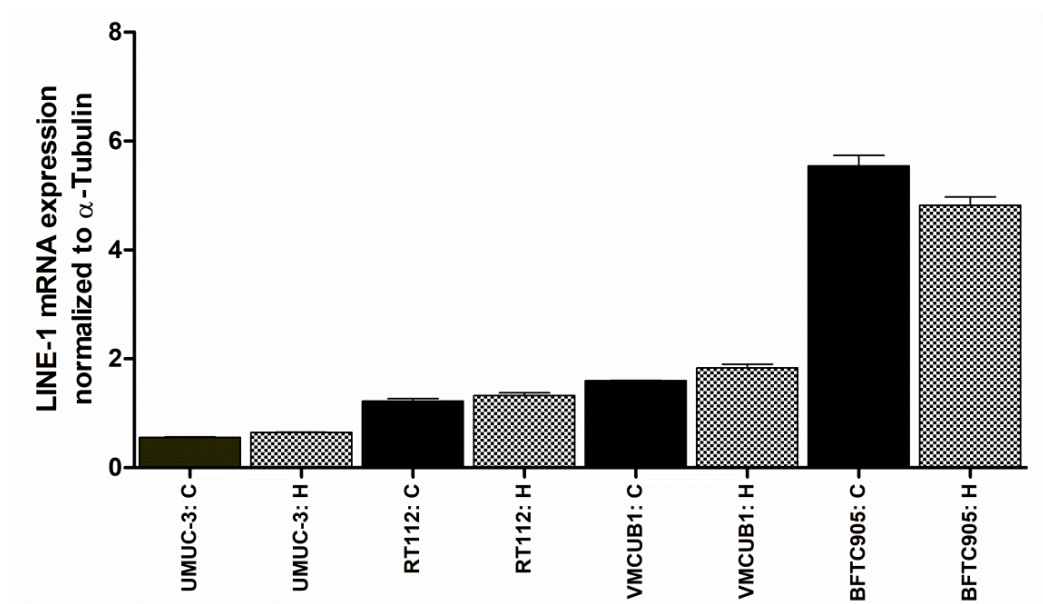
**Figure 69** LINE-1 transcript expression in various bladder cancer cell lines

LINE-1 mRNA expression was evidently varied among cell types.

Additionally, $H_2O_2$ slightly increased LINE-1 mRNA expression.
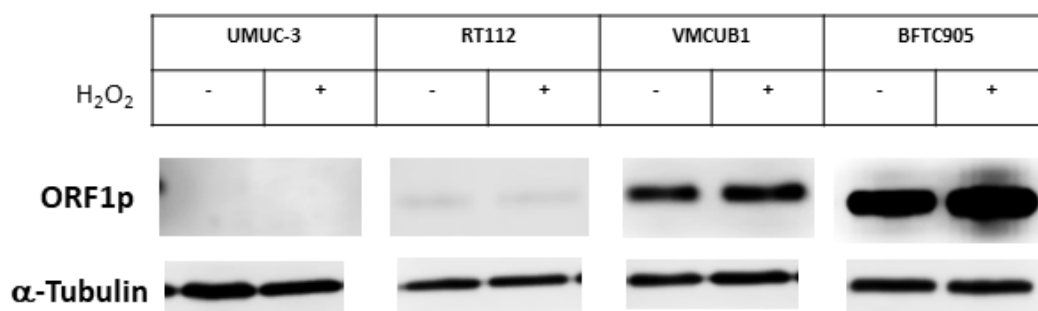


**Figure 70** Western blot analysis for ORF1p expression in various bladder cancer cell lines. ORF1p expression was different between cell types, and $H_2O_2$ could only induce ORF1p expression in VMCUB1 and BFTC905.

Histone modification was explored in this study to investigate whether the regulation of LINE-1 ORF1p expression in different bladder cancer cell lines under oxidative stress condition was mediated through remodeling of chromatin structure. Histone methylation and acetylation were investigated by ChIP-qPCR assay using

histone H3K9me3 and H3K27me3 as heterochromatin or inactive chromatin marks and histone H3K4me3 and H3K18Ac as active chromatin marks. First of all, histone modification of GAPDH, GRM6 and CTCFL gene were analyzed in order to verify efficacy of ChIP-qPCR technique.

GAPDH is highly expressed across human tissues, also in urinary bladder. As shown in figure 71, GAPDH was enriched at active chromatin marks, H3K4me3 and H3K18Ac. This suggested that in the highly expressed genes, such as GAPDH, active chromatin structure or open chromatin was usually formed rather than heterochromatin in order to allow expression of genes.
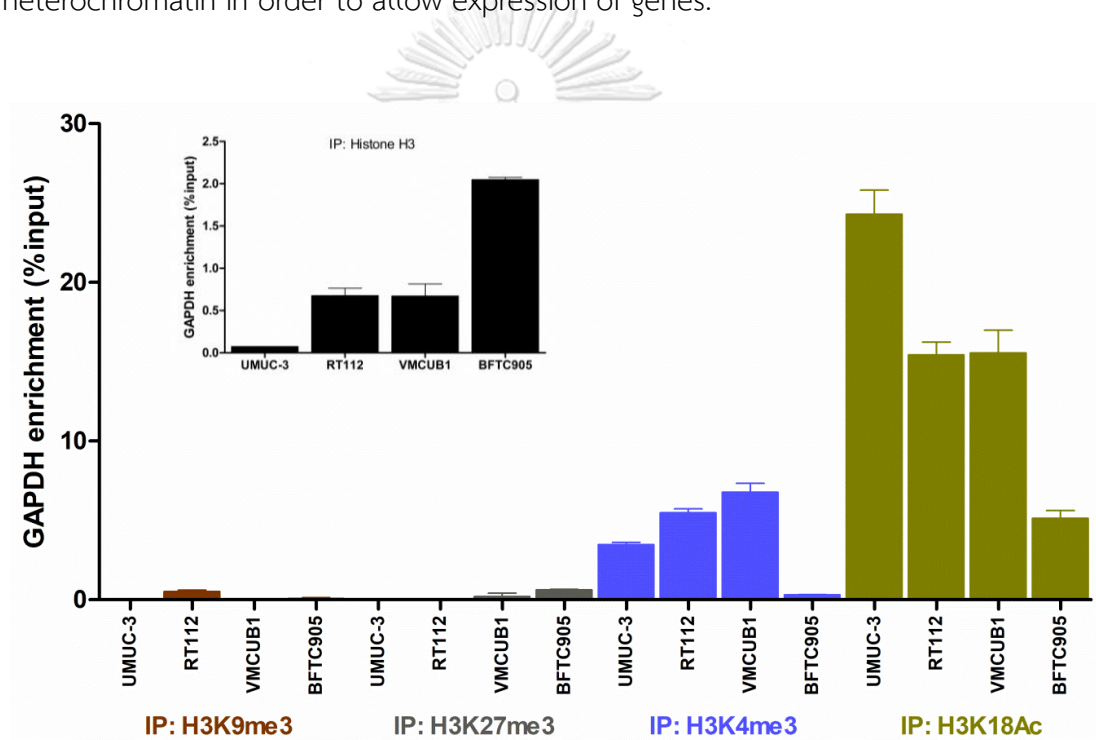


**Figure 71** Histone modifications on GAPDH gene in bladder cancer cell lines
To regulate GAPDH expression, the gene was enriched for active chromatin marks, H3K4me3 and H3K18Ac.

Glutamate metabolic receptor 6 (GRM6) and gene regulator CTCFL are tissue specific genes which expressed at very low level in urinary bladder. Figure 72 showed histone modification on GRM6 gene in bladder cancer cell lines. It was shown that GRM6 was enriched at heterochromatin marks, H3K27me3 and H3K9me3. In contrast

to GAPDH, GRM6 was associated with inactive chromatin structure, and this which led to gene repression or silencing.
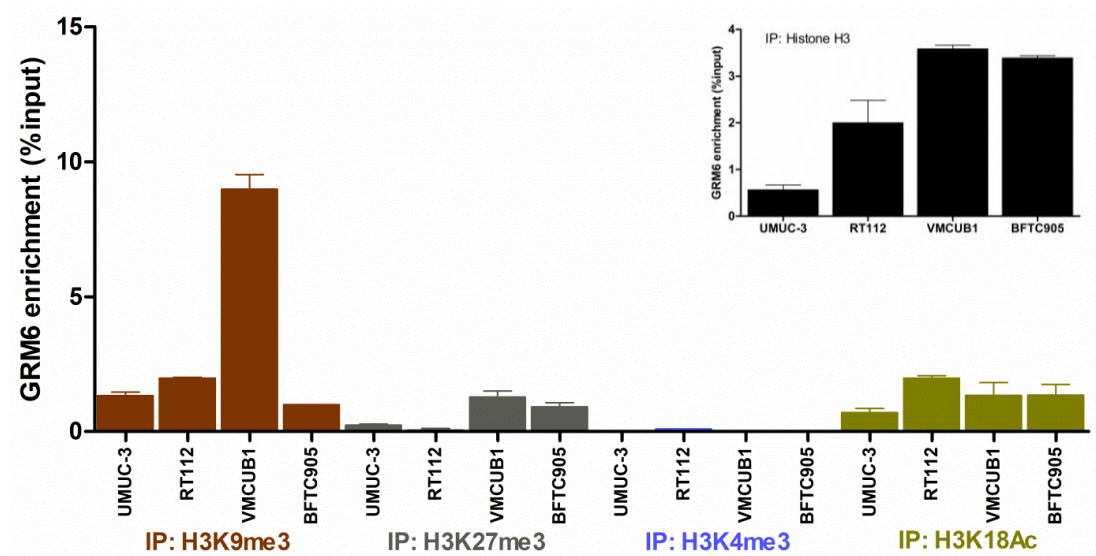


**Figure 72** Histone modifications on GRM6 gene in bladder cancer cell lines
GRM6 was enriched for H3K9me3 and H3K27me3, but not for H3K4me3.

Similar to GRM6, the low expression of CTCFL gene was regulated by methylation at histone H3K9 and H3K27 without H3K4 methylation. CTCFL was enriched for heterochromatin marks, especially H3K27me3 (Figure 73). Compared to GAPDH, enrichment of H3K18Ac for CTCFL was much lower (Figure 73). Therefore, according to ChIP data of these three control genes (GAPDH, GRM6 and CTCFL), it is clearly showed as expected that GAPDH was associated with active chromatin, whereas, GRM6 and CTCFL were enriched for inactive chromatin. These ensured the validity of the current ChIP assay.
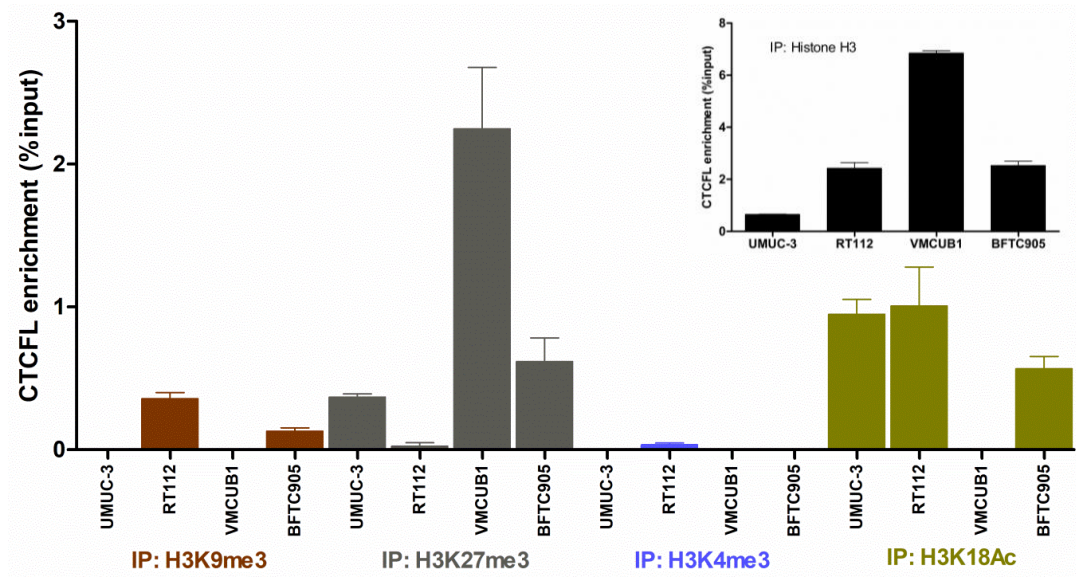
**Figure 73** Histone modifications on CTCFL gene in bladder cancer cell lines
The data showed enrichment of CTCFL for H3K9me3, H3K27me3 and H3K18Ac,
but not H3K4me3.

To study histone modification on LINE-1 elements under oxidative stress (induced by $H_2O_2$), the enrichment of LINE-1-5' (5'-UTR LINE-1 promoter) and LINE-1-3' (3'-UTR LINE-1) for each histone mark were analyzed. The results showed that LINE-1-5' was significantly enriched for H3K4me3 and H3K18Ac, particularly in VMCUB1 and BFTC905 exposed to $H_2O_2$ (Figure 74). These were consistent with increases in LINE-1 mRNA and ORF1p expression in $H_2O_2$-treated VMCUB1 and BFTC905. Enrichment of LINE-1-5' for H3K4me3 was undetectable in UMUC-3 (both $H_2O_2$-treated and untreated conditions), confirming an undetectable level of LINE-1 transcript and ORF1p in UMUC-3 cells. Similarly, enrichment of LINE-1-5' for H3K18Ac in UMUC-3 was very much lower than that in RT112, VMCUB1 and BFTC905. This ChIP data suggested that the expression level of ORF1p was depending on active chromatin formation, as LINE-1 elements were associated with H3K18Ac and H3K4me3 in ORF1p-expressing cells. However, we also observed increased in H3K9me3 and H3K27me3 formation over LINE-1 elements in UMUC-3 and VMCUB-1 exposed to $H_2O_2$. This might be the explanation for a slight induction of ORF1p expression in VMCUB1 treated with $H_2O_2$. .

The histone modification on LINE-1-3' elements under oxidative stress condition was shown in figure 75. The results showed that enrichment of LINE-1-3' was predominantly found at H3K9me3 and H3K27me3, especially in the $H_2O_2$-treated condition. This enrichment of LINE-1-3' for H3K9me3 and H3K27me3 under oxidative stress condition was similar to the LINE-1-5' elements. Enrichment of LINE-1-3' for active chromatin mark H3K4me3 and H3K18Ac was not detectable, and it was not depending on $H_2O_2$ exposure. Majority of LINE-1-3' elements are truncated elements, usually are intragenic elements, and they have to be transcriptionally inactivated. Therefore, our finding of association of LINE-1-3' with inactive chromatin supports this notion.
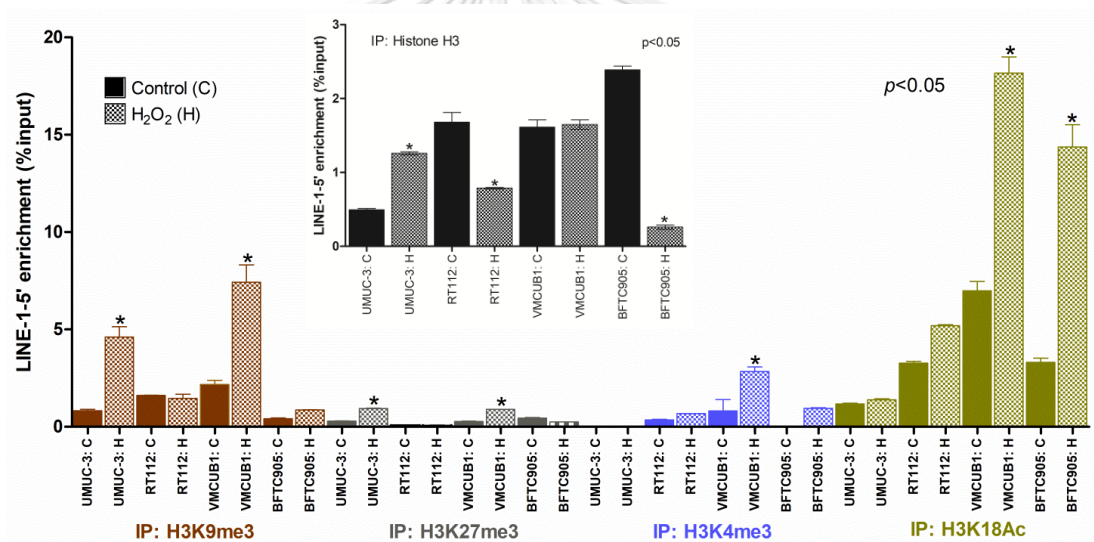


**Figure 74** Enrichment of LINE-1-5' promoter for each chromatin marks under oxidative stress condition in bladder cancer cell lines.
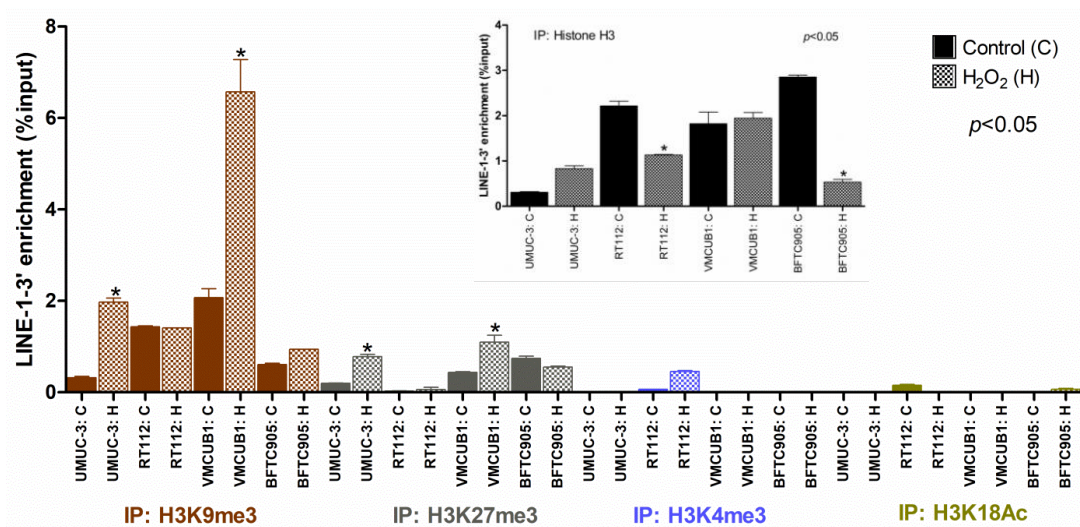
**Figure 75** Enrichment of LINE-1-3' for each chromatin marks under oxidative stress condition in bladder cancer cell lines.

**Oxidative stress triggered cell migration and cell invasion *in vitro***

Wound healing assay was performed in UMUC-3 and VMCUB1 treated with $H_2O_2$. As shown in Figure 76a, the gap was completely closed in UMUC-3 treated with 20 µM $H_2O_2$ compared to the untreated control at 24 hours. Similarly, VMCUB1 treated with 30 µM $H_2O_2$ showed faster closing gap starting at 6 hours treatment compared to the untreated control (Figure 76b). This finding suggested that ROS triggered oxidative stress and increased cell migration in bladder cancer cells.
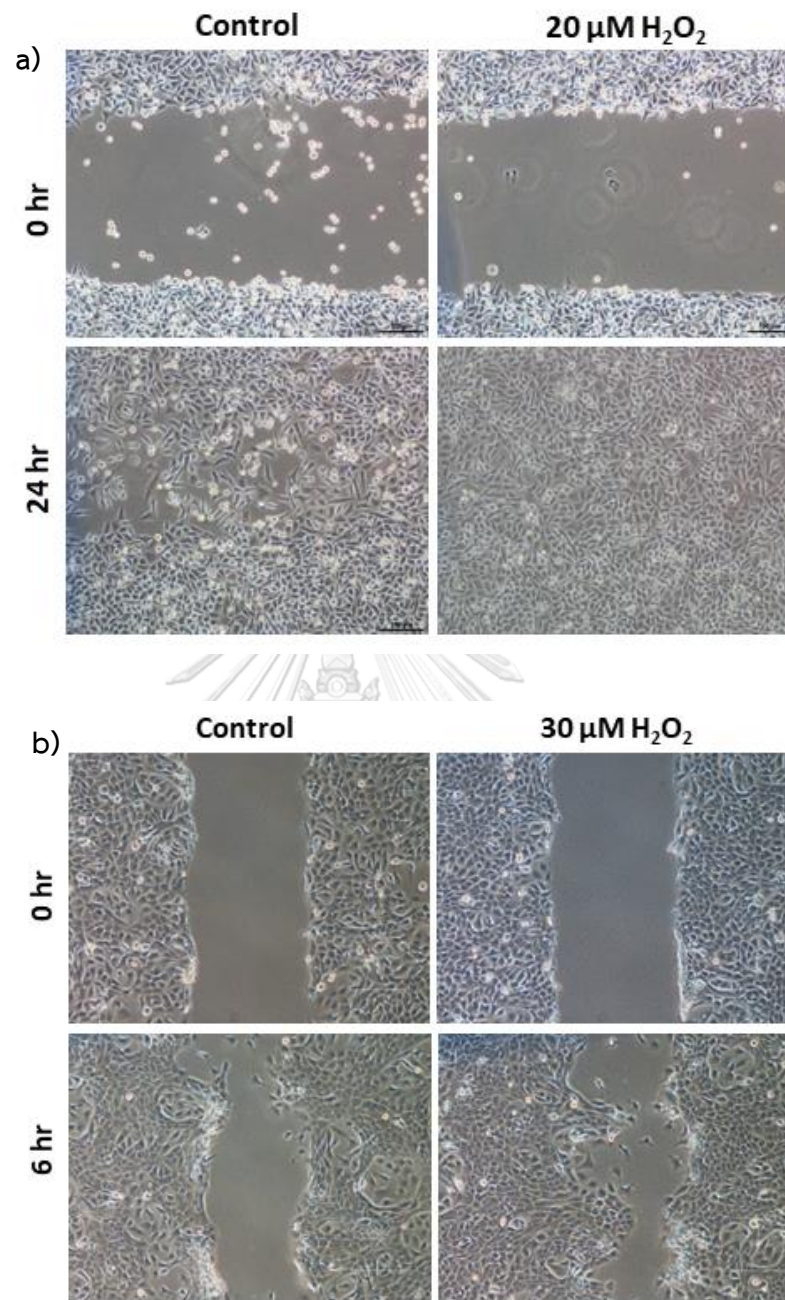
**Figure 76** Wound healing assay in bladder cancer cell lines

    a) $H_2O_2$ increased cell migration in UMUC-3 at 24 hours.

    b) $H_2O_2$ increased cell migration in VMCUB1 starting at 6 hours.

Furthermore, cell migration and cell invasion were studied by Boyden chamber assay. After 24 hours, cells were fixed and stained by crystal violet. Crystal

violet was destained, cells were lyzed and the absorbance was measured at 570 nm. Number of migrated cells and number of invaded cells were calculated from standard curve created from cell number (X axis) and $OD_{570}$ (Y axis) (Figure 77). The positive association represented on standard curve confirmed that the increased $OD_{570}$ was related to the increased number of cells.



The chart shows a standard curve with the equation:

$$y = 3E\text{-}05x + 0.1806$$
$$R^2 = 0.9997$$
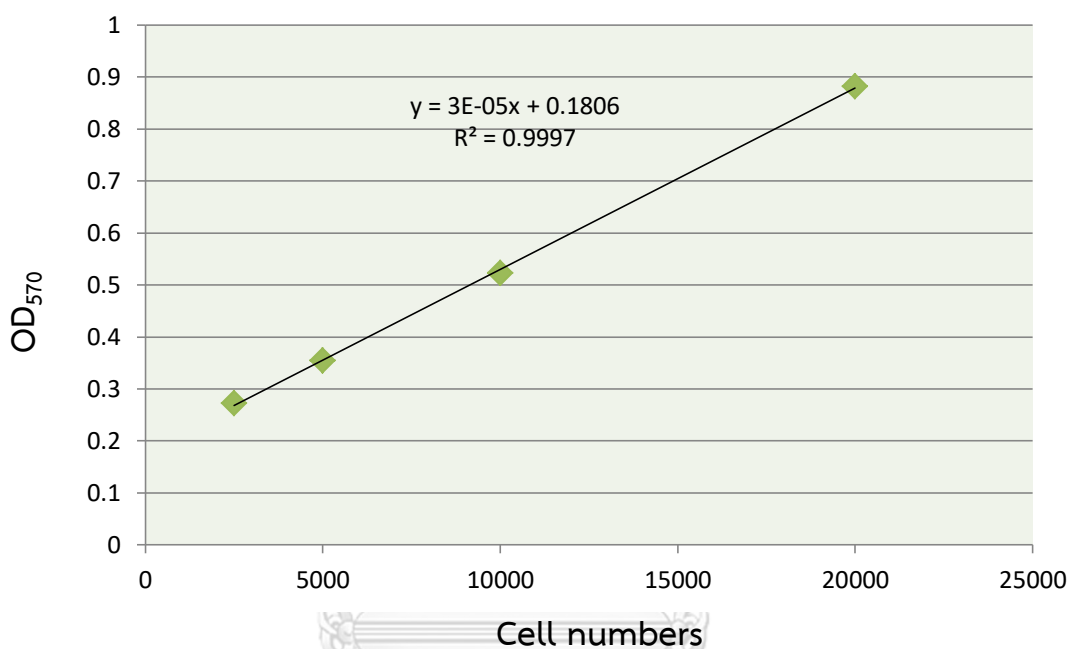
**Figure 77** Standard curve for cell migration and invasion by Boyden chamber assay

Figure 78 represented cell migration by Boyden chamber assay showing that after 24 hours treatment UMUC-3 in untreated control group (77.42% migration) moved slower than UMUC-3 treated with 20 μM $H_2O_2$ (90.95% migration). However, cell migration was slightly decreased in UMUC-3 co-treated with TA (81.4% migration), but not decreased in cells co-treated with HZL (91.33% migration). In VMCUB1, untreated control group showed 31.25% migration, whereas treatment with 30 μM $H_2O_2$ showed 42.23% migration. Cell migration in VMCUB-1 co-treated with TA and HZL were 35.19% and 39.1%, respectively. These results revealed that oxidative stress was able to induce cell migration in both UMUC-3 and VMCUB1. VMCUB1 showed lower migration rate than UMUC-3 in general.
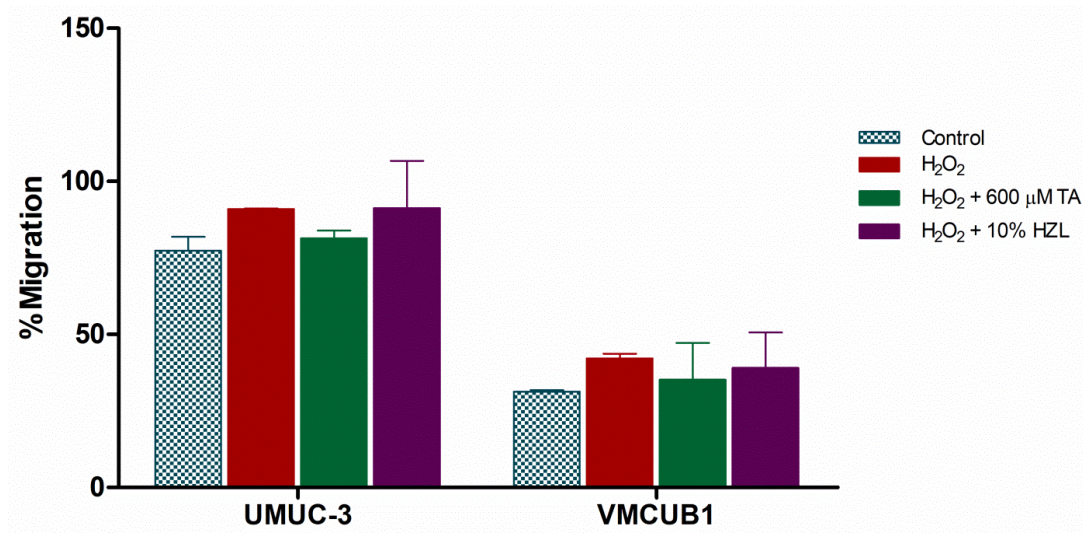
**Figure 78** Cell migration by Boyden chamber assay in bladder cancer cell lines
Cell treated with $H_2O_2$ had higher cell migration than the untreated control.

Cell invasion by Boyden chamber assay was shown in figure 79. The results showed that UMUC-3 in untreated control group (50.89% invasion) had invading capacity lesser than but UMUC-3 treated with 20 µM $H_2O_2$ (58.89% invasion). UMUC-3 co-treated with TA and HZL showed reduced cell invasion capability to 55.2% and 56.7%, respectively. In VMCUB1, untreated control group had 8.34% invasion, but it was increased to 9.36% in VMCUB1 treated with 30 µM $H_2O_2$. VMCUB1 co-treated with TA and HZL showed decreased cell invasion to 7.57% and 7.5%, respectively. These findings indicated that oxidative stress enhanced bladder cancer cell invasion. However, co-treatment with antioxidants could attenuate cell invasion in both UMUC-3 and VMCUB1. It was obvious that VMCUB1 had a much lower invasion capability than UMUC-3.
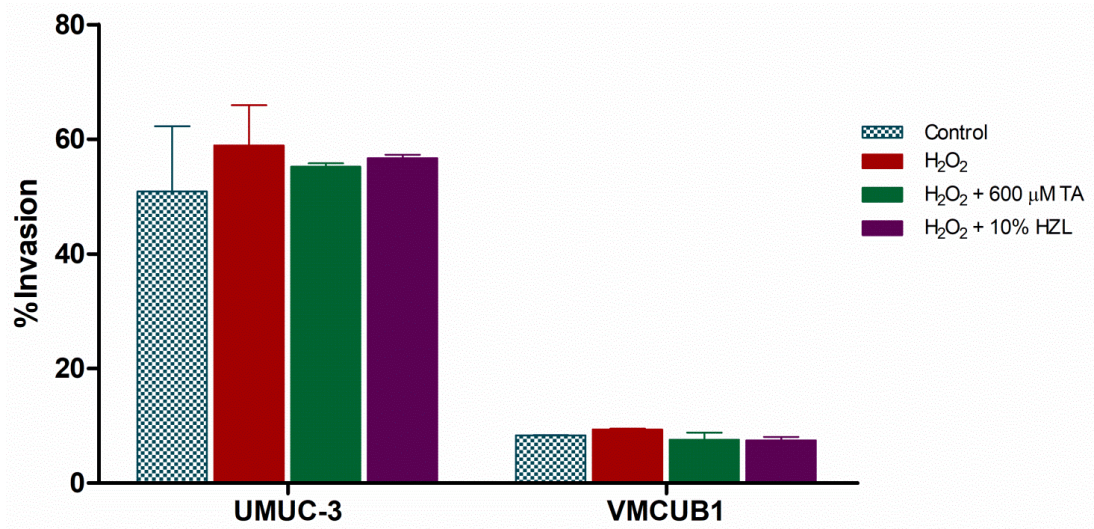
**Figure 79** Cell invasion by Boyden chamber assay in bladder cancer cell lines

Cells treated with $H_2O_2$ had greater cell invasion than the untreated control.
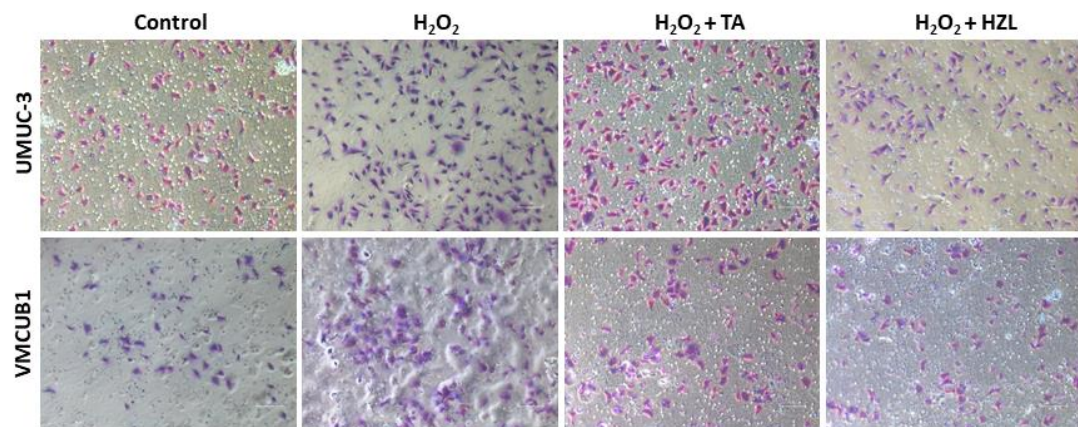


**Figure 80** Micrographs of Boyden chamber for cell invasion assay in

bladder cancer cell lines

## Chapter 5

## Discussion and Conclusion

**Discussion**

Oxidative stress, a condition with excessive production of ROS, has been implicated in various chronic diseases including cancers. ROS directly causes oxidative damage to cellular biomolecules resulting in genetic mutation and alterations of gene expression and signaling pathways (Klaunig et al., 2010). Bladder cancer is the fifth most common cancer worldwide. It is sporadic rather than hereditary cancer, caused by the accumulation of genetic and epigenetic alterations overtime (Al Hussain & Akhtar, 2013; Besaratinia et al., 2013). In addition to genetic mutation, it has been reported that epigenetic alteration such as global DNA hypomethylation or LINE-1 hypomethylation is one of the oncogenic characteristics of bladder cancer (Chalitchagorn et al., 2004; Jürgens et al., 1996). Our previous study found that LINE-1 hypomethylation was strongly correlated with the elevated oxidative stress level in Thai bladder cancer patients (Patchsung et al., 2012). The pioneer investigation in bladder cancer cell lines revealed that 1) oxidative stress was a cause of LINE-1 hypomethylation and 2) one possible mechanism of oxidative stress-induced LINE-1 hypomethylation in bladder cancer cells was that oxidative stress led to S-adenosylmethionine (SAM) depletion resulting in LINE-1 hypomethylation (Kloypan et al., 2015; Wongpaiboonwattana et al., 2013). In this study, global DNA hypomethylation and histone modification on LINE-1 elements in relation to oxidative stress and oxidative DNA damage in bladder cancer were explored to unveil another possible mechanisms driving urothelial bladder carcinogenesis.

Bladder cancerous and non-cancerous tissues were obtained from 39 bladder cancer patients operated by TUR-BT at Buriram hospital. The average age of this studied group was 70.5 ± 13.7 years old and the incidence was found 5.5 times higher in men (84.61%, 33/39) than women (15.39%, 6/39). According to the patient history collected in some cases, 50% (12/24) of patients were former smokers and

43.59% (17/39) were exposed to chemicals such as pesticide. Based on histological evaluation, 71.79% (28/39) were non-muscle invasive bladder cancer and 28.21% (22/39) were muscle invasive bladder cancer. In regard to the histological grading, 8.57% (3/35) were PUNLMP, 37.14% (13/35) were low-grade tumors and 54.29% (19/35) were high-grade tumors. However, all patients had negative family history implying that the studied bladder cancer was not genetic inheritance type.

IHC staining was performed in cancerous bladder tissue compared to its non-cancerous adjacent tissue. DNA methylation level assessed by 5-mC staining showed that nuclear 5-mC expression in cancerous tissues was significantly lower than adjacent tissues ($p$=0.0001) and it was significantly decreased in high-grade tumors compared to PUNLMP/low-grade tumors ($p$=0.037). This indicated that overall DNA methylation was decreased during urothelial bladder cancinogenesis and the global DNA hypomethylation was associated with bladder cancer progression. In consistent with study in Taiwanese patients (Chung et al., 2015) that showed that low 5-mC level was more frequently observed in muscle invasive tumors than in normal urothelium and non-muscle invasive bladder cancer. Comparing among tumor staging, 5-mC level in stage II-IV invasive tumors was significantly different from stage I and non-muscle invasive tumors. Therefore, it was suggested that 5-mC IHC expression could be utilized to predict the muscle invasion of bladder cancer (Chung et al., 2015).

LINE-1 elements contribute about 17% of entire human genome, thus, it is accepted that LINE-1 methylation can be a marker for global DNA methylation and LINE-1 methylation is correlated well with genome-wide methylation (Phokaew et al., 2008). LINE-1 promoter methylation in bladder cancer tissues was previously analyzed by bisulfite Pyrosequencing. The result showed that LINE-1 promoter methylation was significantly decreased in cancerous tissues compared to normal control. LINE-1 mRNA expression was also investigated and a significant increase in full-length LINE-1 transcript expression in bladder cancer tissues was found (Kreimer et al., 2013). In this study, the expression of LINE-1 ORF1p in bladder cancer tissues was analyzed by IHC staining. ORF1p expression was significantly higher in cancerous tissues than adjacent tissues ($p$=0.0464) and it was significantly increased in high-

grade tumors compared to PUNLMP/low-grade tumors ($p$=0.0083). This IHC data indicated that LINE-1 ORF1p expression was associated with bladder cancer progression. ORF1p, as one of two LINE-1 encoded proteins, has been suggested to be a hallmark in cancers, because it was not expressed in normal somatic cells but, as results from immunostaining in lymphomas, pancreatic carcinoma and glioblastoma, upregulated in low-grade and high-grade tumors (Rodic et al., 2014). Reasonably, this can be assumed that global DNA hypomethylation or LINE-1 promoter hypomethylation conduces to increase expression of LINE-1 transcripts and ORF1p which were implicated in bladder cancer progression.

The augment of oxidative stress in bladder cancer tissues was evaluated by two oxidative stress markers including 4-HNE as a byproduct from lipid peroxidation and 8-OHdG as oxidative DNA damage product. Firstly, 4-HNE expression in cancerous tissues was significantly higher than adjacent tissues ($p$=0.020), but it was not statistically different between PUNLMP/low-grade tumors and high-grade tumors. Similarly, nuclear 8-OHdG expression was significantly increased in cancerous tissues compared to adjacent tissues ($p$=0.0206). Inversely, 8-OHdG expression was significantly declined in high-grade tumors compared to PUNLMP/low-grade tumors.

The expression of 8-OHdG in bladder cancer tissues assessed by IHC staining was also studied by Soini and colleagues in 2011. This study reported that 8-OHdG expression was not associated with tumor grading or cancer stages, but they found that high 8-OHdG positive was associated with worse survival rate in bladder tumor patients (Soini et al., 2011). Expressions of 4-HNE and 8-OHdG were also investigated in breast cancer (Karihtala et al., 2011). It was found that 4-HNE and 8-OHdG expressions were significantly increased in breast cancer tissues, but these two oxidative stress markers showed different behavior during breast carcinogenesis. 4-HNE expression was increased towards the progression of breast cancer, as its expression was relatively high in invasive breast tumors. Differently, 8-OHdG expression was declined in invasive carcinoma. It was suggested that lower expression of 8-OHdG in invasive carcinoma might be a result of the induction of DNA repair enzymes under oxidative stress to fix oxidative DNA lesions (Karihtala et al., 2011).

8-oxoguanine DNA glycosylase 1 or OGG1 takes part in base excision repair. It recognizes 8-OHdG lesions formed by ROS attack (David et al., 2007). In this study, the IHC evaluation of OGG1 expression in bladder cancer showed that OGG1 expression was significantly increased in cancerous tissues compared to adjacent tissues ($p$=0.0469). OGG1 level was not statistically different between low- and high-grade, tumors but it was positively related to 8-OHdG level ($p$=0.0015). These findings suggested that OGG1 expression was induced in response to 8-OHdG formation in order to remove this oxidative DNA lesion.

Interestingly, increased 4-HNE expression was significantly correlated with increased ORF1p expression ($p$=0.0002) indicating that oxidative stress was associated with LINE-1 reactivation, and it might be associated with bladder cancer progression through induction of ORF1p expression. The elevated oxidative stress makers (both 4-HNE and 8-OHdG) in bladder cancer tissues suggested that oxidative stress play a critical role in urothelial bladder carcinogenesis.

The *in vitro* study was performed in bladder cancer cell lines and $H_2O_2$ was applied in order to induce the oxidative stress. The physiological concentration of $H_2O_2$ in human body is limited to 20 - 50 µM depending on tissues or cell types (Halliwell et al., 2000). However, $H_2O_2$ secreted into urine in healthy people is found averagely at 17 µM, but it can be varying from very low up to 100 µM (Halliwell et al., 2000). Cell viability assay for bladder cancer cell lines against $H_2O_2$ showed that cells were response to $H_2O_2$ in dose-dependent manner. Low concentration of $H_2O_2$ (10 µM) could induce cell proliferation whereas increasing $H_2O_2$ concentrations (20 – 200 µM) were toxic to cells eventually leading to cell death. In this study, cells were treated at sub-lethal dose of $H_2O_2$ (20 – 30 µM) for 72 hours, and it  showed that intracellular ROS production was provoked resulting in increased oxidative damages including oxidative DNA damage lesion (8-OHdG) and oxidized protein (protein carbonyl). Cells co-treated with antioxidants ($H_2O_2$ + TA or HZL) showed decreased intracellular ROS and protein carbonyl levels compared to cells treated with $H_2O_2$ alone. These indicated that $H_2O_2$ at sub-lethal dose could induce the oxidative stress whereas antioxidants could attenuate the oxidative stress in bladder cancer cells.

Bisulfite pyrosequencing was performed in bladder cancer cell lines including UMUC-3 and VMCUB1 to measure the methylation level of 4 CpG sites on LINE-1 promoter. DNA methylation can regulate gene expression through the addition of methyl group to cytosine base, especially at CpG dinucleotide sites. The methyl group added on cytosine base blocks the binding of transcription factors or recruit methyl-binding domain protein (MBD) which further interacts with histone deacetylases (HDACs) resulting in gene silencing (Sharma et al., 2010). Therefore, the change in DNA methylation level leads to the aberrant expression of the gene. In this study, the overall methylation level of LINE-1 promoter in UMUC-3 and VMCUB1 were largely different (69.25% in UMUC-3 and 40.5% in VMCUB1). LINE-1 mRNA and LINE-1 ORF1p expression in VMCUB1 were markedly higher than UMUC-3. Additionally, ORF1p expression was undetectable in UMUC-3. This data clearly demonstrated that a lower promoter methylation caused a higher gene expression. To reactivate LINE-1 elements in UMUC-3, LINE-1 methylation level in UMUC-3 has to be as low as in VMCUB1.

Cells treated with $H_2O_2$ showed decreased methylation level. The methylation level in all 4 CpG sites were reduced in UMUC-3 treated with $H_2O_2$ leading to decreased overall methylation to 64.75% whereas, in VMCUB1 treated with $H_2O_2$, the methylation was reduced in 3 CpG sites but increased in 1 CpG site resulting in slightly decreased overall methylation level to 40%. LINE-1 mRNA expression was investigated and it was found that LINE-1 mRNA expression was slightly increased in UMUC-3 and VMCUB1 treated with $H_2O_2$. LINE-1 ORF1p expression was undetectable in UMUC-3, but it showed significant increase in VMCUB1 treated with $H_2O_2$. Cells co-treated with $H_2O_2$ and TA showed increased methylation in all reduced CpG sites compared to cells treated with $H_2O_2$ alone. LINE-1 ORF1p expression was slightly decreased in VMCUB1 co-treated with $H_2O_2$ and TA compared to cells treated with $H_2O_2$ alone. These implied that oxidative stress was implicated in the reactivation of LINE-1 elements by inducing LINE-1 promoter hypomethylation leading to increased LINE-1 expression in both mRNA and protein levels. Interestingly, the antioxidant supplement could restore the methylation status and reduce LINE-1 expression in bladder cancer cells.

It is interesting to elucidate the mechanism of how oxidative stress induces LINE-1 hypomethylation in bladder cancer. In this study, we asked if LINE-1 hypomethylation was a consequence of increased formation of oxidative DNA damage lesion 8-OHdG. As mentioned previously in bladder cancer tissues, 8-OHdG was significantly increased in cancerous tissues compared to non-cancerous control. $H_2O_2$ at sub-lethal dose induced 8-OHdG formation in UMUC-3 and VMCUB1. Subsequently, 8-OHdG lesions were found to be accumulated in 5'-UTR LINE-1 promoter, as shown by quantitative real-time PCR. Basically, *in vitro* DNA polymerase activity can be inhibited by DNA adducts such as hydroxyl group on guanosine base, and the PCR amplification will stop at DNA damage sites resulting in less efficacy of amplification (Furda et al., 2014; Kumari et al., 2008). Based on this principle, DNA damage lesions on specific region can be detected by quantitative real-time PCR based technique which has been applied in various studies to detect lesion frequency on genomic strand or DNA repair rate (Ayala-Torres et al., 2000; Hunter et al., 2010; Sawyera et al., 2003; Van Houten et al., 2000). In this study, UMUC-3 and VMCUB1 treated with $H_2O_2$ exhibited significantly increased 8-OHdG lesions on LINE-1 promoter, and the lesions on LINE-1 promoter were decreased in cells co-treated with antioxidants. It should be noted that 8-OHdG lesions were detected not only on LINE-1 promoter, but also on LINE-1-3' and GAPDH. This indicated that 8-OHdG lesions induced by ROS are randomized, perhaps, depending on accessibility of DNA to ROS. Our additional study in Dnmt1 expression found that $H_2O_2$ could enhance Dnmt1 expression in UMUC-3, but LINE-1 hypomethylation was obviously found in UMUC-3 after $H_2O_2$ exposure. The kinetic study by Weitzman and colleagues in 1994 showed that the activity of DNA methyltransferase (DNMT) enzyme was inhibited by 8-OHdG residues (Weitzman et al., 1994). Capability of the DNMT enzyme to methylate C residue next to 8-OHdG was greatly low compared to the capability to methylate the normal CpG. This study suggested that, in addition to causing mutagenesis, 8-OHdG could alter epigenetic control by causing DNA hypomethylation which was implicated in tumorigenesis (Weitzman et al., 1994). Therefore, our findings suggest that 8-OHdG formation on LINE-1 promoter possibly leads to LINE-1 promoter hypomethylation in bladder cancer.

OGG1 expression was also evaluated in bladder cancer cell lines. OGG1 expression was elevated in cells treated with $H_2O_2$ and decreased after co-treated with antioxidant TA indicating that OGG1 expression was upregulated by oxidative stress. Moreover, the oxidative stress-induced OGG1 expression was related to increased 8-OHdG level in both UMUC-3 and VMCUB1. OGG1 has been suggested to be a rate-limiting step in base excision repair to remove 8-OHdG (Ruchko et al., 2011). This indicated the function of OGG1 to retain genomic stability of cells under oxidative stress exposure. OGG1 is expressed in order to initiate base excision repair, and it functions to recognize and cleave 8-OHdG lesion on genomic DNA, hence generating abasic site. Then, this abasic site is removed by abasic site endonuclease 1 (APE1) followed by DNA polymerase β (POLB) and, finally, DNA ligase III to complete base repairing process (Q. Li et al., 2013). In addition to BER pathway, OGG1 is involved in DNA demethylation in two aspects. During repairing step operated by OGG1 and APE1 enzymes, the 5-mC on CpG dinucleotides was potentially removed together with 8-OHdG (Kasymova et al., 2013). Moreover, OGG1 can interact with TET1 enzyme and recruit it to 8-OHdG site resulting in DNA demethylation at the neighboring cytosine base (Zhou et al., 2016). Taken together, oxidative stress-induced OGG1 expression can lead to DNA demethylation on CpG sites. This could be an explanation for LINE-1 hypomethylation induced by ROS in bladder cancer. However, we believe that the increased LINE-1 expression by oxidative stress was not solely a consequence of LINE-1 hypomethylation, histone modification change leading to remodeling of chromatin structure may also play a vital role.

The alteration of histone modification patterns is documented in bladder cancer. Compared to normal urothelial, histone methylation and histone acetylation were globally decreased in bladder cancer and they were even more declined in muscle invasive tumors (Ellinger et al., 2014; Ellinger et al., 2016; Schneider et al., 2011). In this study, expression of H3K9me3 and its recognized protein, heterochromatin protein 1 (HP1α), in cancerous tissues were significantly increased compared to adjacent tissues. A trend of decreased expression of H3K9me3 and HP1α was observed in high-grade tumors relative to low-grade tumors. This suggested that heterochromatin was progressively decreased towards high-grade

tumors. Similarly, the previous study by Ellinger and colleagues in 2014 reported the decreased histone H3K9me3 level in muscle invasive bladder cancer compared to non-muscle invasive bladder cancer (Ellinger et al., 2014). The discrepancy between the current study and Ellinger's study was that they found decreased H3K9me3 expression, but we found increased H3K9me3 expression in cancerous bladder tissues. However, , increased histone H3K9me3 similar to our current finding was reported in patients with early-stage of colon cancer (Benard et al., 2014), and the elevated H3K9me3 was positively correlated with lymph node metastasis in colorectal cancer.  In addition, increased H3K9me3 expression was demonstrated to associate with tumor formation in mice (Yokoyama et al., 2013).

The positive correlation between histone H3K9me3 level and 8-OHdG level was found in this study ($p$=0.0021). Many *in vitro* studies have confirmed the link between histone H3K9me3 and DNA damage response. Breast cancer cell lines were treated with DNA damage reagent leading to the increase in H3K9me3 expression, and it was shown that elevation of histone H3K93me3 was associated with decreased sensitivity of the cells to DNA damage and promoted genomic stabilization (Q.-L. Li et al., 2017). In regard to DNA repair mechanism, H3K9me3 is initially recognized by HP1$\alpha$. Subsequently, HP1$\alpha$ is a signaling target to recruit Tip60 to DNA damage site. Finally, Tip60, as an acetyltransferase enzyme, activates DNA repairing process by acetylating proteins involving in DNA damage response such as ATM kinase to initiate DNA repair process (Ayrapetova et al., 2014; Cann & Dellaire, 2011; Sun et al., 2009).

HP1$\alpha$ is a non-histone protein that recognizes histone H3K9me3 on histone tails tethering the formation of heterochromatin structure. Interestingly, the deregulation of HP1$\alpha$ has been implicated in various cancers (Dialynas et al., 2008; Vad-Nielsen & Nielsen, 2015), such as breast cancer (Thomsen et al., 2011), colon cancer (Espada et al., 2004) and papillary thyroid carcinoma (Wasenius et al., 2003). In concordance with this study, HP1$\alpha$ was possibly related to bladder cancer progression, since it was decreased in high-grade tumors. Remarkably, HP1$\alpha$ expression was found to be significantly correlated with 8-OHdG expression in bladder cancer ($p$=0.0388) suggesting that it was associated with DNA damage response. The previous study demonstrated in Hela cells reported that HP1 protein

was recruited at the site of oxidative DNA damage together with OGG1 and gradually decreased overtime (Dinant & Luijsterburg, 2009; Zarebski et al., 2009).

Taken together, presumably, histone H3K9me3 and HP1α were accumulated in response to oxidative DNA damage to recruit DNA repair proteins at the damage sites and initiate the base excision repair process. After that, loss of heterochromatin formation with decreased H3K9me3 and decreased HP1α led to a relax heterochromatin state which was beneficial for downstream repairing process in bladder cancer. Besides, it was reported that histone H3K9me3 and HP1α were required for LINE-1 promoter silencing in mouse fibroblast cells (Danny Rangasamy, 2013). Therefore, loss of heterochromatin in high-grade tumors might be related to the reactivation of LINE-1 elements in bladder cancer.

The previous *in vitro* study on the regulation of LINE-1 expression revealed that LINE-1 elements are repressed by histone H3K9me3 and H3K27me3 binding around promoter region (Walter et al., 2016). On the other hand, the expression of LINE-1 depends on histone H3K4me3 (Walter et al., 2016). ChIP-qPCR assay was performed in this study in 4 bladder cancer cell lines (UMUC-3, RT112, VMCUB1 and BFTC905) to investigate histone modification patterns on LINE-1 elements. The enrichment of LINE-1 elements (both LINE-1-5' and LINE-1-3' regions) for histone marks was measured. According to LINE-1 expression level determined by LINE-1 mRNA and LINE-1 ORF1p expressions, LINE-1 was low expressed in UMUC-3 and RT112 whereas it was highly expressed in VMCUB1 and BFTC905. This indicates the difference of actively expressed LINE-1 elements among cell lines which, possibly, is a consequence of different histone modification patterns. The enrichment of LINE-1 for active chromatin mark H3K4me3 and H3K18Ac was related to LINE-1 expression level in bladder cancer cell lines. LINE-1-5' region (a full-length LINE-1) was low enriched in UMUC-3 and RT112, but highly enriched in VMCUB1 and BFTC905.

Histone H3K4me3 is an active histone mark on promoter region that recruits other chromatin modifiers such as histone acetylase and histone demethylase leading to nucleosome repositioning. Moreover, H3K4me3 can recruit transcription factors, RNA polymerase and also impede the binding of transcriptional repressor, for example NuRD complex, and DNMT3L resulting in gene transcription (Bannister &

Kouzarides, 2011; Sawan & Herceg, 2010). The nucleosome repositioning is also regulated by histone acetylation. The acetylation of lysine residue results in neutralizing the positive charge on lysine residues and disrupting the binding between DNA and histone protein leading to chromatin relaxation and gene transcription (Bannister & Kouzarides, 2011). These suggested that the reactivation of LINE-1 elements is regulated through histone H3K4me3 and H3K18Ac on LINE-1 promoters.

The enrichments of histone H3K9me3 and H3K27me3 on LINE-1 elements were explored, and we believed that histone H3K9me3 and H3K27me3 would be involved with LINE-1 repression. Histone H3K9me3 and H3K27me3 were found to be enriched on both LINE-1-5' and LINE-1-3', but H3K9me3 was rather more enriched on LINE-1 elements than H3K27me3. Based on this finding, the repression of LINE-1 elements in bladder cancer was preferably regulated by histone H3K9me3. It has been reported that about 500,000 copies of LINE-1 elements distribute throughout the human genome, but most of them are inactive because of the mutations, truncations or some repressive cellular mechanisms. Only human specific Ta1 (L1HS-Ta1) subfamily are potentially active and mobilizing in human genome (D. Rangasamy et al., 2015). Therefore, the inactive LINE-1 elements might be suppressed through H3K9me3-associated heterochromatin. To form constitutive heterochromatin, H3K9me3 together with HP1 protein directly recruit DNA methylation and histone deacetylase enzymes to the sites for permanent gene silencing (Gessaman & Selker, 2017; Lehnertz et al., 2003). The previous study in mouse model found that H3K9me3 along with HP1$\alpha$ were co-localized at LINE-1 promoter to regulate the expression of retrotransposon (Danny Rangasamy, 2013).

Furthermore, the effect of oxidative stress on histone modification pattern was explored in bladder cancer cells treated with sub-lethal dose of $H_2O_2$. LINE-1 mRNA expression was slightly increased in $H_2O_2$ treated cells. ORF1p expression was also slightly increased in VMCUB1and BFTC905 exposed to $H_2O_2$. In low ORF1p-expressiong cells, ORF1p expression was not obviously changed in RT112 treated with $H_2O_2$, and it was still undetectable in UMUC-3 even after exposure to $H_2O_2$. Histone methylation and acetylation levels were significantly increased in $H_2O_2$

treated cells compared to untreated control. Histone H3K4me3 and H3K18Ac were significantly elevated in $H_2O_2$ treated cells, which was related to the increased expression of LINE-1 elements. Concerning the aberrant pattern of histone modifications, oxidative stress possibly disturbs the expression or activity of histone modifying enzymes. ROS is shown to inhibit the activity of the JmjC-domain containing histone demethylase leading to increased H3K4me3 level (Niu et al., 2015). Increased H9K3me3 is a result of oxidative stress-induced histone methyltransferase Suv39H1 expression (Bosch-Presegue et al., 2011). Furthermore, ROS triggers phosphorylation on EZH2, histone methyltransferase specific to H3K27me3, resulting in hyperactivation of this enzyme (L. Li et al., 2014). Moreover, it has been suggested that oxidative stress is implicated in histone acetylation. HDAC expression can be regulated by ROS since ROS is able to either inhibit or stimulate all classes of HDACs leading to the aberrant histone acetylation level (Kreuz & Fischle, 2016). However, the effect of oxidative stress on histone modifying enzymes in bladder cancer has to be investigated in further study.

The increased enrichment of H3K9me3 and H3K27me3 on LINE-1 elements in bladder cancer cells under oxidative stress condition is possibly involved with DNA damage response because heterochromatin is required to maintain genomic stability at the early-stage of DNA damage response in order to prevent the attack of DNA damage agents, such as ROS, to DNA and to block the transcription (Cann & Dellaire, 2011; Cao et al., 2016). Later, the relaxation of chromatin is taken place for the accessibility of DNA repair protein to the damage site through many mechanisms, for example histone acetylation by Tip60 (Cann & Dellaire, 2011; Cao et al., 2016). In this study, the increase of H3K18Ac on LINE-1 promoters was found in cells treated with $H_2O_2$, and this might lead to chromatin relaxation or formation of active chromatin on LINE-1 promoters. Presumably, in addition to increased LINE-1 expression, this oxidative stress-induced chromatin rearrangement might be beneficial for DNA repair on LINE-1 promoter as well. Taken together, the chromatin changes on LINE-1 elements governed by ROS, demonstrated in both bladder cancer tissues and cell lines, were presumably involved with the regulation of LINE-1 reactivation and oxidative DNA damage response.

The aberrant DNA methylation and histone modification has been intensively explored in cancers, and the interplay between DNA methylation and histone modification has been discussed in many aspects. To maintain gene silencing, heterochromatin and DNA methylation are linked together. Histone H3K9me3 is a target for DNA methylation since SUV39H1 or G9a, histone methyltransferase specific for H3K9me3, can recruit DNA methyltransferase Dnmt3a or Dnmt3b to methylated sites to extent gene silencing. Moreover, the methyl DNA binding proteins such as MeCP2 and MBD1 which localize around methylated CpG promoter can recruit histone deacetylases (HDACs) and histone methyltransferases to form higher order of chromatin structure for gene inactivation (Cedar & Bergman, 2009; Kondo, 2009; Rose & Klose, 2014). On the other hand, gene transcription has been link to DNA methylation and active histone marks. Histone H3k4me3 can block the binding of DNMTs especially at promoter region. Moreover, it was revealed that H3K4me3 can target Gadd45a and Ing1 for DNA demethylation at the specific site. Therefore, H3K4me3 seems to play a role in DNA demethylation (Rose & Klose, 2014; Schäfer et al., 2013). Due to gene transcription, it was found that unmethylated DNA at the specific location is associated with acetylated histone and they are essential for transcriptional regulation (Irvine et al., 2002).

Our study found that oxidative stress induced LINE-1 hypomethylation and altered histone modification patterns on LINE-1 promoter leading to LINE-1 reactivation in bladder cancer cells. LINE-1 elements are normally repressed in normal tissues, but highly expressed in various cancers (Ardeljan et al., 2017; Rodic et al., 2014). However, once LINE-1 becomes active, LINE-1 copies can be increased by copy-and-paste leading to LINE-1 retrotransposition mechanism. As a result of retrotranspostion, LINE-1 can insert into another genomic region, eventually, resulting in insertional mutation, genomic deletion, tumor suppressor gene inactivation or oncogene activation which are implicated in tumorigenesis(D. Rangasamy et al., 2015). As an example, LINE-1 could activate c-MET oncogene which involved in cell proliferation, invasion and metastasis in cancer (Kemp & Longworth, 2015; D. Rangasamy et al., 2015). Interestingly, the previous study in bladder cancer showed that LINE-1 hypomethylation and increased H3K4me3 on LINE-1 promoter lead to

the activation of MET oncogene that located near LINE-1 elements (L1-MET) (Wolff et al., 2010). In this study, oxidative stress and LINE-1 expression were implicated with bladder cancer progression, as elevated LINE-1 ORF1p expression in high-grade tumors was associated with augmented oxidative stress. Moreover, oxidative stress triggered LINE-1 expression and provoked the migration and invasion in bladder cancer cell lines. Therefore, it could be assumed that oxidative stress enhanced LINE-1 expression leading to, at least in part, activation of MET oncogene which was implicated in bladder cancer progression. However, further experimental study is required to warrant this speculation.

Epigenetic applications have a potential role in cancer management either for diagnosis, prognosis or therapy. It has been suggested that methylation of LINE-1 has a potential to be a post-diagnosis marker for bladder cancer (Harb-de la Rosa et al., 2015). Since LINE-1 expression is elevated in cancers, LINE-1 ORF2p protein, as a reverse transcriptase, is a promising target for cancer therapy. Efavirenz, a reverse transcriptase inhibitor, showed the anti-cancer efficacy in *in vitro*, *in vivo* and phase II human trial on prostate cancer (Sciamanna et al., 2018). Interestingly, LINE-1 ORF1p protein could be a potential target for bladder cancer therapy as well. Epigenetics can be utilized for cancer therapy due to its reversibility (Ahuja et al., 2016). Therefore, LINE-1 reprogramming through epigenetic controls either by DNA methylation or histone modifications would be promising. In addition to epigenetic applications, antioxidants would be potentially useful for bladder cancer therapy. Our *in vitro* study suggested that antioxidants could attenuate the oxidative damage and restore LINE-1 methylation level leading to reduced ORF1p expression. Moreover, the cohort study in bladder cancer patients in the US reported that the long-term use (more than 10 years) of tocopherol acetate or vitamin E at high dose (200 – 1000 IU per day) could reduce risk of bladder cancer mortality (Jacobs et al., 2002).

## Conclusion

Oxidative stress-driven epigenetic alteration was investigated in bladder cancer. In bladder cancer tissues, global DNA hypomethylation was observed together with increased oxidative DNA damage. Regarding base excision repair protein, OGG1 expression was increased in bladder cancer tissues and it was positively correlated with 8-OHdG level, perhaps, it used to remove oxidized lesion 8-OHdG. LINE-1 encoded protein, ORF1p was low expressed in normal urothelium, but it was highly expressed in cancerous bladder tissues. Additionally, ORF1p expression was higher in high-grade tumors than low-grade tumors. Furthermore, increased ORF1p expression was correlated with the increment of oxidative stress in cancerous tissues. Besides, expressions of H3K9me3 and heterochromatin protein 1 were elevated in bladder cancer tissues, but their expressions were potentially decreased in high-grade tumors relative to low-grade tumors. This might indicate a loss of heterochromatin during urothelial bladder carcinogenesis. Moreover, expression of heterochromatin marks was linearly correlated with increased formation of oxidative DNA lesions. Our current IHC data clearly demonstrated that oxidative DNA damage was associated with epigenetic alterations in bladder cancer tissues.

The *in vitro* study revealed that $H_2O_2$ at sub-lethal dose was able to provoke the oxidative stress in bladder cancer cells, and oxidative stress induced LINE-1 hypomethylation. This ROS-induce LINE-1 hypomethylation was potentially occurred through the formation of 8-OHdG on LINE-1 promoter. Perhaps, 8-OHdG inhibits the methylation of DNMTs on LINE-1 promoter leading to hypomethylation. Alternatively, LINE-1 is demethylated through removal of methylated C together with 8-OHdG in CpG dinucleotides during the base excision repair process. The other possible mechanism of ROS-induced LINE-1 hypomethylation is that OGG1 recruits TET enzyme to the target site (LINE-1) resulting in active DNA demethylation. As a result of oxidative stress-induced LINE-1 hypomethylation, both LINE-1 mRNA and ORF1p expression were upregulated. However, the co-treatment with antioxidants was advantageous in abolishing the oxidative damage, restoration of LINE-1 methylation level and reduction of ORF1p expression.

In addition to DNA methylation, the regulation of LINE-1 elements in bladder cancer was controlled by histone modifications. The repression of LINE-1 elements was preferably controlled by heterochromatin marks, H3K9me3 and H3K27me3. Contrarily, expression of LINE-1 was regulated by active chromatin marks, H3K4me3 and H3K18Ac. Oxidative stress obviously altered histone modification patterns in bladder cancer cells. ChIP data clearly showed that LINE-1 promoters were enriched for H3K4me3 and H3K18Ac under oxidative stress condition and this enrichment was associated with elevated ORF1p expression. Nevertheless, H3K9me3 and H3K27me3 were also increased under oxidative status possibly in regard to DNA damage response since heterochromatin is the initial step in DNA damage response process.

Limitation of the present study should be mentioned. In the part of IHC staining in bladder cancer tissues, this study was performed in the relatively small number of patients. Clinical data of the patients used for clinical association analysis was not complete. The present study is cross-sectional study, and prospective study should be further conducted for validation of the findings. To verify the effect of LINE-1 expression on bladder cancer progression, overexpression of LINE-1 proteins should be performed in further study.

Taken together, oxidative stress caused LINE-1 reactivation through the deregulation of epigenetic mechanisms in bladder cancer. Moreover, this study revealed that oxidative stress-induced LINE-1 reactivation was implicated in bladder cancer progression. Therefore, LINE-1 expression, epigenetic applications and the use of antioxidants would be promising targets for bladder cancer management in the future.
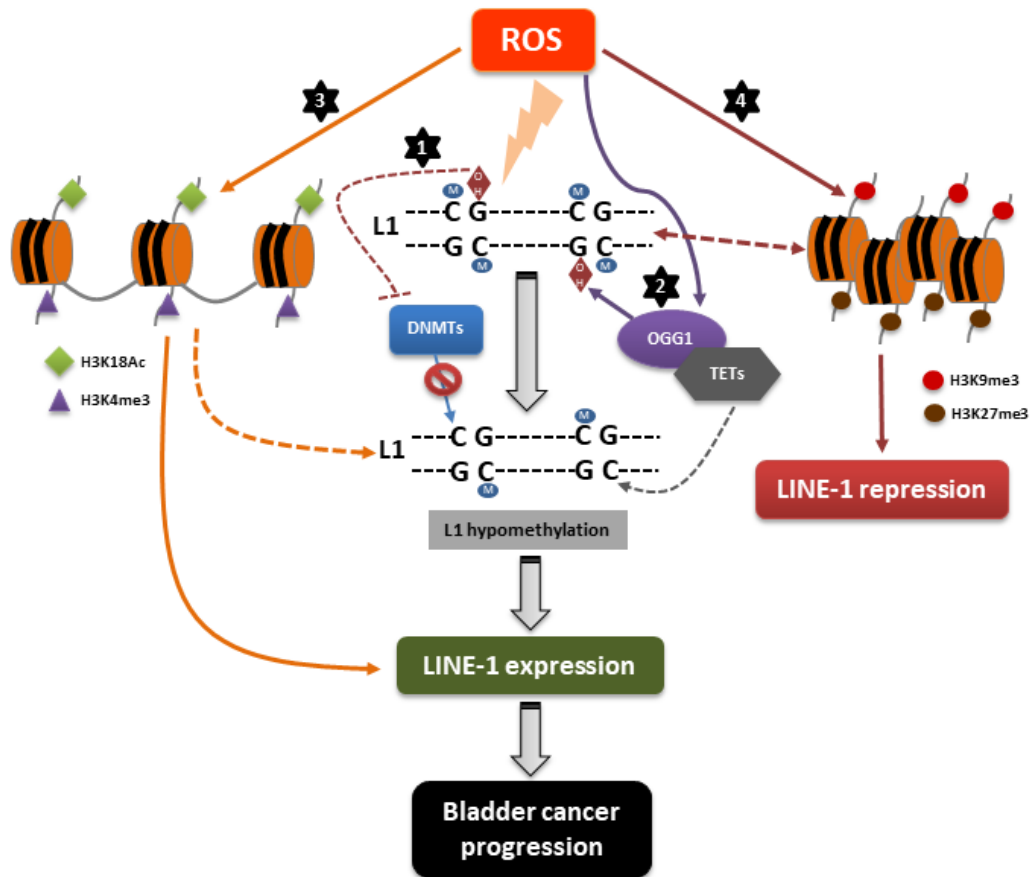
**Figure 81** Schematic diagram for the conclusion of LINE-1 regulation
by ROS in bladder cancer

1) LINE-1 hypomethylation through the inhibition of DNMTs by 8-OHdG

2) 2) LINE-1 hypomethylation through base excision repair

3) LINE-1 expression by ROS-induced euchromatin formation

4) LINE-1 repression by heterochromatin coupled with DNA methylation and
the initiation of DNA damage response by heterochromatin formation

REFERENCES

Ahuja, N., Sharma, A. R., & Baylin, S. B. (2016). Epigenetic therapeutics: a new weapon in the war against cancer. *Annual Review of Medicine, 67*, 73–89. doi: 10.1146/annurev-med-111314-035900

Akçay, T., Saygılı, I., Andican, G., & Yalçın, V. (2003). Increased formation of 8-Hydroxy-2'-Deoxyguanosine in peripheral blood leukocytes in bladder cancer. *Urologia Internationalis, 71*(3), 271–274. doi: 10.1159/000072677

Al Hussain, T. O., & Akhtar, M. (2013). Molecular basis of urinary bladder cancer. *Advances in Anatomic Pathology, 20*(1), 53-60. doi: 10.1097/PAP.0b013e31827bd0ec

Ali, K., Mahjabeen, I., Sabir, M., Mehmood, H., & Kayani, M. A. (2015). OGG1 mutations and risk of female breast cancer: meta-analysis and experimental data. *Disease Markers, 2015*. doi: 10.1155/2015/690878

Ardeljan, D., Taylor, M. S., Ting, D. T., & Burns, K. H. (2017). The Human Long Interspersed Element-1 retrotransposon: an emerging biomarker of neoplasia. *Clinical Chemistry, 63*(4). doi: 10.1373/clinchem.2016.257444

Ashktorab, H. (2009). Global histone H4 acetylation and HDAC2 expression in colon adenoma and carcinoma. *Digestive Diseases and Scieces, 54*(10), 2109–2117. doi: 10.1007/s10620-008-0601-7.

Ayala-Torres, S., Chen, Y., Svoboda, T., Rosenblatt, J., & Houten, B. V. (2000). Analysis of gene-specific DNA damage and repair using quantitative polymerase chain reaction. *Methods, 22*(2), 135–147. doi: 10.1006/meth.2000.1054

Ayrapetova, M. K., Gursoy-Yuzugullua, O., Xua, C., Xua, Y., & Price, B. D. (2014). DNA double-strand breaks promote methylation of histone H3 on lysine 9 and transient formation of repressive chromatin. *PNAS, 111*(25), 9169–9174. doi: 10.1073/pnas.1403565111

Badjatia, N., Satyam, A., Singh, P., Seth, A., & Sharma, A. (2010). Altered antioxidant status and lipid peroxidation in Indian patients with urothelial bladder

carcinoma. *Urologic Oncology: Seminars and Original Investigations, 28*(4), 360–367. doi: 10.1016/j.urolonc.2008.12.010

Bannister, A. J., & Kouzarides, T. (2011). Regulation of chromatin by histone modifications. *Cell Research, 21*(3), 381-395. doi: 10.1038/cr.2011.22

Benard, A., Goossens-Beumer, I. J., Hoesel, A. Q. v., Graaf, W. d., Horati, H., Putter, H., Zeestraten, E. C., Velde, C. J. v. d., & Kuppen, P. J. (2014). Histone trimethylation at H3K4, H3K9 and H4K20 correlates with patient survival and tumor recurrence in early-stage colon cancer. *BMC Cancer, 14*(531). doi: 10.1186/1471-2407-14-531

Besaratinia, A., Cockburn, M., & Tommasi, S. (2013). Alterations of DNA methylome in human bladder cancer. *Epigenetics, 8*(10), 1013–1022. doi: 10.4161/epi.25927

Betteridge, D. J. (2000). What Is Oxidative Stress? *Metabolism, 49*(2 Suppl 1), 3-8.

Borrego, S., Vazquez, A., Dasí, F., Cerdá, C., Iradi, A., Tormos, C., Sánchez, J. M., Bagán, L., Boix, J., Zaragoza, C., Camps, J., & Sáez, G. (2013). Oxidative stress and DNA damage in human gastric carcinoma: 8-Oxo-7'8-dihydro-2'-deoxyguanosine (8-oxo-dG) as a possible tumor marker. *International Journal of Molecular Sciences, 14*(2), 3467-3486. doi: 10.3390/ijms14023467

Bosch-Presegue, L., Raurell-Vila, H., Marazuela-Duque, A., Kane-Goldsmith, N., Valle, A., Oliver, J., Serrano, L., & Vaquero, A. (2011). Stabilization of Suv39H1 by SirT1 is part of oxidative stress response and ensures genome protection. *Mol Cell, 42*(2), 210-223. doi: 10.1016/j.molcel.2011.02.034

Campalans, A., Moritz, E., Kortulewski, T., Biard, D., Epe, B., & Radicella, P. (2015). Interaction with OGG1 is required for fffficient recruitment of XRCC1 to base excision repair and maintenance of genetic stability after exposure to oxidative stress. *Molecular and Cellular Biology, 35*(9), 1648–1658. doi: 10.1128/MCB.00134-15

Cann, K. L., & Dellaire, G. (2011). Heterochromatin and the DNA damage response: the need to relax. *Biochemistry and Cell Biology, 89*(1), 45–60. doi: 10.1139/O10-113

Cao, L.-L., Shen, C., & Zhu, W.-G. (2016). Histone modifications in DNA damage response. *Science China Life Science, 59*(3), 257–270. doi: 10.1007/s11427-016-5011-z

Cash, H. L., Tao, L., Yuan, J.-M., Marsit, C. J., Houseman, E. A., Xiang, Y.-B., Gao, Y.-T., Nelson, H. H., & Kelsey, K. T. (2012). LINE-1 hypomethylation is associated with bladder cancer risk among nonsmoking Chinese. *International Journal of Cancer, 130*(5), 1151–1159. doi: 10.1002/ijc.26098

Cedar, H., & Bergman, Y. (2009). Linking DNA methylation and histone modification: patterns and paradigms. *Nature Reviews Genetics, 10*, 295-304. doi: 10.1038/nrg2540

Chalitchagorn, K., Shuangshoti, S., Hourpai, N., Kongruttanachok, N., Tangkijvanich, P., Thong-ngam, D., Voravud, N., Sriuranpong, V., & Mutirangura, A. (2004). OncogeneDistinctive pattern of LINE-1 methylation level in normal tissues and the association with carcinogenesis. *Oncogene, 23*(54), 8841–8846. doi: 10.1038/sj.onc.1208137

Choudhury, A., Elliott, F., MarkMIles, Churchman, M., Bristow, R. G., Bishop, D. T., & Kiltie, A. E. (2008). Analysis of variants in DNA damage signalling genes in bladder cancer. *BMC Medical Genetics, 9*(69), 1-11. doi: 10.1186/1471-2350-9-69

Chung, C.-J., Chang, C.-H., Chuu, C.-P., Yang, C.-R., Chang, Y.-H., Huang, C.-P., Chen, W.-C., Chung, M.-C., & Chang, H. (2015). Reduced 5-methylcytosine level as a potential progression predictor in patients with T1 or non-invasive urothelial carcinoma. *International Journal of Molecular Sciences, 16*(1), 677-690. doi: 10.3390/ijms16010677

David, S. S., O'Shea, V. L., & Kundu, S. (2007). Base-excision repair of oxidative DNA damage. *Nature, 447*(7147), 941-950. doi: 10.1038/nature05978

Dialynas, G. K., Vitalini, M. W., & Wallrath, L. L. (2008). Linking Heterochromatin Protein 1 (HP1) to cancer progression. *Mutation Research, 647*(1-2), 13–20. doi: 10.1016/j.mrfmmm.2008.09.007

Dinant, C., & Luijsterburg, M. S. (2009). The emerging role of HP1 in the DNA damage response. *Molecular and Cellular Biology, 29*(24), 6335–6340. doi: 10.1128/MCB.01048-09

Ellinger, J., Bachmann, A., Baumann, C., Göke, F., Heukamp, L. C., Behbahani, T. E., Rogenhofer, S., & Müller, S. C. (2014). Alterations of global histone H3K9 and H3K27 methylation levels in bladder cancer. *Urologia Internationalis, 93*(1), 113–118. doi: 10.1159/000355467

Ellinger, J., Schneider, A.-C., Bachmann, A., Kristiansen, G., Müller, S. C., & Rogenhofer, S. (2016). Evaluation of global histone acetylation levels in bladder cancer patients. *Anticancer Research, 36*(8), 3961-3964.

Espada, J., Ballestar, E., Fraga, M. F., Villar-Garea, A., Juarranz, A., Stockert, J. C., Robertson, K. D., Fuks, F., & Esteller, M. (2004). Human DNA methyltransferase 1 is required for maintenance of the histone H3 modification pattern. *Journal of Biological Chemistry, 279*(35), 37175-37184. doi: 10.1074/jbc.M404842200

Esteller, M. (2008). Epigenetics in cancer. *The New England Journal of Medicine, 358*(11), 1148-1159. doi: 10.1056/NEJMra072067

Florl, A., Löwer, R., Schmitz-Dräger, B., & Schulz, W. (1999). DNA methylation and expression of LINE-1 and HERV-K provirus sequences in urothelial and renal cell carcinomas. *British Journal of Cancer, 80*(9), 1312–1321.

Franco, R., Schoneveld, O., Georgakilas, A. G., & Panayiotidis, M. I. (2008). Oxidative stress, DNA methylation and carcinogenesis. *Cancer Letters, 266*(1), 6–11. doi: 10.1016/j.canlet.2008.02.026

Fritzsche, F. R., Weichert, W., Röske1, A., Gekeler, V., Beckers, T., Stephan, C., Jung, K., Scholman, K., Denkert, C., Dietel, M., & Kristiansen, G. (2008). Class I histone deacetylases 1, 2 and 3 are highly expressed in renal cell cancer. *BMC Cancer, 8*(381), 1-10. doi: 10.1186/1471-2407-8-381

Furda, A., Santos, J. H., Meyer, J. N., & Houten, B. V. (2014). Quantitative PCR-based measurement of nuclear and mitochondrial DNA damage and repair in mammalian cells. *Methods in Molecular Biology, 1105*, 419–437. doi: 10.1007/978-1-62703-739-6_31

Garcia-Perez, J. L., Morell, M., Scheys, J. O., Kulpa, D. A., Morell, S., Carter, C. C., Hammer, G. D., Collins, K. L., O'Shea, K. S., Menendez, P., & Moran, J. V. (2010). Epigenetic silencing of engineered L1 retrotransposition events in human embryonic carcinoma cells. *Nature, 466*(7307), 769–773. doi: 10.1038/nature09209

Gecit, I., Aslan, M., Gunes, M., Pirincci, N., Esen, R., Demir, H., & Ceylan, K. (2012). Serum prolidase activity, oxidative stress, and nitric oxide levels in patients with bladder cancer. *Journal of Cancer Research and Clinical Oncology, 138*(5), 739–743. doi: 10.1007/s00432-011-1136-4

Gessaman, J. D., & Selker, E. U. (2017). Induction of H3K9me3 and DNA methylation by tethered heterochromatin factors in *Neurospora crassa*. *Proceedings of the National Academy of Sciences*. doi: 10.1073/pnas.1715049114

Giacomo, M. D., Comazzetto, S., Sampath, S. C., Sampath, S. C., & O'Carroll, D. (2014). G9a co-suppresses LINE1 elements in spermatogonia. *Epigenetics & Chromatin, 7*(24), 1-7. doi: 10.1186/1756-8935-7-24

Habib, S. L., Bhandari, B. K., Sadek, N., Abboud-Werner, S. L., & Abboud, H. E. (2010). Novel mechanism of regulation of the DNA repair enzyme OGG1 in tuberin-deficient cells. *Carcinogenesis, 31*(11), 2022–2030. doi: 10.1093/carcin/bgq189

Halliwell, B., Clement, M. V., & Long, L. H. (2000). Hydrogen peroxide in the human body. *FEBS Letters, 486*, 10-13. doi: 10.1016/S0014-5793(00)02197-9

Han, J. S., & Boeke, J. D. (2005). LINE-1 retrotransposons: modulators of quantity and quality of mammalian gene expression? *BioEssays, 27*(8), 775–784. doi: 10.1002/bies.20257

Harb-de la Rosa, A., Acker, M., Kumar, R. A., & Manoharan, M. (2015). Epigenetics application in the diagnosis and treatment of bladder cancer. *Can J Urol, 22*(5), 7947-7951.

Hempel, N., Ye, H., Abessi, B., Mian, B., & Melendez, J. A. (2009). Altered redox status accompanies progression to metastatic human bladder cancer. *Free Radical Biology & Medicine, 46*(1), 42–50. doi: 10.1016/j.freeradbiomed.2008.09.020

Hernandez-Blazquez, F. J., Habib, M., Dumollard, J.-M., Barthelemy, C., Benchaib, M., Capoa, A. d., & Niveleau, A. (2000). Evaluation of global DNA hypomethylation

in human colon cancer tissues by immunohistochemistry and image analysis. *Gut, 47*(5), 689–693. doi: 10.1136/gut.47.5.689

Holm, K., Grabau, D., Lovgren, K., Aradottir, S., Gruvberger-Saal, S., Howlin, J., Saal, L. H., Ethier, S. P., Bendahl, P. O., Stal, O., Malmstrom, P., Ferno, M., Ryden, L., Hegardt, C., Borg, A., & Ringner, M. (2012). Global H3K27 trimethylation and EZH2 abundance in breast tumor subtypes. *Molecular Oncology, 6*(5), 494-506. doi: 10.1016/j.molonc.2012.06.002

Hon, G. C., Hawkins, R. D., Caballero, O. L., Lo, C., Lister, R., Pelizzola, M., Valsesia, A., Ye, Z., Kuan, S., Edsall, L. E., Camargo, A. A., Stevenson, B. J., Ecker, J. R., Bafna, V., Strausberg, R. L., Simpson, A. J., & Ren, B. (2012). Global DNA hypomethylation coupled to repressive chromatin domain formation and gene silencing in breast cancer. *Genome Research, 22*(2), 246–258. doi: 10.1101/gr.125872.111

Hunter, S. E., Jung, D., Giulio, R. T. D., & Meyer, J. N. (2010). The QPCR assay for analysis of mitochondrial DNA damage, repair, and relative copy number. *Methods, 51*(4), 444–451. doi: 10.1016/j.ymeth.2010.01.033

Hwang, S., Byun, J. W., Yoon, J. S., & Lee, E. J. (2016). Inhibitory Effects of α-Lipoic Acid on Oxidative Stress-Induced Adipogenesis in Orbital Fibroblasts From Patients With Graves Ophthalmopathy. *Medicine, 95*(2), e2497. doi: 10.1097/MD.0000000000002497

Irvine, R. A., Lin, I. G., & Hsieh, C.-L. (2002). DNA methylation has a local effect on transcription and histone acetylation. *Molecular and Cellular Biology, 22*(19), 6689–6696. doi: 10.1128/MCB.22.19.6689–6696.2002

Jacobs, E. J., Henion, A. K., Briggs, P. J., Connell, C. J., McCullough, M. L., Jonas, C. R., Rodriguez, C., Calle, E. E., & Thun, M. J. (2002). Vitamin C and vitamin E supplement use and bladder cancer mortality in a large cohort of US men and women. *American Journal of Epidemiology, 156*(11), 1002–1010. doi: 10.1093/aje/kwf147

Jantip, J., Tanthanuch, M., Kanngurn, S., Karnchanawanichkul, W., Pripatnanont, C., Sangkhathat, S., & Thongsuksai, P. (2013). Mutations of Fibroblast Growth Factor Receptor 3 Gene (FGFR3) in transitional cell Carcinoma of urinary

bladder in Thai patients [Revision-2a]†. *Journal of the Medical Association of Thailand, 96*(8), 976-983.

Jürgens, B., Schmitz-Dräger, B. J., & Schulz, W. A. (1996). Hypomethylation of Li LINE sequences prevailing in human urothelial carcinoma. *Cancer Research, 56*(24), 5698-5703.

Kandimalla, R., Tilborg, A. A. v., & Zwarthoff, E. C. (2013). DNA methylation-based biomarkers in bladder cancer. *Nature Reviews Urology, 10*(6), 327–335. doi: 10.1038/nrurol.2013.89

Karihtala, P., Kauppila, S., Puistola, U., & Jukkola-Vuorinen, A. (2011). Divergent behaviour of oxidative stress markers 8-hydroxydeoxyguanosine (8-OHdG) and 4-hydroxy-2-nonenal (HNE) in breast carcinogenesis. *Histopathology, 58*(6), 854–862. doi: 10.1111/j.1365-2559.2011.03835.x

Kasymova, R. D., Grin, I. R., Endutkin, A. V., Smirnov, S. L., Ishchenko, A. A., Saparbaev, M. K., & Zharkov, D. O. (2013). Excision of 8-oxoguanine from methylated CpG dinucleotides by human 8-oxoguanine DNA glycosylase. *FEBS Letters, 587*(18), 3129–3134. doi: 10.1016/j.febslet.2013.08.008

Kemp, J. R., & Longworth, M. S. (2015). Crossing the LINE toward genomic instability: LINE-1 retrotransposition in cancer. *Frontiers in Chemistry, 3*(68). doi: 10.3389/fchem.2015.00068

Kim, J., Akbani, R., Creighton, C. J., Lerner, S. P., Weinstein, J. N., Getz, G., & Kwiatkowski, D. J. (2015). Invasive Bladder Cancer: Genomic Insights and Therapeutic Promise. *Clinical cancer research : an official journal of the American Association for Cancer Research, 21*(20), 4514-4524. doi: 10.1158/1078-0432.CCR-14-1215

Kitkumthorn, N., & Mutirangura, A. (2011). Long interspersed nuclear element-1 hypomethylation in cancer: biology and clinical applications. *Clinical Epigenetics, 2*(2), 315–330. doi: 10.1007/s13148-011-0032-8

Klaunig, J. E., Kamendulis, L. M., & Hocevar, B. A. (2010). Oxidative stress and oxidative damage in carcinogenesis. *Toxicologic Pathology, 38*(1), 96-109. doi: 10.1177/0192623309356453

Kloypan, C., Srisa-art, M., Mutirangura, A., & Boonla, C. (2015). LINE-1 hypomethylation
induced by reactive oxygen species is mediated via depletion of S-
adenosylmethionine. *Cell Biochemistry and Function, 33*(6), 375-385. doi:
10.1002/cbf.3124

Kondo, Y. (2009). Epigenetic cross-talk between DNA methylation and histone
modifications in human cancers. *Yonsei Medical Journal, 50*(4), 455-463. doi:
10.3349/ymj.2009.50.4.455

Kreimer, U., Schulz, W. A., Koch, A., Niegisch, G., & Goering, W. (2013). HERV-K and
LINE-1 DNA methylation and reexpression in urothelial carcinoma. *Frontiers in
Oncology, 3*(255), 1-12. doi: 10.3389/fonc.2013.00255

Kreuz, S., & Fischle, W. (2016). Oxidative stress signaling to chromatin in health and
disease. *Epigenomics, 8*(6), 843–862. doi: 10.2217/epi-2016-0002

Kumari, S., Rastogi, R. P., Singh, K. L., Singh, S. P., & Sinha, R. P. (2008). DNA Damages:
detection strategies. *EXCLI Journal, 7*, 44-62.

Lehnertz, B., Ueda, Y., Derijck, A. A. H. A., Braunschweig, U., Perez-Burgos, L., Kubicek,
S., Chen, T., Li, E., Jenuwein, T., & Peters, A. H. F. M. (2003). Suv39h-mediated
Histone H3 lysine 9 methylation directs DNA methylation to major satellite
repeats at pericentric heterochromatin. *Current Biology, 13*(14), 1192–1200.
doi: 10.1016/S0960-9822(03)00432-9

Li, H.-T., Duymich, C. E., Weisenberger, D. J., & Liang, G. (2016). Genetic and epigenetic
alterations in bladder cancer. *International Neurourology Journal, 20*(Suppl 2),
S84-94. doi: 10.5213/inj.1632752.376

Li, L., Qiu, P., Chen, B., Lu, Y., Wu, K., Thakur, C., Chang, Q., Sun, J., & Chen, F. (2014).
Reactive oxygen species contribute to arsenic-induced EZH2 phosphorylation
in human bronchial epithelial cells and lung cancer cells. *Toxicology and
Applied Pharmacology, 276*(3), 165–170. doi: 10.1016/j.taap.2014.02.005.

Li, Q.-L., Lei, P.-J., Zhao, Q.-Y., Li, L., Wei, G., & Wu, M. (2017). Epigenomic analysis in a
cell-based model reveals the roles of H3K9me3 in breast cancer
transformation. *Epigenomics, 9*(8), 1077–1092. doi: 10.2217/epi-2016-0183

Li, Q., Wang, J.-M., Peng, Y., Zhang, S.-H., Ren, T., Luo, H., Cheng, Y., & Wang, D. (2013).
Association of DNA sase-excision repair XRCC1, OGG1 and APE1 gene

polymorphisms with nasopharyngeal carcinoma susceptibility in a Chinese population. *Asian Pacific Journal of Cancer Prevention, 14*(9), 5145-5151. doi: 10.7314/APJCP.2013.14.9.5145

Mahalingaiah, P. K., Ponnusamy, L., & Singh, K. P. (2017). Oxidative stress-induced epigenetic changes associated with malignant transformation of human kidney epithelial cells. *Oncotarget, 8*(7), 11127-11143. doi: 10.18632/oncotarget.12091

Mair, B., Kubicek, S., & Nijman, S. M. B. (2014). Exploiting epigenetic vulnerabilities for cancer therapeutics. *Trends in Pharmacological Sciences, 35*(3), 136-145. doi: 10.1016/j.tips.2014.01.001

Michaud, D. S. (2007). Chronic inflammation and bladder cancer. *Urologic Oncology: Seminars and Original Investigations, 25*(3), 260–268. doi: 10.1016/j.urolonc.2006.10.002

Moodie, F. M., Marwick, J. A., Anderson, C. S., Szulakowski, P., Biswas, S. K., Bauter, M. R., Kilty, I., & Rahman, I. (2004). Oxidative stress and cigarette smoke alter chromatin remodeling but differentially regulate NF-kappaB activation and proinflammatory cytokine release in alveolar epithelial cells. *The FASEB Journal, 18*(15), 1897-1899. doi: 10.1096/fj.04-1506fje

Moore, L. E., Pfeiffer, R. M., Poscablo, C., Real, F. X., Kogevinas, M., Silverman, D., Garcia-Closas, R., Chanock, S., Tardón, A., Serra, C., Carrato, A., Dosemeci, M., García-Closas, M., Esteller, M., Fraga, M., Rothman, N., & Malats, N. (2008). Genomic DNA hypomethylation is a biomarker for bladder cancer susceptibility in the Spanish bladder cancer case-control study. *The Lancet Oncology, 9*(4), 359–366. doi: 10.1016/S1470-2045(08)70038-X

Mosashvilli, D., Kahl, P., Mertens, C., Holzapfel, S., Rogenhofer, S., Hauser, S., Büttner, R., Ruecker, A. v., Müller, S. C., & Ellinger, J. (2010). Global histone acetylation levels: Prognostic relevance in patients with renal cell carcinoma. *Cancer Science, 101*(12), 2664–2669. doi: 10.1111/j.1349-7006.2010.01717.x

Ngollo, M., Lebert, A., Daures, M., Judes, G., Rifai, K., Dubois, L., Kemeny, J.-L., Penault-Llorca, F., Bignon, Y.-J., Guy, L., & Bernard-Gallon, D. (2017). Global

analysis of H3K27me3 as an epigenetic marker in prostate cancer progression. *BMC Cancer, 17*(261), 1-8. doi: 10.1186/s12885-017-3256-y

Nishida, N., Arizumi, T., Takita, M., Kitai, S., Yada, N., Hagiwara, S., Inoue, T., Minami, Y., Ueshima, K., Sakurai, T., & Kudo, M. (2013). Reactive oxygen species induce epigenetic instability through the formation of 8-hydroxydeoxyguanosine in human hepatocarcinogenesis. *Digestive Diseases, 31*(5-6), 459–466. doi: 10.1159/000355245

Niu, Y., DesMarais, T. L., Tong, Z., Yao, Y., & Costa, M. (2015). Oxidative stress alters global histone modification and DNA methylation. *Free Radical Biology & Medicine, 82*, 22–28. doi: 10.1016/j.freeradbiomed.2015.01.028

Oberley, T. D. (2002). Oxidative damage and cancer. *American Journal of Pathology, 160*(2), 403-408.

Opanuraks, J., Boonla, C., Saelim, C., Kittikowit, W., Sumpatanukul, P., Honglertsakul, C., & Tosukhowong, P. (2010). Elevated urinary total sialic acid and increased oxidative stress in patients with bladder cancer. *Asian Biomedicine, 4*(5), 703-710.

Patchsung, M., Boonla, C., Amnattrakul, P., Dissayabutra, T., Mutirangura, A., & Tosukhowong, P. (2012). Long Interspersed Nuclear Element-1 hypomethylation and oxidative stress: correlation and bladder cancer diagnostic potential. *PLoS ONE, 7*(5), e37009. doi: 10.1371/journal.pone.0037009

Phokaew, C., Kowudtitham, S., Subbalekha, K., Shuangshoti, S., & Mutirangura, A. (2008). LINE-1 methylation patterns of different loci in normal and cancerous cells. *Nucleic Acids Research, 36*(17), 5704–5712. doi: 10.1093/nar/gkn571

Poungpairoj, P., Whongsiri, P., Suwannasin, S., Khlaiphuengsin, A., Tangkijvanich, P., & Boonla, C. (2015). Increased Oxidative Stress and RUNX3 Hypermethylation in Patients with Hepatitis B Virus-Associated Hepatocellular Carcinoma (HCC) and Induction of RUNX3 Hypermethylation by Reactive Oxygen Species in HCC Cells. *Asian Pacific journal of cancer prevention : APJCP, 16*(13), 5343-5348.

Rangasamy, D. (2013). Distinctive patterns of epigenetic marks are associated with promoter regions of mouse LINE-1 and LTR retrotransposons. *Mobile DNA, 4*(1), 27. doi: 10.1186/1759-8753-4-27

Rangasamy, D., Lenka, N., Ohms, S., Dahlstrom, J. E., Blackburn, A. C., & Board, P. G. (2015). Activation of LINE-1 retrotransposon increases the risk of epithelial-mesenchymal transition and metastasis in epithelial cancer. *Current Molecular Medicine, 15*(7), 588-597.

Reuter, S., Gupta, S. C., Chaturvedi, M. M., & Aggarwal, B. B. (2010). Oxidative stress, inflammation, and cancer: How are they linked? *Free Radical Biology and Medicine, 49*(11), 1603–1616. doi: 10.1016/j.freeradbiomed.2010.09.006

Rodic, N., & Burns, K. H. (2013). Long Interspersed Element–1 (LINE-1): passenger or driver in human neoplasms? *PLoS Genetics, 9*(3), e1003402. doi: 10.1371/journal.pgen.1003402

Rodic, N., Sharma, R., Sharma, R., Zampella, J., Dai, L., Taylor, M. S., Hruban, R. H., Iacobuzio-Donahue, C. A., Maitra, A., Torbenson, M. S., Goggins, M., Shih, I.-M., Duffield, A. S., Montgomery, E. A., Gabrielson, E., Netto, G. J., Lotan, T. L., Marzo, A. M. D., Westra, W., Binder, Z. A., Orr, B. A., Gallia, G. L., Eberhart, C. G., Boeke, J. D., Harris, C. R., & Burns, K. H. (2014). Long Interspersed Element-1 protein expression is a hallmark of many human cancers. *The American Journal of Pathology, 184*(5), 1280-1286. doi: 10.1016/j.ajpath.2014.01.007

Romanenko, A., Morimura, K., Wei, M., Zaparin, W., Vozianov, A., & Fukushima, S. (2002). DNA damage repair in bladder urothelium after the Chernobyl accident in Ukraine. *Journal of Urology, 168*(3), 973-977. doi: 10.1097/01.ju.0000026808.26025.3b

Rose, N. R., & Klose, R. J. (2014). Understanding the relationship between DNA methylation and histone lysine methylation. *Biochimica et Biophysica Acta, 1839*(12), 1362–1372. doi: 10.1016/j.bbagrm.2014.02.007

Ruchko, M. V., Gorodnya, O. M., Zuleta, A., Pastukh, V. M., & Gillespie, M. N. (2011). The DNA Glycosylase, Ogg1, defends against oxidant-induced mtDNA damage and apoptosis in pulmonary artery endothelial cells. *Free Radical Biology & Medicine, 50*(9), 1107–1113. doi: 10.1016/j.freeradbiomed.2010.10.692

Salim, E. I., Morimura, K., Menesi, A., El-Lity, M., Fukushima, S., & Wanibuchi, H. (2008). Elevated oxidative stress and DNA damage and repair levels in urinary bladder carcinomas associated with Schistosomiasis. *International Journal of Cancer, 123*(3), 601–608. doi: 10.1002/ijc.23547

Sawan, C., & Herceg, Z. (2010). Histone modifications and cancer. *Advances in Genetics, 70*, 57-85. doi: 10.1016/B978-0-12-380866-0.60003-4

Sawyera, D. E., Mercera, B. G., M.Wiklendt, A., & Aitken, R. J. (2003). Quantitative analysis of gene-specific DNA damage in human spermatozoa. *Mutation Research, 529*(1-2), 21–34. doi: 10.1016/S0027-5107(03)00101-5

Schabath, M. B., Spitz, M. R., Grossman, H. B., Zhang, K., Dinney, C. P., Zheng, P.-J., & Wu, X. (2003). Genetic instability in bladder cancer assessed by the comet assay. *Journal of the National Cancer Institute, 95*(7), 540-547.

Schäfer, A., Karaulanov, E., Stapf, U., Döderlein, G., & Niehrs, C. (2013). Ing1 functions in DNA demethylation by directing Gadd45a to H3K4me3. *Genes & Development, 27*(3), 261–273. doi: 10.1101/gad.186916.112

Schieber, M., & Chandel, N. S. (2014). ROS function in redox signaling and oxidative stress. *Current Biology, 24*(10), R453–R462. doi: 10.1016/j.cub.2014.03.034

Schneider, A. C., Heukamp, L. C., Rogenhofer, S., Fechner, G., Bastian, P. J., von Ruecker, A., Muller, S. C., & Ellinger, J. (2011). Global histone H4K20 trimethylation predicts cancer-specific survival in patients with muscle-invasive bladder cancer. *BJU International, 108*(8 Pt 2), E290-296. doi: 10.1111/j.1464-410X.2011.10203.x

Schulz, W. A., & Goering, W. (2016). DNA methylation in urothelial carcinoma. *Epigenomics, 8*(10), 1415-1428. doi: 10.2217/epi-2016-0064

Sciamanna, I., Sinibaldi-Vallebona, P., Serafino, A., & Spadafora, C. (2018). LINE-1-encoded reverse Transcriptase as a target in cancer therapy. *Frontiers In Bioscience (Landmark Ed), 23*, 1360-1369.

Sharma, S., Kelly, T. K., & Jones, P. A. (2010). Epigenetics in cancer. *Carcinogenesis, 31*(1), 27–36. doi: 10.1093/carcin/bgp220

Soini, Y., Haapasaari, K.-M., Vaarala, M. H., Turpeenniemi-Hujanen, T., Kärjä, V., & Karihtala, P. (2011). 8-hydroxydeguanosine and nitrotyrosine are prognostic

factors in urinary bladder carcinoma. *International Journal of Clinical and Experimental Pathology, 4*(4), 267-275.

Sova, H., Jukkola-Vuorinen, A., Puistola, U., Kauppila, S., & Karihtala, P. (2010). 8-Hydroxydeoxyguanosine: a new potential independent prognostic factor in breast cancer. *British Journal of Cancer, 102*(6), 1018 – 1023. doi: 10.1038/sj.bjc.6605565

Sun, Y., Jiang, X., Xu, Y., Ayrapetov, M. K., Moreau, L. A., Whetstine, J. R., & Price, B. D. (2009). Histone H3 methylation links DNA damage detection to activation of the tumour suppressor Tip60. *Nature Cell Biology, 11*(11), 1376-1382. doi: 10.1038/ncb1982

The Cancer Genome Atlas Research, N. (2014). Comprehensive molecular characterization of urothelial bladder carcinoma. *Nature, 507*, 315. doi: 10.1038/nature12965

Thomsen, R., Christensen, D. B., Rosborg, S., Linnet, T. E., Blechingberg, J., & Nielsen, A. L. (2011). Analysis of HP1alpha regulation in human breast cancer cells. *Molecular Carcinogenesis, 50*(8), 601–613. doi: 10.1002/mc.20755

Toraño, E. G., Petrus, S., Fernandez, A. F., & Fraga, M. F. (2012). Global DNA hypomethylation in cancer: review of validated methods and clinical significance. *Clinical Chemistry and Laboratory Medicine, 50*(10), 1733–1742. doi: 10.1515/cclm-2011-0902

Vad-Nielsen, J., & Nielsen, A. L. (2015). Beyond the histone tale: HP1alpha deregulation in breast cancer epigenetics. *Cancer Biology & Therapy, 16*(2), 189-200. doi: 10.1080/15384047.2014.1001277

Valavanidis, A., Vlachogianni, T., & Fiotakis, C. (2009). 8-hydroxy-2'-deoxyguanosine (8-OHdG): a critical biomarker of oxidative stress and carcinogenesis. *Journal of Environmental Science and Health Part C, 27*(2), 120–139. doi: 10.1080/10590500902885684

Van Houten, B., Cheng, S., & Chen, Y. (2000). Measuring gene-specific nucleotide excision repair in human cells using quantitative amplification of long targets from nanogram quantities of DNA. *Mutation Research, 460*(2), 81-94. doi: 10.1016/S0921-8777(00)00018-5

Walter, M., Teissandier, A., Pérez-Palacios, R., & Bourc'his, D. (2016). An epigenetic switch ensures transposon repression upon dynamic loss of DNA methylation in embryonic stem cells. *eLife, 5*, e11418. doi: 10.7554/eLife.11418

Wasenius, V.-M., Hemmer, S., Kettunen, E., Knuutila, S., Franssila, K., & Joensuu, H. (2003). Hepatocyte Growth Factor Receptor, Matrix Metalloproteinase-11, tissue inhibitor of Metalloproteinase-1, and Fibronectin are up-regulated in papillary thyroid carcinoma: a cDNA and tissue microarray study. *Clinical Cancer Research, 9*(1), 68–75.

Weitzman, S. A., Turk, P. W., Milkowski, D. H., & Kozlowski, K. (1994). Free radical adducts induce alterations in DNA cytosine methylation. *PNAS, 91*, 1261-1264.

Wilhelm, C. S., Kelsey, K. T., Butler, R., Plaza, S., Gagne, L., Zens, S., Andrew, A. S., Morris, S., Nelson, H. H., Schned, A. R., Karagas, M. R., & Marsit, C. J. (2010). Implications of LINE1 methylation for bladder cancer risk in women. *Clinical Cancer Research, 16*(5), 1682–1689. doi: 10.1158/1078-0432.CCR-09-2983

Wilson, A. S., Power, B. E., & Molloy, P. L. (2007). DNA hypomethylation and human diseases. *Biochimica et Biophysica Acta, 1775*(1), 138–162. doi: 10.1016/j.bbcan.2006.08.007

Wolff, E. M., Byun, H.-M., Han, H. F., Sharma, S., Nichols, P. W., Siegmund, K. D., Yang, A. S., Jones, P. A., & Liang, G. (2010). Hypomethylation of a LINE-1 promoter activates an alternate transcript of the MET oncogene in bladders with cancer. *PLoS Genetics, 6*(4), e1000917. doi: 10.1371/journal.pgen.1000917

Wongpaiboonwattana, W., Tosukhowong, P., Dissayabutra, T., Mutirangura, A., & Boonla, C. (2013). Oxidative stress induces hypomethylation of LINE-1 and hypermethylation of the RUNX3 promoter in a bladder cancer cell line. *Asian Pacific Journal of Cancer Prevention, 14*(6), 3773-3778. doi: 10.7314/APJCP.2013.14.6.3773

Wu, L. L., Chiou, C.-C., Chang, P.-Y., & Wu, J. T. (2004). Urinary 8-OHdG: a marker of oxidative stress to DNA and a risk factor for cancer, atherosclerosis and diabetics. *Clinica Chimica Acta, 339*(1-2), 1-9. doi: 10.1016/j.cccn.2003.09.010

Wu, Q., & Ni, X. (2015). ROS-mediated DNA methylation pattern alterations in carcinogenesis. *Current Drug Targets, 16*(1), 13-19.

Wu, S., Yang, Z., Ye, R., An, D., Li, C., Wang, Y., Wang, Y., Huang, Y., Liu, H., Li, F., He, L., Sun, D., Yu, Y., Li, Q., Huang, P., Zhang, M., Zhao, X., Bi, T., Zhuang, X., Zhang, L., Lu, J., Sun, X., Zhou, F., Liu, C., Yang, G., Hou, Y., Fan, Z., & Cai, Z. (2016). Novel variants in MLL confer to bladder cancer recurrence identified by whole-exome sequencing. *Oncotarget, 7*(3), 2629-2645. doi: 10.18632/oncotarget.6380

Wu, X., Gu, J., Grossman, H. B., Amos, C. I., Etzel, C., Huang, M., Zhang, Q., Millikan, R. E., Lerner, S., Dinney, C. P., & Spitz, M. R. (2006). Bladder cancer predisposition: a multigenic approach to DNA-repair and cell-cycle–control genes. *The American Journal of Human Genetics, 78*(3), 464–479. doi: 10.1086/500848

Xu, X., Wang, Y., Guo, W., Zhou, Y., Lv, C., Chen, X., & Liu, K. (2013). The significance of the alteration of 8-OHdG in serous ovarian carcinoma. *Journal of Ovarian Research, 6*(74), 1-9. doi: 10.1186/1757-2215-6-74

Yang, B., Sun, H., Lin, W., Hou, W., Li, H., Zhang, L., Li, F., Gu, Y., Song, Y., Li, Q., & Zhang, F. (2013). Evaluation of global DNA hypomethylation in human prostate cancer and prostatic intraepithelial neoplasm tissues by immunohistochemistry. *Urologic Oncology: Seminars and Original Investigations, 31*(5), 628–634. doi: 10.1016/j.urolonc.2011.05.009

Yokoyama, Y., Hieda, M., Nishioka, Y., Matsumoto, A., Higashi, S., Kimura, H., Yamamoto, H., Mori, M., Matsuura, S., & Matsuura, N. (2013). Cancer-associated upregulation of histone H3 lysine 9 trimethylation promotes cell motility *in vitro* and drives tumor formation *in vivo*. *Cancer Science, 104*(7), 889–895. doi: 10.1111/cas.12166

Zarebski, M., Wiernasz, E., & Dobrucki, J. W. (2009). Recruitment of Heterochromatin Protein 1 to DNA repair sites. *Cytometry Part A, 75*(7), 619-625. doi: 10.1002/cyto.a.20734

Zhou, X., Zhuang, Z., Wang, W., He, L., Wu, H., Cao, Y., Pan, F., Zhao, J., Hua, Z., Sekhar, C., & Guo, Z. (2016). OGG1 is essential in oxidative stress induced DNA demethylation. *Cellular Signalling, 28*(9), 1163–1171. doi: 10.1016/j.cellsig.2016.05.021

APPENDIX

# Reagents used in this study

1. 10X PBS, pH 7.4
    - ○ 80 g/L  NaCl
    - ○ 2 g/L   KCl
    - ○ 14.4 g/L $Na_2HPO_4$
    - ○ 2.4 g/L  $KH_2PO_4$

2. RIPA buffer, pH 7.4
    - ○ 6 g/L   Tris
    - ○ 8.7 g/L NaCl
    - ○ 1 g/L   SDS
    - ○ 1% Triton X-100
    - ○ Store at $4^{\circ}C$

3. Reagents for protein carbonyl assay
    - 3.1 2 N HCl
    - 3.2 10 mM DNPH in 2 N HCl
    - 3.3 20% w/v Trichloroacetic acid (TCA)
    - 3.4 Ethanol: Ethyl acetate (1:1 V/V)
    - 3.5 6 M Guanidine hydrochloride in 0.5 M potassium phosphate, pH 2.5

4. DCFH-DA reagent
    - ○ 50 mM DCFH-DA in DMSO
    - ○ Store at $-20^{\circ}C$
    - ○ Workging DCFH-DA: 0.5 mM DCFH-DA in serum-free media

5. MTT reagent
    - ○ 5 mg/mL MTT in PBS
    - ○ Store at $-20^{\circ}C$
    - ○ Working MTT: 0.5 mg/mL MTT in serum-free media

6. 10X sodium citrate buffer (0.1 M), pH 6.0
    - ○ 29.41 g/L Sodium citrate dihydrate ($C_6H_3Na_3O_7 \cdot 2H_2O$)
    - ○ Store at $4^{\circ}C$
    - ○ Working citrate buffer: 1X sodium citrate buffer + 0.05% Tween 20

7     Reagents for 8-OHdG immunoprecipitation

     7.1 10X IP buffer, pH 7.0

         O    100 mM $Na_2HPO_4$

         O    1.4 M NaCl

         O    0.5% Triton X-100

     7.2 Digestion buffer, pH 8.0

         O    50 mM Tris

         O    10 mM EDTA

         O    0.5% w/v SDS

     7.3 TE buffer, pH 8.0

         O    10 mM Tris

         O    1 mM EDTA

     7.4 3 M sodium acetate

8     Reagents for western blot

     8.1 Separating gel (10% acrylamide for 10 mL)

| | | | |
|---|---|---|---|
| O | $H_2O$ | 5 | mL |
| O | 40% Polyacrylamide | 2.5 | mL |
| O | 1.5 M Tris pH 8.8 | 2.5 | mL |
| O | 10% SDS | 100 | µL |
| O | 10% APS | 100 | µL |
| O | TEMED | 5 | µL |

     8.2 Stacking gel (2.5% acrylamide for 5 mL)

| | | | |
|---|---|---|---|
| O | $H_2O$ | 3.61 | mL |
| O | 40% Polyacrylamide | 0.62 | mL |
| O | 1 M Tris pH 6.8 | 2.5 | mL |
| O | 10% SDS | 50 | µL |
| O | 10% APS | 50 | µL |
| O | TEMED | 5 | µL |

     8.3 1X Running buffer

         O    3 g/L Tris

- 14.41 g/L Glycine
- 0.1% SDS

8.4 10X Transfer buffer

- 30.3 g/L Tris
- 144 g/L Glycine
- Store at $4^{\circ}$C
- Working transfer buffer: 100 mL 10X transfer buffer + 200 mL methanol + 700 mL distilled waster
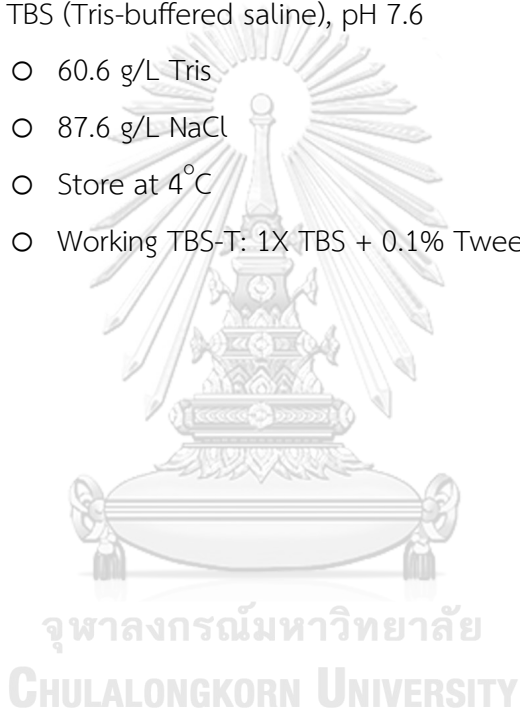
8.5 10X TBS (Tris-buffered saline), pH 7.6

- 60.6 g/L Tris
- 87.6 g/L NaCl
- Store at $4^{\circ}$C
- Working TBS-T: 1X TBS + 0.1% Tween 20

# VITA

Name            Patcharawalai Whongsiri

Date of birth    5th October 1986   Place of birth       Lopburi

Education        M.Sc. in Zoology, Department of Biology, Faculty of Science,

Chulalongkorn Universiry

B.Sc. in Biology, Department of Biology, Faculty of Science,

Chulalongkorn University

Scholarship     Development and Promotion of Science and Technology talents Project

Award           Outstanding student of Faculty of Medicine, Chulalongkorn University in the academic year of 2015

Conferences     E-poster presentation at Joint Conference in Medical Science: Chula-Rama-Siriraj in Bangkok, Thailand, 13 – 15 September 2017

Poster presentation at EMBO conference: Chromatin and Epigenetics in

Heidelberg, Germany, 6 – 10 May 2015

Publications

Whongsiri, P., Pimrattana, C., Wijitsettakul, U., Jindatip, D., Sanpavat, A., Schulz, W. A., & Boonla, C. (2018). LINE-1 ORF1 protein is up-regulated by reactive oxygen species and associated with bladder urothelial carcinoma progression. Cancer Genomics & Proteomics, 15(2), 143–151.

Whongsiri, P., Phoyen, S., & Boonla, C. (2018). Oxidative stress in urothelial carcinogenesis: measurements of protein carbonylation and intracellular production of reactive oxygen species. Methods in Molecular Biology, 1655, 109-117.

Ma-On, C., Sanpavat, A., Whongsiri, P., Suwannasin, S., Hirankarn, N., Tangkijvanich, P., & Boonla, C. (2017). Oxidative stress indicated by elevated expression of Nrf2 and 8-OHdG promotes hepatocellular carcinoma progression. Medical Oncology, 34(4), 57.

Poungpairoj, P., Whongsiri, P., Suwannasin, S., Khlaiphuengsin, A., Tangkijvanich, P., & Boonla, C. (2015). Increased oxidative stress and RUNX3 Hypermethylation in patients with hepatitis B virus-associated hepatocellular carcinoma (HCC) and induction of RUNX3 hypermethylation by reactive oxygen species in HCC cells. Asian Pacific journal of cancer prevention, 16(13), 5343-5348.